

# POLITECNICO DI TORINO

Department of Mechanical and Aerospace Engineering

## CAE Model Characterization of an Iveco Daily Airbag



**Politecnico  
di Torino**

### **Tutors**

Prof. Alessandro Scattina

Prof. Giovanni Belingardi

### **Iveco tutors**

Ing. Marco Barbi

Ing. Giuseppe Cordua

### **Candidate**

Filippo Luzzi

April 2022



## Summary

Abstract .....	11
1. Introduction .....	12
2. Commercial vehicles safety .....	16
2.1 Commercial Vehicles .....	16
2.2 Restraint systems in commercial vehicles .....	17
2.3 Airbag .....	19
2.4 Iveco Daily airbag .....	21
2.5 Iveco Daily steering wheel .....	24
3. Used methods .....	26
3.1 Hyperworks software .....	26
3.2 Airbag modelling with Hyperworks <sup>[3]</sup> .....	26
4. Tests description .....	29
4.1. Linear impactor test .....	29
4.2. Body Block test .....	32
5. Linear impactor .....	40
5.1. Model description .....	40
5.1.1. Steering wheel .....	41
5.1.2. Bag model .....	43
5.1.3. Impactor .....	45
5.2. Airbag model parameters .....	46
5.2.1. Airbag volume and inflation definition .....	46
5.2.2. Material properties .....	49
5.2.3. Porosity definition .....	51
5.2.4. Vent Hole definition .....	54
5.3. Results discussion .....	57

5.3.1.	Model with no porosity and no vent hole .....	57
5.3.2.	Model with porosity definition but no vent hole.....	60
5.3.3.	Model with porosity and vent hole definition .....	61
5.3.4.	Comparison with experimental results.....	63
5.3.5.	Final results of Madymo comparison.....	65
6.	Body Block .....	67
6.1.	Model description.....	67
6.1.1.	Body Block .....	68
6.1.2.	Steering wheel and steering column .....	70
6.1.3.	Final configuration of body block model.....	73
6.2.	Results discussion.....	76
6.2.1.	0 degrees steering wheel .....	76
6.2.2.	90 degrees steering wheel .....	79
6.2.3.	180 degrees steering wheel .....	82
7.	Airbag folding.....	85
7.1.	Airbag folding tool in HyperWorks 2021.1 .....	86
7.2.	Airbag folding process .....	87
7.2.1.	Folding plan .....	87
7.2.2.	Airbag folding process .....	88
7.2.3.	Folded airbag deployment.....	91
	Conclusions.....	93
	Bibliography.....	94

## Figures index

Figure 1: experimental linear impactor test .....	12
Figure 2: finite element model of linear impactor test.....	12
Figure 3: Madymo model of linear impactor test .....	13
Figure 4: body block test with fixed steering wheel. ....	14
Figure 5: finite element model of a body block test. ....	14
Figure 6: Iveco Daily in two different versions, van on the left and truck on the right.....	16
Figure 7: airbag deployment after a crash test .....	17
Figure 8: general scheme of an airbag .....	19
Figure 9: section view of an Iveco Daily airbag .....	21
Figure 10: airbag module of an Iveco Daily .....	22
Figure 11: a bag housing after its deployment.....	22
Figure 12: deployed airbag .....	23
Figure 13: airbag tear lines.....	23
Figure 14: Iveco Daily steering wheel, front view.....	24
Figure 15: Iveco Daily steering wheel partial section.....	24
Figure 16: trigonometric view of the steering wheel .....	25
Figure 17: monitored volume parameters. ....	26
Figure 18: vent hole data definition. ....	27
Figure 19: porosity data definition.....	28
Figure 20: Linear impactor test bench .....	29
Figure 21: linear impactor test frame sequency. ....	30
Figure 22: Steering wheel at 0 degrees. ....	31
Figure 23: body block test with rigid steering wheel.....	32
Figure 24: body block test with steering wheel mounted on the steering column.....	33
Figure 25: steering wheel at 0 degrees for body bock test.....	34

Figure 26: steering wheel at 90 degrees for body block test.....	34
Figure 27: steering wheel at 180 degrees for body block test.....	35
Figure 28: frame sequence of body bock test with steering wheel mounted on a steering column...	36
Figure 29: frame sequence of body block test with steering wheel fixed on a support .....	37
Figure 30: detail of the airbag behaviour in the moment of maximum penetration of the dummy; test configurations with the steering wheel at 0 degrees. ....	38
Figure 31: detail of the airbag behaviour in the moment of maximum penetration of the dummy; test configuration with the steering wheel at 90 degrees. ....	38
Figure 32: detail of the airbag behaviour in the moment of maximum penetration of the dummy; test configuration with the steering wheel at 180 degrees. ....	39
Figure 33: linear impactor model.....	40
Figure 34: detail of the punch .....	41
Figure 35: rigid body definition of the steering wheel.....	41
Figure 36: rigid body with boundary condition .....	42
Figure 37: boundary condition on master node .....	42
Figure 38:airbag model, upper face (left) and lower face (right).....	43
Figure 39: detail of the airbag seams .....	43
Figure 40: airbag straps.....	44
Figure 41: vent hole detail .....	44
Figure 42: impactor for Madymo comparison .....	45
Figure 43: impactor for experimental test comparison .....	45
Figure 44: surfaces of the airbag monitored volume .....	47
Figure 45: detail of the surfaces shell elements with 3 or 4 nodes. ....	47
Figure 46: mass of injected gas function in time .....	48
Figure 47: temperature of injected gas function vs time.....	48
Figure 48: Radioss material card .....	49
Figure 49: upper view of the comparison between Madymo and finite element airbag.....	50

Figure 50: side view of the comparison between Madymo and finite element airbag .....	50
Figure 51: porous surfaces of the cushion .....	51
Figure 52: surfaces for seams porosity .....	52
Figure 53: outflow velocity function of seams porosity .....	52
Figure 54: outflow velocity function of surfaces porosity .....	53
Figure 55: left, a deployed bag; right, zoom on the vent hole .....	54
Figure 56: vent hole in finite element model .....	54
Figure 57: venting coefficient function.....	55
Figure 58: venting coefficient function of definitive model .....	56
Figure 59: comparison between impactor deceleration of fe and Madymo models with no porosity and no vent hole. ....	57
Figure 60: simulation frames of linear impactor test .....	58
Figure 61: comparison between contact force of fe and Madymo models with no porosity and no vent hole.....	59
Figure 62: comparison between contact force vs displacement of fe and Madymo models with no porosity and no vent hole .....	59
Figure 63: comparison between impactor deceleration of fe and Madymo models with porosity and no vent hole.....	60
Figure 64: comparison between contact force of fe and Madymo models with porosity and no vent hole.....	60
Figure 65: comparison between contact force vs displacement of fe and Madymo models with porosity and no vent hole .....	61
Figure 66: comparison between impactor deceleration of fe and Madymo models with porosity and vent hole.....	61
Figure 67: comparison between contact force of fe and Madymo models with porosity and vent hole .....	62
Figure 68: comparison between contact force vs displacement of fe and Madymo models with porosity and vent hole.....	62

Figure 69: comparison between deceleration of finite element model and ZF experimental test at high energy.....	63
Figure 70: comparison between contact force of finite element model and ZF experimental test at high energy.....	64
Figure 71: comparison between deceleration of finite element model and ZF experimental test at low energy.....	64
Figure 72: comparison between contact force of finite element model and ZF experimental test at low energy.....	65
Figure 73: comparison between deceleration of finite element model and Madymo.....	65
Figure 74: comparison between contact force of finite element model and Madymo.....	66
Figure 75: comparison between contact force versus displacement of finite element model and Madymo .....	66
Figure 76: body block finite element model .....	67
Figure 77: body block finite element model, 2nd view .....	68
Figure 78: drawing of body block as described in the UNCE R12 normative. ....	69
Figure 79: body block finite element model. Left: plywood (rear of the body block) and wood. Centre: wood covered by elastomeric material. Right: all the components are covered with scotch tape. ....	69
Figure 80: deformable steering wheel.....	70
Figure 81: steering wheel model definition .....	71
Figure 82: comparison between steering wheel set in finite element model and experimental test. .	72
Figure 83: Left, original section of the support derived from the column one. Right, section of the support that more fit its real behaviour .....	72
Figure 84: final body block model, side view.....	73
Figure 85: body block model with 0 degrees steering wheel.....	74
Figure 86: body block model with 90 degrees steering wheel.....	74
Figure 87: body block model with 180 degrees steering wheel.....	75
Figure 88: body block deceleration with 0 degrees steering wheel .....	76



Figure 89: body block test with 0 degrees steering wheel .....	77
Figure 90: body block simulation with 0 degrees steering wheel.....	78
Figure 91: body block deceleration with 90 degrees steering wheel .....	79
Figure 92: comparison between the real steering wheel and the model, where the are the controls missing .....	79
Figure 93: body block test with 90 degrees steering wheel .....	80
Figure 94: body block simulation with 90 degrees steering wheel.....	81
Figure 95: body block deceleration with 180 degrees steering wheel .....	82
Figure 96: comparison between the long arc deformation in experimental test and in finite element model.....	82
Figure 97: body block test with 180 degrees steering wheel .....	83
Figure 98: body block simulation with 180 degrees steering wheel.....	84
Figure 99: left, unfolded airbag initial configuration; right, pre-formed airbag second configuration .....	85
Figure 100: HyperWorks airbag solution options.....	86
Figure 101: folding plan example for driver airbag.....	87
Figure 102: airbag first symmetric simple fold.....	88
Figure 103: airbag second symmetric simple fold .....	88
Figure 104: airbag symmetric roll fold .....	89
Figure 105: airbag housing .....	89
Figure 106: final folded airbag configuration .....	89
Figure 107: steering wheel and folded airbag .....	90
Figure 108: comparison between finite element folded airbag and real airbag deployment, part 1 ..	91
Figure 109: comparison between finite element folded airbag and real airbag deployment, part 2 ..	92



## **Abstract**

In the last years, safety regulations have become more stringent also in the area of the commercial vehicles, from vans to trucks. All security systems require an ever greater attention in their design, both the ones for active and passive safety. Among these, a crucial role is always played by the airbags. The object of this thesis is the characterization of an Iveco Daily airbag finite element model comparing the results of the experimental tests conducted on the real airbag and that of the computer simulations. The work was done in collaboration with Iveco.

The airbag is a cushion of various fabric material components that inflates after an accident. Therefore it has gas losses due to the material porosity and to the vent hole. The vent hole is a hole in the rear side of the airbag that let a certain amount of gas out to reduce the cushion stiffness with the aim of avoiding injuries for the passenger impacting on it. To define properly which is the effect on the airbag behaviour due to the porosity and that due to the vent hole, it has been modelled following some steps and introducing one by one these phenomena. The characterization is done, in a first step, comparing the finite element model results of a linear impactor test with the ones of a Madymo model, provided by Iveco, and then with the experimental results of the tests done at STELLANTIS Safety Center. The results obtained show a finite element model that is well correlated with the Madymo one and with the experimental results of the tests done on the real airbag. After this, the characterized model has been used to simulate an experimental test with a mannequin impacting on the airbag, like what can happen to the driver in case of accident, to do a comparison with the experimental test results. Even this comparison shows a good correlation between simulation and experimental results.

Lastly, a new tool from the HyperWorks 2021.2 has been used to fold the airbag into its housing.

# 1. Introduction

This thesis work, done at Iveco with some tests conducted at STELLANTIS Safety Center, is about the characterization of an airbag CAE model, in order to replicate some tests that usually are done experimentally to verify the security standards required for commercial vehicles. The goal is to reduce the number of the tests, and consequently the time and the costs spent by the manufacturer, in order to validate the components. The object of this analysis is the airbag of an Iveco Daily.

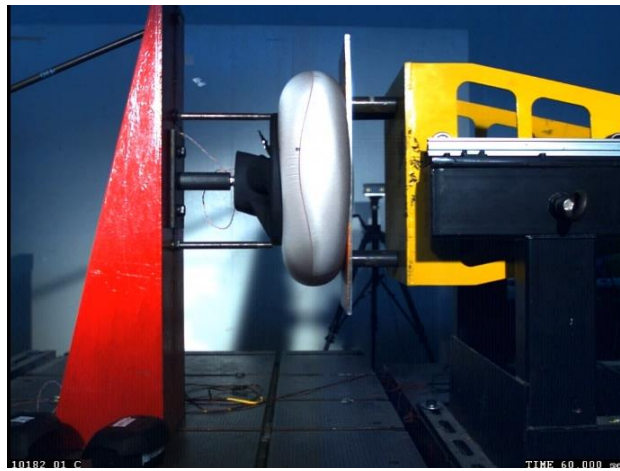


*Figure 1: experimental linear impactor test*

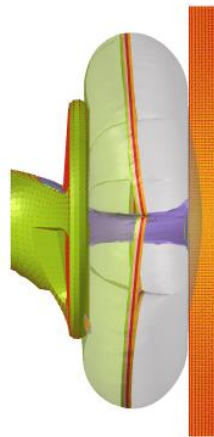


*Figure 2: finite element model of linear impactor test*

For what concern the characterization of the airbag, it has been done, in a first moment, working on a linear impactor test and comparing the results between the finite element model (*Figure 2*) and the

Madymo model (*Figure 3*), a multibody one. This characterization of the finite element model has been done considering what is that defines the airbag behaviour, so there have been identified various parameters like the components materials, the porosity of the material and the effect of the vent hole (a hole in the airbag rear side useful to let the cushion deflate during the impact so to reduce the stiffness on the airbag). The full study consists of three parts:

- Correlation of the ideal airbag model, with no material porosity and no vent hole defined on the bag;
- Correlation of the airbag model introducing only the porosity, with no vent hole definition;
- Correlation of the complete model, with both porosity and vent hole.

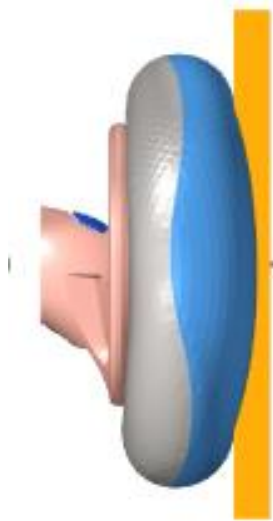


*Figure 3: Madymo model of linear impactor test*

Introducing initially the porosity only and then the vent hole is useful to split the effects of the two phenomena on the final results.

The second step is to compare the finite element model results with the ones done at STELLANTIS Safety Center and those of the validation tests done by ZF Friedrichshafen, the company manufacturer of the airbag which the Daily is equipped with. Since the validation tests have been done with two different velocities of the impactor, one with an impactor of 7 m/s (high energy test) and the other of 6 m/s (low energy test), the comparison has been done for both the tests and this has allowed to make a better correlation, obtaining a more robust finite element model.

Lastly, the correlated airbag model has been introduced into a model simulating a body block test, a test where a mannequin is launched with a certain initial velocity against the steering wheel with the

airbag mounted on it (*figure 4 and 5*). The airbag is inflated before the mannequin hits the steering wheel to simulate what can happen to the driver in case of an accident. The test is conducted with the steering wheel fixed on a rigid frame.

This analysis has been conducted to understand how the component works, after it has been correlated, in a more complex subsystem. In fact, the system composed by body block, steering wheel and steering column was already correlated in a previous activity from Iveco, and introducing the airbag it is possible to have a complete simulation of a realistic phenomenon.



*Figure 4: body block test with fixed steering wheel.*

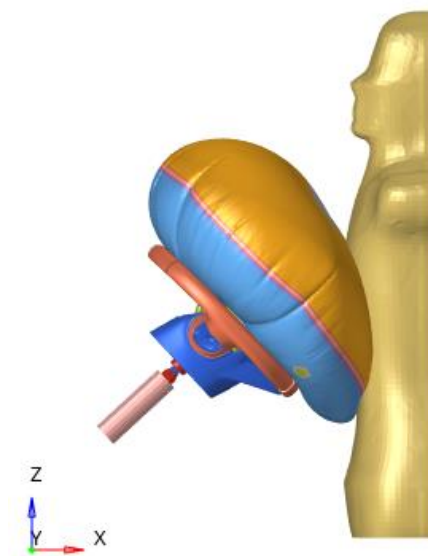


*Figure 5: finite element model of a body block test.*

All the details of the analysis presented before are discussed in the following starting from the driver airbag (DAB) working principles that have been discussed in the chapter two. The third chapter is about some specific functions of the software used to work with finite element analysis: the Hyperworks suite from Altair. Chapter four focuses on the experimental tests characteristics done at the STELLANTIS Safety Center. In chapter five and six the attention is focused respectively on the linear impactor and on the body block tests, comparing experimental and computer simulation results to improve the model. The last chapter is about the airbag folding and how it can be done with the new tool implemented in HyperWorks since the 2021.2 version.

## 2. Commercial vehicles safety

### 2.1 Commercial Vehicles

Since there are many authorities legislating over different countries (Europe, USA, China, etc.) about each single vehicle market, it is important to have safety standards to be observed by all the manufacturers. For what concerns Europe, it is the European Commission that establishes the rules for safety and environmental protection and the conditions under which a vehicle can be put in the EU market. In order to have, all around the world, the same conditions to enter a certain market, during the last years it has been improved a technical harmonization carried on by the UNECE (United Nations Economic Commission for Europe), that has constant contacts whit authorities in other countries to seek solutions to regulatory issues.

Vehicles classification is an important step of the approval system as for European market as for worldwide market.

There are four main categories:

- M: vehicles carrying passengers;
- N: vehicles carrying goods;
- L: two and three wheels vehicles;
- T: agricultural vehicles.

Categories M and N can have both light-duty vehicles, such as cars or vans, and heavy-duty vehicles, such as coaches, buses and trucks <sup>[1]</sup>.

The Iveco Daily, whom airbag is the object of the study of this thesis, is present on the market in various versions (*figure 6*), like bus or van, so it belongs to category M or N vehicle, depending on his configuration.



*Figure 6: Iveco Daily in two different versions, van on the left and truck on the right*



## 2.2 Restraint systems in commercial vehicles

For every type of vehicle there are active safety and passive safety approaches:

- Active safety is about what can be done to avoid an accident. This includes all the systems that help the driver to control the vehicle, like traction control system, ABS or AEB;
- Passive safety is about what can be done to minimize the damages for the driver and the occupants once that the accident has happened. In this scenario airbags and seat belts have a fundamental role (*figure 7*).



*Figure 7: airbag deployment after a crash test*

Due to their mass and their size, very often, in accidents between vans and cars or other smaller vehicles, the former are subjected to minor damage. Also, safety systems of commercial vehicles are less developed than those of the cars, this because of:

- Safety rules that are less stringent for the commercial vehicles than for other categories;
- Safety systems that usually don't benefit from the researches done in the last years, because all the new technologies developed by manufacturer are applied mostly to the cars.

On the other side, the number of vans or trucks on the road is increasing constantly, so there is the necessity to grant a certain safety level also to the occupants of this vehicles.

A study from Euro NCAP <sup>[2]</sup> says that of nineteen vans commonly present on the roads, only six of them have two frontal airbags and no one of them has at least one side airbag. Many times it happens that the protection and the safety of the vans passengers are not considered equivalent to that of a car passenger. In this sample of nineteen vans, sometimes seat belt reminders for passengers or airbag

and seat belt load limiters are missing. Also, there are other systems equipped nowadays in almost all the cars on the market that are absent in vans and other commercial vehicles. So, because of the necessity to update the rules about safety standards, it has been approved that, from 2022 on, all vans must have cameras and sensors to help the driver during the reverse gear, a black box that stores all the data of the vehicle in case of accident, a system that awake the driver if he fell asleep or call for his attention if it is not on the road, aided braking system in case of emergency breaking and better seat belts designed on the base of the crash tests done. Furthermore, it has been approved that all N1 category vehicles (vans and trucks for goods carriage up to 3,5 tons) must respect the following norms:

- UNECER137, about frontal impact;
- UNECER95, about side impact;
- UNECER153, about rear impact.

In order to reduce this gap in the safety of different type of vehicles and be ready for the forthcoming regulations, it is important, for all the manufacturers, to study all safety systems and subsystems. Obviously, it is fundamental that the results of this analysis are truthful and useful, so, instead of doing numerous experimental tests, the finite element analysis can be used to model this safety systems and, thanks to the computer simulation, reduce the costs both in terms of time and money.

It's with this aim that this thesis work has been done: to characterize a model of an airbag and use it in the study of a subsystem, the body block test simulating the impact of the driver into the steering wheel in case of accident.

FEM analysis permits to do the initial and the biggest part of the tests, that should be done to validate a vehicle (that must have certain safety standards), by computer simulation, and then to do only a few experimental tests to confirm the results obtained from it.

## 2.3 Airbag

The airbag is a restraint system with the aim of reducing injuries for the driver or the other occupants of the vehicle in case of accident. In a vehicle there are many airbags, the main one is the driver airbag, located into the steering wheel. It inflates in about a tenth of a second after an accident has occurred and avoid the driver to crash into the steering wheel that is rigid. There is also the passenger airbag, located on the dashboard, to prevent damages for the front occupant of the vehicle. Side airbags and central airbags are located, respectively, on the side of the seats and between them and by now at least all the cars are equipped with them, they have a fundamental role during side collisions or in case of overturning. And more, there are also headbags on the upper side of the body, to prevent damages on the head occupant. For what concerns commercial vehicles it is not obvious that there are all the same airbags like on the cars. For sure they are equipped with driver and passenger airbags, side airbags are being introduced in the last years.

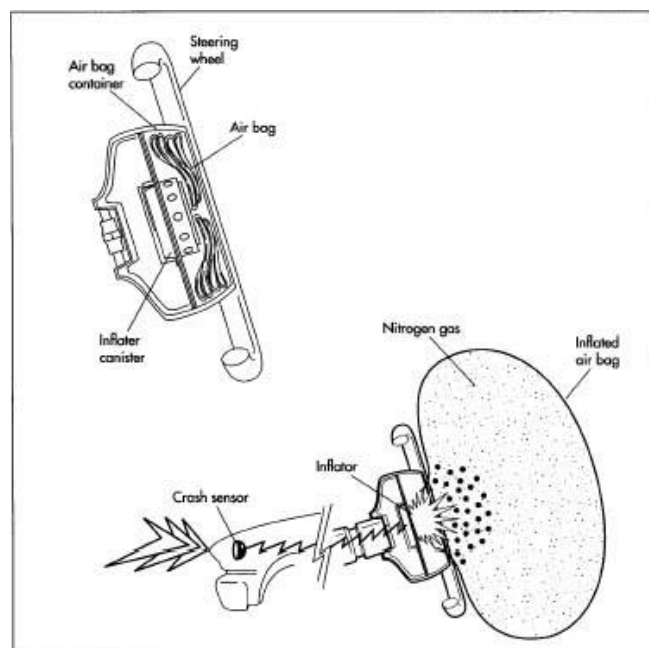


Figure 8: general scheme of an airbag

In general, an airbag consists of a cushion, made by fabric material, an inflator module and various sensors. When the vehicle crashes the sensors record data about the accident and send them to the airbag electronic controller unit (ECU) and the calibrated algorithm of the ECU determines if the airbag must be deployed or not. Real world accidents are not like crash tests where there is always a frontal impact, so the sensor that gives the signal whether or not to deploy the airbag can't make its

decision on the velocity of the vehicle. So the sensor is a microelectromechanical accelerometer, the mechanical part is a microscopic element that moves following a rapid deceleration and cause a change in the capacitance of the circuit; this gives the signal to fire the inflator. The inflator module has a thin wire and a chamber where is located a solid propellant, generally sodium azide. The signal of the ECU determines the wire to heat up, like in a light bulb, and this starts the pyrotechnic chain: the propellant undergoes to a chemical reaction that produces azote and inflate the bag. During the deployment of the cushion the nitrogen undergoes a process that reduces the temperature and remove all the combustion residues and ash.

This decision process by the ECU and the consequent inflation of the bag must be very quick. The algorithm that analyses the data from the sensors has to run in about 15 to 30 milliseconds and the bag is inflated in about 30-40 milliseconds after the first moment of the crash contact. If the bag inflates slower than this time, the risk for the occupant is to hit the bag during his inflation with the consequence of major injuries for the driver.

For the front passenger the distance between him and the dashboard is greater so the passenger airbag must be bigger and requires more gas; in fact, while for the DAB is necessary about 40 g of sodium azide, for the passenger airbag they become 250 g.

## 2.4 Iveco Daily airbag

In the following the main components of an airbag will be presented focusing on the Iveco Daily driver airbag.

In *figure 9* it is represented a section of the airbag module showing the housing of the bag while in *figure 10* there is a complete airbag like it is mounted on the steering wheel.

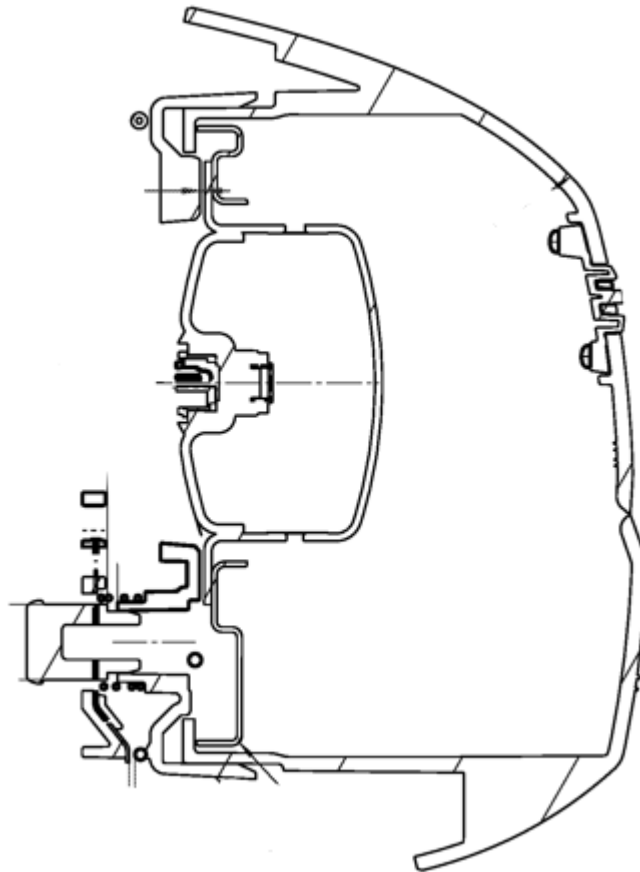


*Figure 9: section view of an Iveco Daily airbag*

The *figure 11* shows the housing after the bag inflation, to give a proper view of the real aspect of this part the bag has been cut.

While in *figure 12* there is a back view of an airbag module so it is possible to identify the vent hole on the back of the bag, and, on the upper part of the module, the open cover. How the cover opens to let the bag out and how this part is made are very important for the right deployment of the bag, particularly for the passenger airbag that is located into the dashboard; in this case also the surface roughness of the dashboard can determine the correct functioning of the airbag.

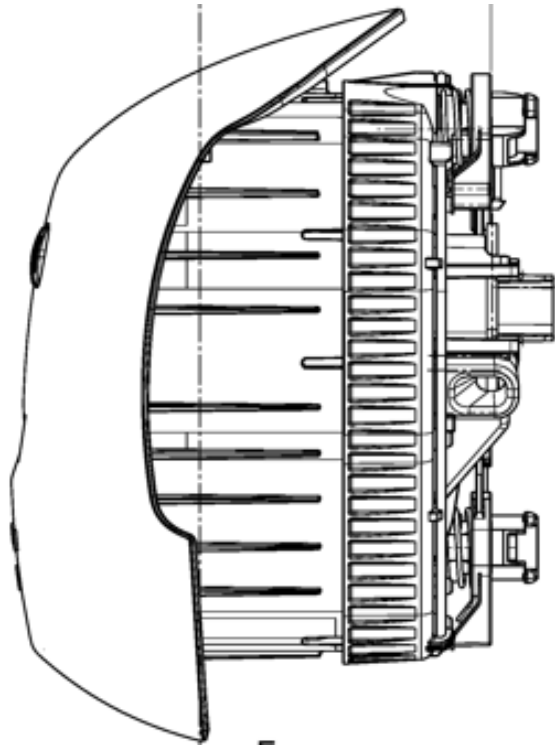


*Figure 10: airbag module of an Iveco Daily*



*Figure 11: a bag housing after its deployment*



Figure 12: deployed airbag

Another particular to focus on is the design of the tear lines and how the cover really opens to allow the bag to inflate. This can be seen in *figure 11* and *13*. As designed, the upper part of the cover, the one with the Iveco line, is cut from the lower part exactly in the way it is shown in *figure 11*.

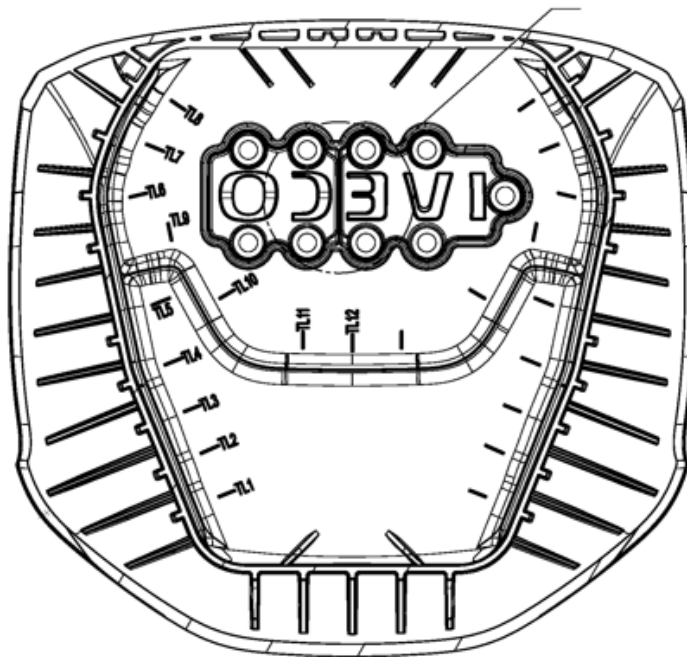
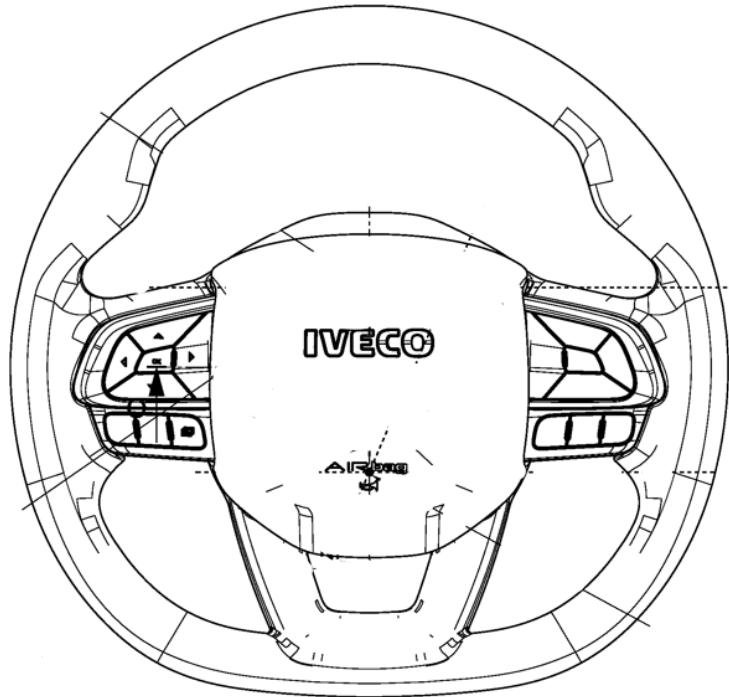


Figure 13: airbag tear lines



## 2.5 Iveco Daily steering wheel



*Figure 14: Iveco Daily steering wheel, front view*

Made by elastomeric materials, with a magnesium core, the Iveco Daily steering wheel is represented in the figure above with the airbag module mounted in its site.

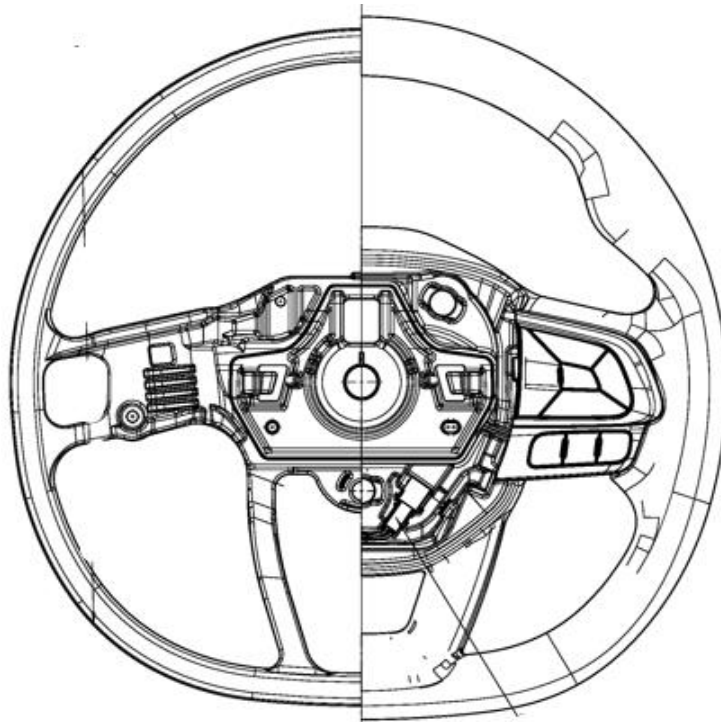


*Figure 15: Iveco Daily steering wheel partial section*



In *figure 15* it is possible to see how the steering wheel is made, with the inner part (in the figure the one on the left cut with a section) that is the structural one, it absorbs the energy during an impact with possible deformations (as will be seen in the body block test). While the outer part is a cover of elastomeric material.

In *figure 16* however is showed a trigonometric view of the steering wheel and it is possible to identify the site of the airbag on the centre where there is also the linking interface between the steering wheel and the steering column.

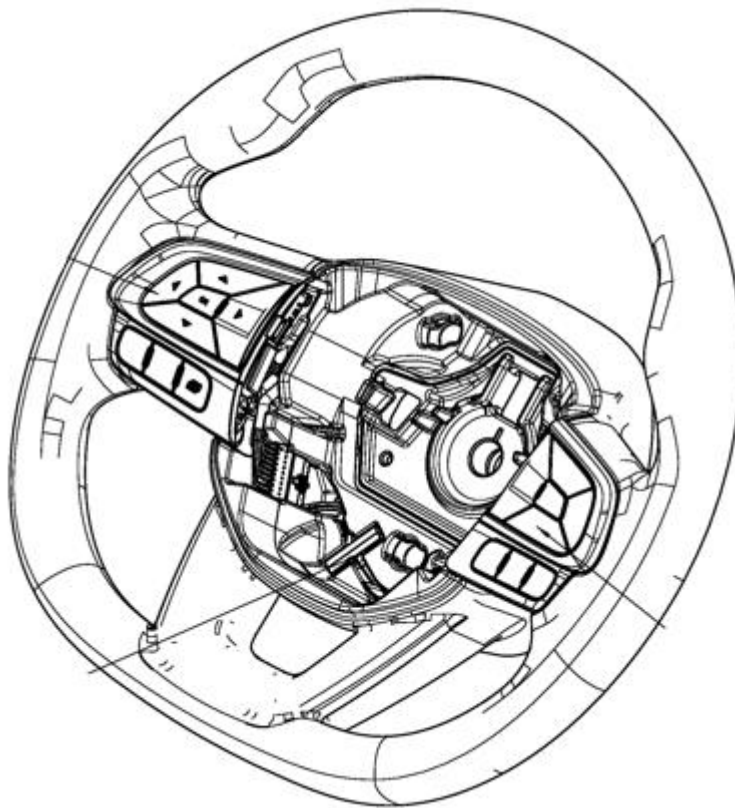


*Figure 16: trigonometric view of the steering wheel*

### 3. Used methods

#### 3.1 Hyperworks software

In this thesis work it has been used the Hyperworks Suite by Altair Engineering for CAE model pre and post-processor and Radioss as solver. The Fem of the various components have been realized with Hypermesh, while the characterization of the submodels has been done with Hypercrash that is dedicated to the study of impacts and bag modelling and is also the preprocessor dedicated to Radioss. Hyperview and Hypergraph have been used to read the outputs of the simulations and done the post-processing of the results.

#### 3.2 Airbag modelling with Hyperworks <sup>[3]</sup>

As mentioned, for the characterization of the airbag it has been used Radioss and its pre-processor HyperCrash, in fact this dedicated software has some specific functions to model the airbag and its behaviour, like *Monitored Volume* with the definition of *Vent Holes* and *Porous Fabric Surfaces*.

MONVOL x	
AIRBAG1	
ID	1000001
Title	AIRBAGD00_volume_1
[surf_IDex] External surface*	[1000052] MONVOL_group_6000005_of_PART
▸ [surf_IDex] External surface (Advanced selector)	
[Hconv] Heat transfer coefficient	0
[AscaleT] X-Scale factor for time based function	1
[AscaleP] X-Scale factor for pressure based function	1
[AscaleS] X-Scale factor for area based function	1
[AscaleA] X-Scale factor for angle based function	1
[AscaleD] X-Scale factor for distance based function	1
[mat_ID] Material ID*	[1001001] AIR, g, mm, ms
[Mu] Volumetric viscosity	.001
[Pext] External pressure	0
[T0] Init. temperature	0
[lequi] Flag for initial thermodynamic equilibrium	1: Mass is of gas is determined wrt volume at b
[lttf] Flag for venting time shift	3: Venting start time is shifted by Tinj +Tstart
▸ Injectors	
▸ Vent holes	
▸ Porous Fabric Surfaces	

Figure 17: monitored volume parameters.

In the *figure 17* is shown the menu for the definition of the monitored volume. This function can be used to model airbags, tanks or other component of closed volume. For what concerns airbags, they can be modelled in three ways:

- Uniform pressure airbag, */MONVOL/AIRBAG1*;
- Uniform pressure airbag whit communicating chamber, */MONVOL/COMMUI*;
- Non uniform pressure airbag with finite volume method, */MONVOL/FVMBAG1*.

In this analysis it has been used a uniform pressure airbag, as can be seen also from the name of the card in the figure. The card also requires other parameters, among which the most important are:

- the closed surface that represents the bag (*External surface*),
- the *Material\_ID*, i.e. the identification number of the card material representing the air inside the bag;
- *Iequil*, that is a flag to define the initial thermodynamic equilibrium;
- *Ittf*, another flag to define the time at which venting and porosity start acting, requires the definition of at least one injection sensor.

As can be seen, in the card can be specified also the *Injectors*, the *Vent Holes* and the *Porous Fabric Surfaces*, that will be discussed in the following.

MONVOL x	
AIRBAG1	
[surf_IDv] Vent hole membrane	[1000051] group_6000005_of_PART
[Avent] Surface for vent hole or scale fact	0
[Bvent] Scale factor on impacted surface	0
[Iform] Formulation flag	1: Isenthalpic (default)
[Tstart] Start time for venting	0
[Tstop] Stop time for venting	0
[dPdef] Pressure diff. to open vent hole me	0
[dtPdef] Min. duration press. exceeds Pdef	0
[ldtPdef] Flag : time for delay	0: Pressure should be over dPdef during a
[vent_title] Vent hole title	Venthole
[fct_IDt] Venting vs time	None
[fct_IDP] Venting vs press.	[1000007] New FUNCT 6000007
[fct_IDA] Venting vs area	None
[Fscalet] Scale factor for venting vs time	0
[FscaleP] Scale factor for venting vs press	0
[FscaleA] Scale factor for venting vs area	0
[fct_IDt] Venting vs time when contact	None
[fct_IDP] Venting vs press. when contact	None
[fct_IDA] Venting vs area when contact	None
[Fscalet] Scale factor for venting vs time w	0
[FscaleP] Scale factor for venting vs press	0
[FscaleA] Scale factor for venting vs area	0
[fct_IDv] Outflow velocity	None
[Fscalev] Scale factor for outflow velocity	0

► Porous Fabric Surfaces

Figure 18: vent hole data definition.

The *Injector* section requires the definition of one or more injectors, a card that is a property where is defined the mass injected in the volume, and its temperature, each by a function versus time.

The *Vent Holes* require the definition of various parameters (*Figure 18*) but the most important are:

- The *Vent hole membrane*, i.e. the surface of the vent hole;
- The *Iform*, a flag that defines the formulation type of the flow through the vent hole;
- *Tstart*, *Tstop*, *dPdef*, *dtPdef*, *IdtPdef* that are parameters defining three different ways to activate or deactivate the vent hole.

If *Iflag*=2, i.e. it is used the Chemkin formulation for the flow through the vent hole, it must be defined (in *fct\_IDv*) also a function of the outflow velocity versus the difference of pressure between the inside and the outside of the bag.

The *Porous Fabric Surfaces* tool requires more or less the same parameters as for *Vent Holes*, as can be seen in the (*Figure 19*). *Iformps* has the same meaning of *Iform* for *Vent Holes*. When defining a porous surface, it is important, in the model, to divide two porous surface or a porous surface from a non-porous surface whit a line of “neutral” element so to not have problem in the assignation of the nodes to a surface or another.

[surf_IDps] Porous Fabric Surface	None
[Iformps] Porosity formulation	0: Bernoulli (Wang & Nefske) without any c
[Iblockage] Flag to block leakage if contact	<input type="checkbox"/>
[Tstart] Start time for porosity	0
[Tstop] End time for porosity	0
[dPdef] Pressure difference to open vent h	0
[dtPdef] Minimum duration pressure exceed	0
[IdtPdef] Time delay flag when dPdef is rea	<input type="checkbox"/>
[Cps] Scale factor on leakage area	0
[Areaps] Leakage area	0
[fct_IDcps] Function defining Cps versus tir	None
[fct_IDaps] Function defining Areaps versu	None
[Fscalecps] Scale factor for FCT_ID_CPS	0
[Fscaleaps] Scale factor for FCT_ID_AREA	0
[fct_IDv] Outflow velocity function identifier	None
[Fscalev] Scale factor for FCT_IDV	0
[surface_title] Porous Surface title	

Figure 19: porosity data definition.

## 4. Tests description

During this thesis work, there have been done two types of tests to characterize and evaluate the airbag model: the linear impactor test and the body block test. In the following both tests will be presented in detail.

### 4.1. Linear impactor test

The linear impactor test is a test done to characterize an airbag. The work bench has been prepared to have a plate hitting an airbag mounted on a steering wheel rigidly fixed to a support. In the *figure 20* is presented the work bench ready for the test, in this case the plate hitting the airbag is an aluminium plate fixed to a runner; the airbag is in its housing and the steering wheel is fixed to the red support on the right.



*Figure 20: Linear impactor test bench*

There are also two bars, mounted on the upper and lower side of the steering wheel to reduce the deformation of the steering wheel during the impact. The finite element model steering wheel is rigid, so it does not deform during the simulation. Instead, the real steering wheel can deform being made of metallic and elastomeric materials. This deformation dissipates energy during the impact and the dissipated energy can be a cause of different results between simulation and experimental ones.



Another loss of energy in the test execution is represented by the red support that is not perfectly fixed on the ground so it can oscillate a bit during the impact.

The test is conducted in this way: a pneumatic circuit gives the impulse to a piston that hits the yellow runner on the right, by specifications the runner must have a velocity of 7 m/s. Previously, few velocity tests must be conducted to heat the circuit and to have the minimum loss of velocity between the one imposed by the piston and the one of the runner registered by the velocimeter. The airbag is activated through its sensor when the plate reaches the trigger distance, two accelerometers register the plate deceleration during the impact and the result is assumed to be the medium curve of the two.

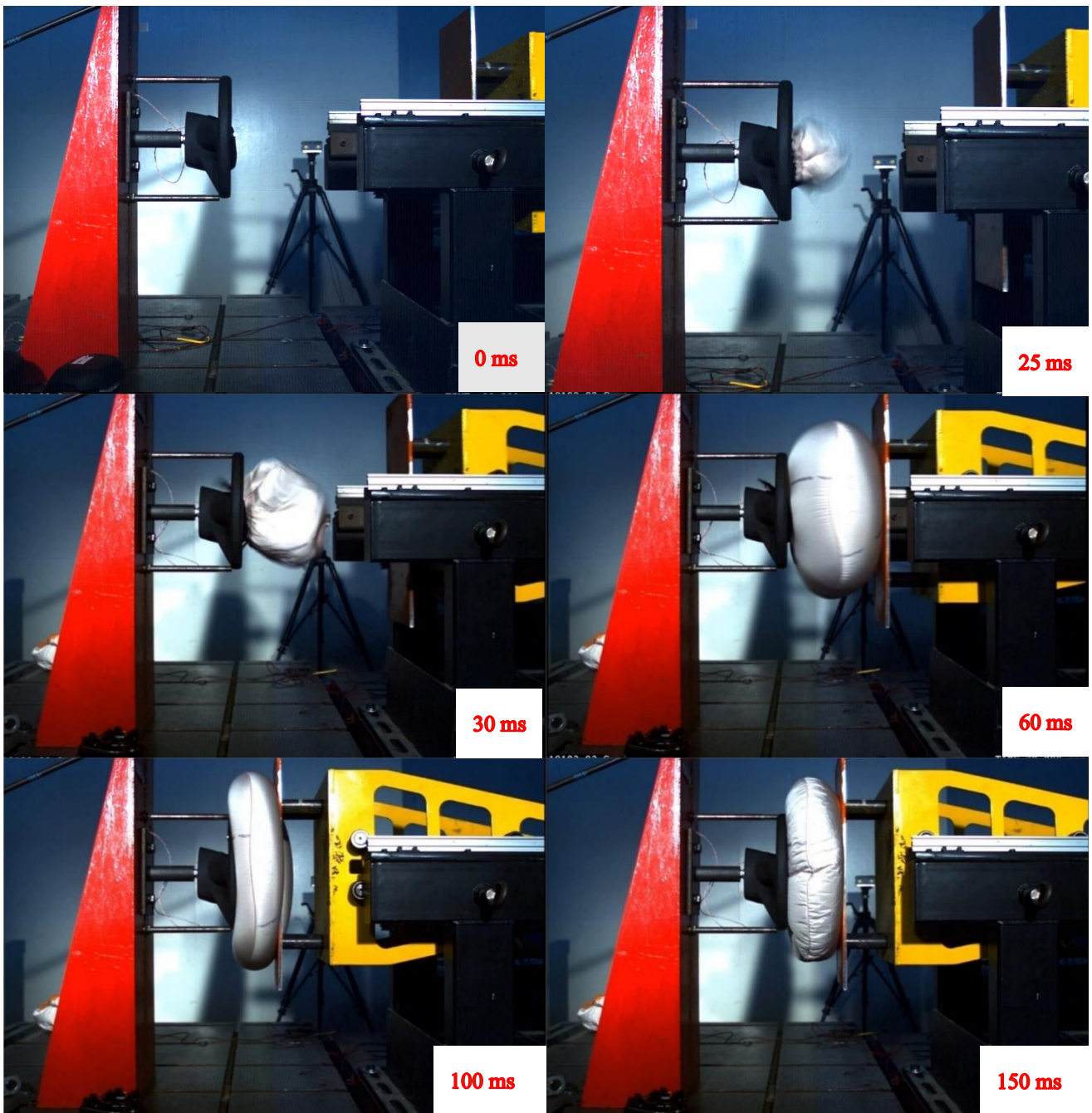


Figure 21: linear impactor test frame sequence.

As can be seen from the *figure 21*, the full test last about 150 ms and the bag is fully inflated after about 40 ms, the penetration of the impactor in the bag reaches its maximum in about 80 ms. Looking carefully at the sequence of the test, it can be seen how the steering wheel is deformed and the red support oscillate after the impactor hits the bag, giving the energy loss explained before.

The linear impactor test has been conducted with the steering wheel at 0 degrees (*figure 22*), meaning it was in the same position it has when the car is going straight. It has been repeated two times to have a better confidence in the results.



*Figure 22: Steering wheel at 0 degrees.*

Being the airbag supplied by ZF Friedrichshafen, they have done the same test to validate the airbag before putting it on the market, repeating it three times. Their test has a better confidence because the structure on which is fixed the steering wheel is more rigid, the steering wheel itself is also made stiffer with four bars instead of two like in the test done at STELLANTIS Safety Center.

## 4.2. Body Block test

The body block test is an experimental one to simulate the impact of the driver on the steering wheel with inflated airbag, when a frontal impact happens.

This type of accident is different from the one of cars due to the structure of the van that has the steering wheel in a different position and oriented in a different way with respect to the seat. The steering column is more vertical with respect to the floor of the vehicle in a van than in a car, also the driver seat is higher and so, during a frontal impact, it happens that the dummy of the driver, that is projected forward by inertia, can hit the steering wheel.



*Figure 23: body block test with rigid steering wheel*





Figure 24: body block test with steering wheel mounted on the steering column

The test has been done in two different configurations:

- The first with the steering wheel mounted to a rigid support (*figure 23*);
- The second with the steering wheel mounted on the steering column (*figure 24*).

The first test has also been done with three different orientations of the steering wheel with respect to the steering column axis for six tests overall:

- Two with the steering wheel at 0 degrees, like the linear impactor test (*figure 25*);
- Two with the steering wheel at 90 degrees, like the vehicle is turning left or right (*figure 26*);
- Two with the steering wheel at 180 degrees (*figure 27*).

The body block test with the steering wheel on the columns has been done only with a 0 degrees configuration for two times.



*Figure 25: steering wheel at 0 degrees for body block test*



*Figure 26: steering wheel at 90 degrees for body block test*



Figure 27: steering wheel at 180 degrees for body block test

The test is conducted so that the dummy is initially on a runner, the runner is pushed by a piston and then, after a short run, is immediately stopped so that the dummy continues on its path with a free fly until it hits the airbag that in the meanwhile is inflated activating the sensor when the dummy reaches the trigger distance. For the correct execution of the test, the dummy must have an initial velocity at least equal to 24,1 km/h (about 6,7 m/s). Like for the linear impactor test, the circuit that activates the piston is pneumatic and must be heated so that the velocity given by the piston is equal to the one of the runner, measured by a velocimeter, and it is more than 24,1 km/h. Therefore, also in this case some velocity tests are necessary. More details about the test procedure can be found in the regulation UNCE R12 [4].

The *figure 28* shows the sequence of frames of a body block test with the steering wheel mounted on the steering column, while the *figure 29* shows the frames of the test conducted with the steering wheel mounted on a rigid support. After 20 ms the bag starts inflating and it is fully inflated after 60 ms. As shown also in the frames, the airbag does not work like it could be on a car, with the dummy hitting it frontally, but the impact occurs on the lower part of the bag, this because of the relative position between the seat and the steering wheel. With this dynamic of the accident, can happen that the occupant hits directly the steering wheel, if the bag does not inflate so fast to cover it completely. An amount of the impact energy is dissipated by the steering wheel that is low or high deformed depending on its orientation.



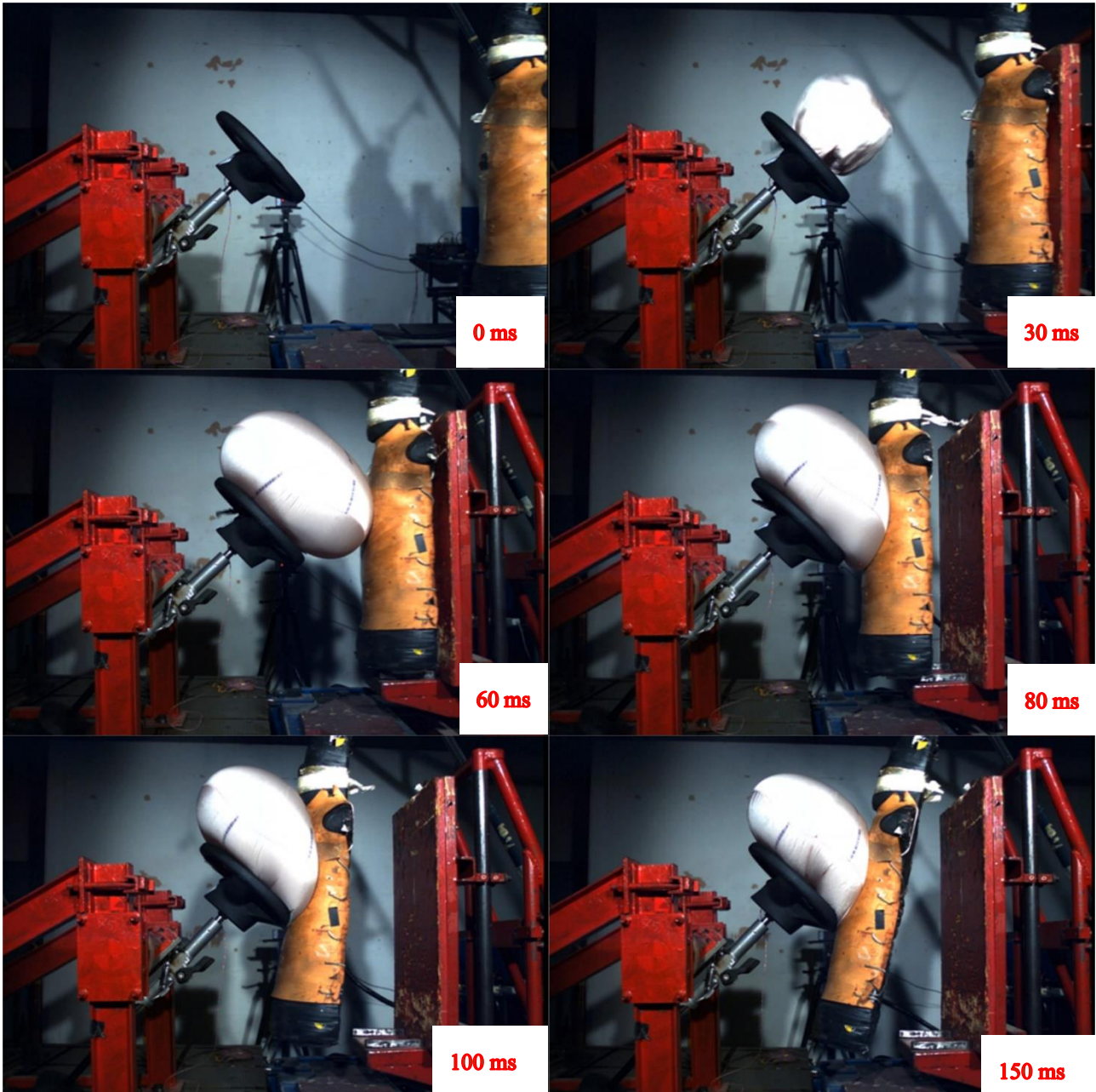


Figure 28: frame sequence of body bock test with steering wheel mounted on a steering column



Figure 29: frame sequence of body block test with steering wheel fixed on a support

The impact between the driver and the steering wheel can happen also if the bag cover completely the steering wheel when the contact starts, this depends also on the orientation of the latter.

With the steering wheel at 90 degrees the bag is more likely stuck between the dummy and the steering wheel (figure 31) with respect to the case of 0 degrees (figure 30). With the steering wheel



at 180 degrees the role of this one in the absorption of the impact energy is more evident being the steering wheel sharply deformed during the contact (*figure 32*).



*Figure 30: detail of the airbag behaviour in the moment of maximum penetration of the dummy; test configurations with the steering wheel at 0 degrees.*

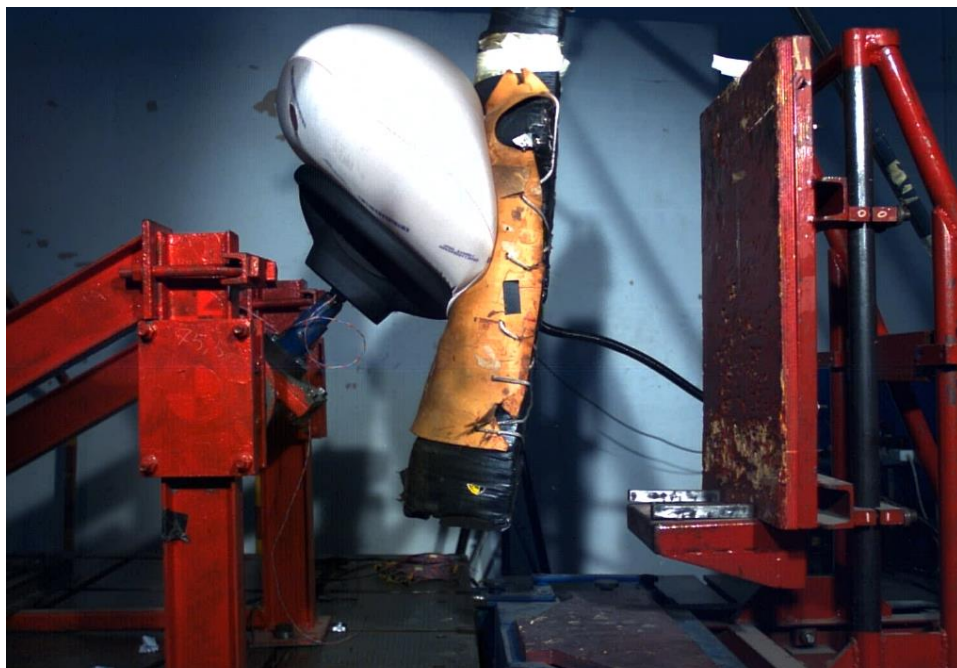


*Figure 31: detail of the airbag behaviour in the moment of maximum penetration of the dummy; test configuration with the steering wheel at 90 degrees.*

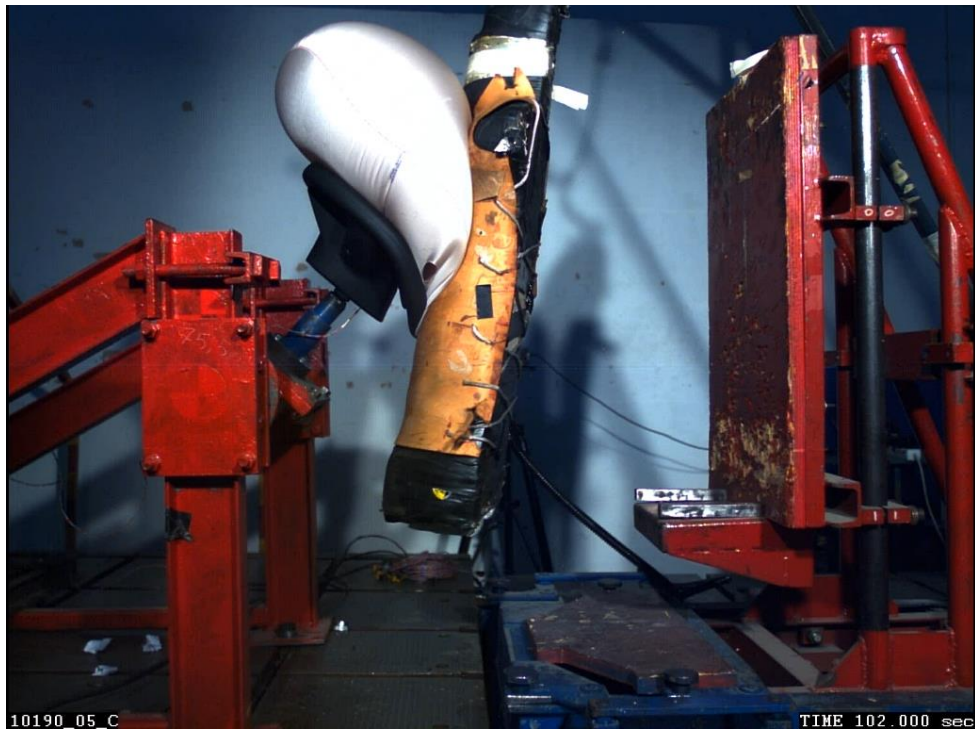


*Figure 32: detail of the airbag behaviour in the moment of maximum penetration of the dummy; test configuration with the steering wheel at 180 degrees.*

In the following, for the comparison between the experimental and the simulation results only the data deriving from the test with the steering wheel fixed on a rigid frame will be used. This choice derives from the video analysis of the two tests conducted with the steering wheel mounted on the steering column. It shows that the steering column was not correctly fixed to the red frame on the left, so the results of this tests cannot be considered valid for a comparison with the simulation ones.

## 5. Linear impactor

### 5.1. Model description

In *figure 33* there is an image of the linear impactor model. It is possible to identify the various components: the steering wheel, in pink on the left, the bag, in blue, and the impactor, in red on the right. In this case the impactor has two wings, even if the one of the experimental tests does not have them, because this model is done to be correlated with the Madymo one. Another peculiarity is that the bag is not in its housing at the beginning of the simulation but it is already opened, this because the aim of this analysis is not the study of its deployment but only the modelling of its behaviour during its functioning.

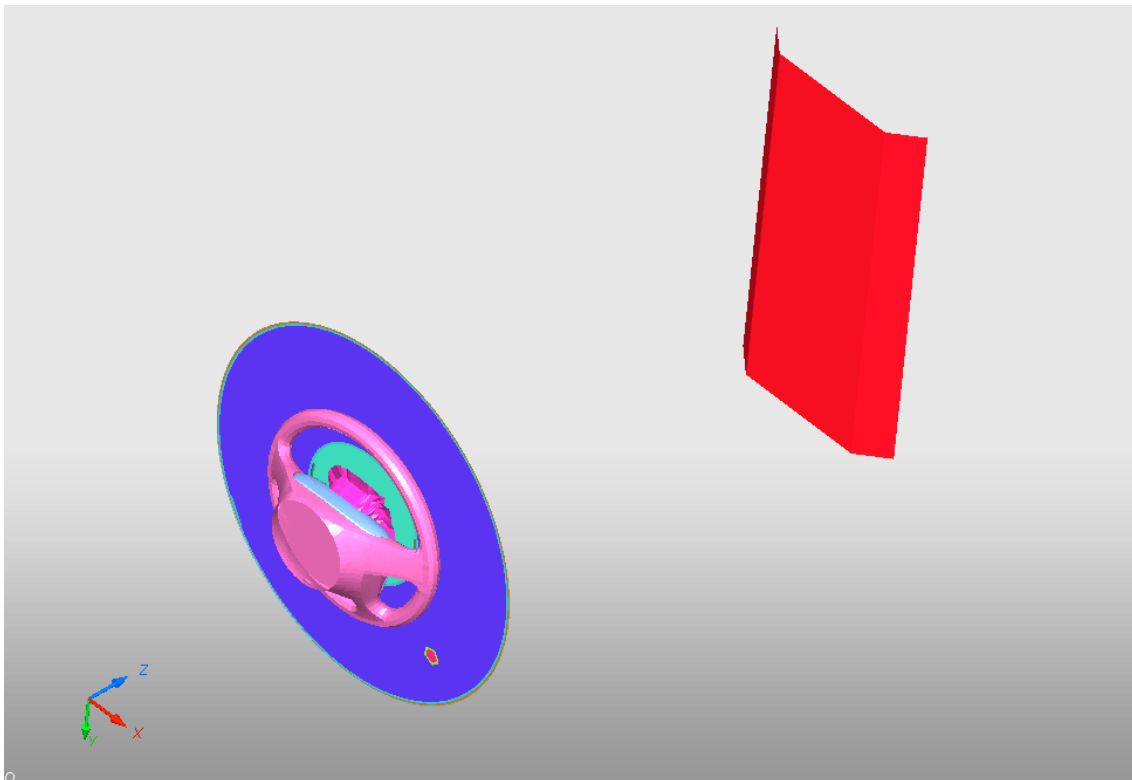


*Figure 33: linear impactor model*

A particular component is the punch (*figure 34*), in purple, between the steering wheel and the bag. This part has a primary role because it gives to the bag the correct shape like it was in its housing before the inflation started. Being the bag completely deployed at the start of the simulation, it is very important that it inflates having the correct shape. Therefore, in the first instants of the simulation the lower part of the bag, the one facing the steering wheel, is thrown inside the punch and only after the bag starts to inflate.



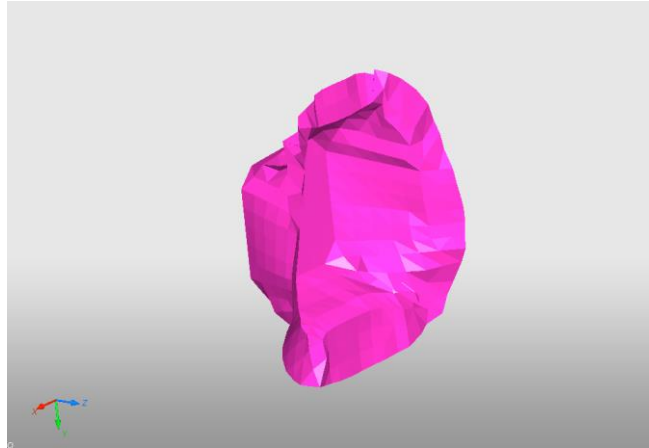


Figure 34: detail of the punch

### 5.1.1. Steering wheel

In this model the steering wheel is defined like a rigid body and it is bonded so it cannot neither translate nor rotate in space. Being a rigid body means that the relative displacement between the nodes of the steering wheel is fixed and cannot change during the entire simulation, basically it is not deformable, so all the energy dissipation occurring during the impact of the impactor on the bag is caused by the deformation and the deflation of the bag.

As can be seen in *figure 35*, the lite blue segments connect all the nodes of the various parts of the steering wheel to a master node where a boundary condition is applied. This boundary condition lock all the six degrees of freedom.

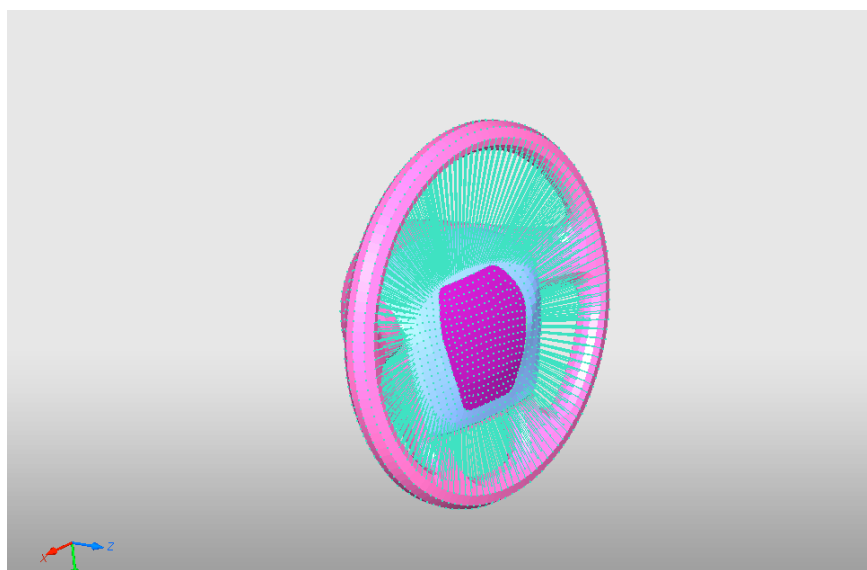
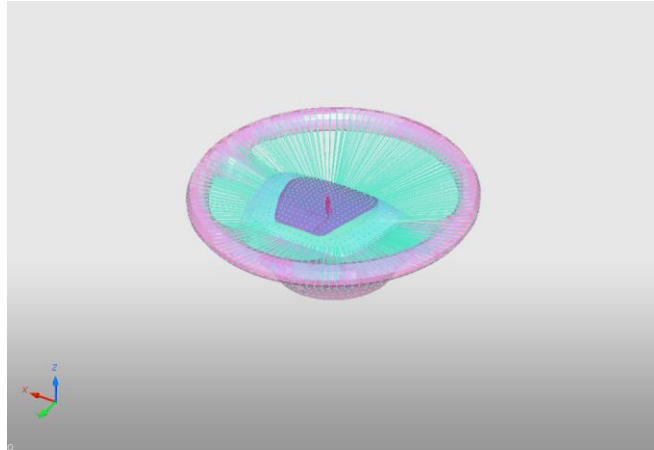
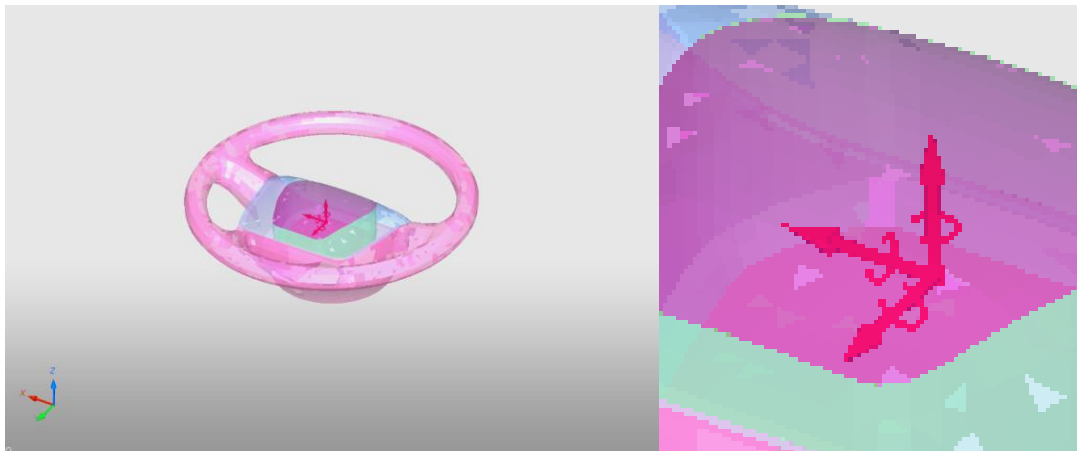


Figure 35: rigid body definition of the steering wheel

In *figure 36 and 37* there are the steering wheel in transparency with the rigid body and the master node that can be identified as the point from which six red arrows start, they represent the boundary condition applied to the rigid body master node, three for the translational dofs and three for the rotational ones, the colour red means that they are all blocked.



*Figure 36: rigid body with boundary condition*



*Figure 37: boundary condition on master node*

### 5.1.2. Bag model

The bag cushion is made of various parts, each one modelled with a fabric material. In the *figure 38* the upper and the lower parts of the cushion can be identified, respectively in yellow (left) and purple (right). To have a correct definition of the porosity of the material there must be a line of elements between a porous surface and another one or between a porous surface and a non-porous one. This is useful to avoid errors in the assignment of the nodes to different surfaces. Being both the upper and the lower surface of the bag porous surfaces, it has been defined this line of element dividing them from the surfaces of the seams.

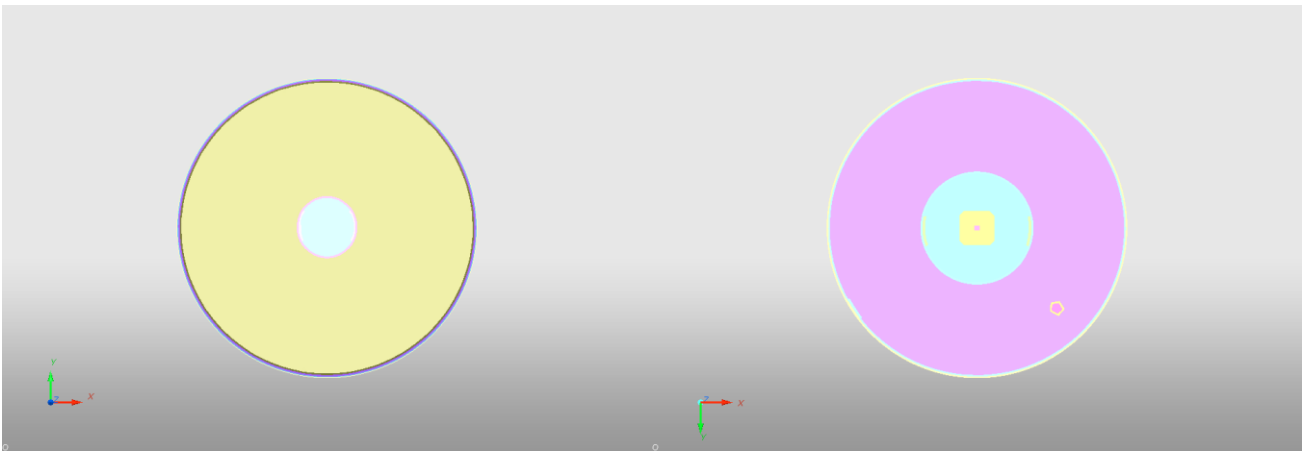


Figure 38: airbag model, upper face (left) and lower face (right)

In *figure 39* there is a zoom on the seams to show the line of element dividing the various porous surfaces, a purple one on the upper side (left) and a light blue one on the lower side (right). In blue (left) and orange (right) there are the seams.

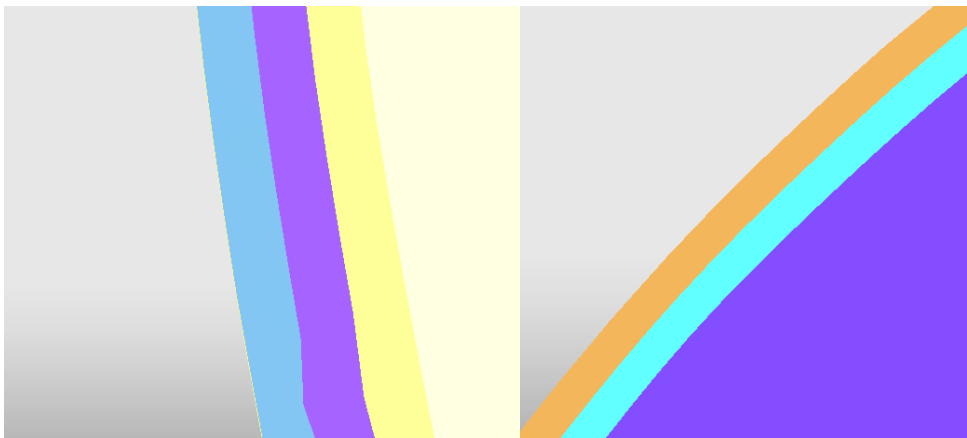


Figure 39: detail of the airbag seams

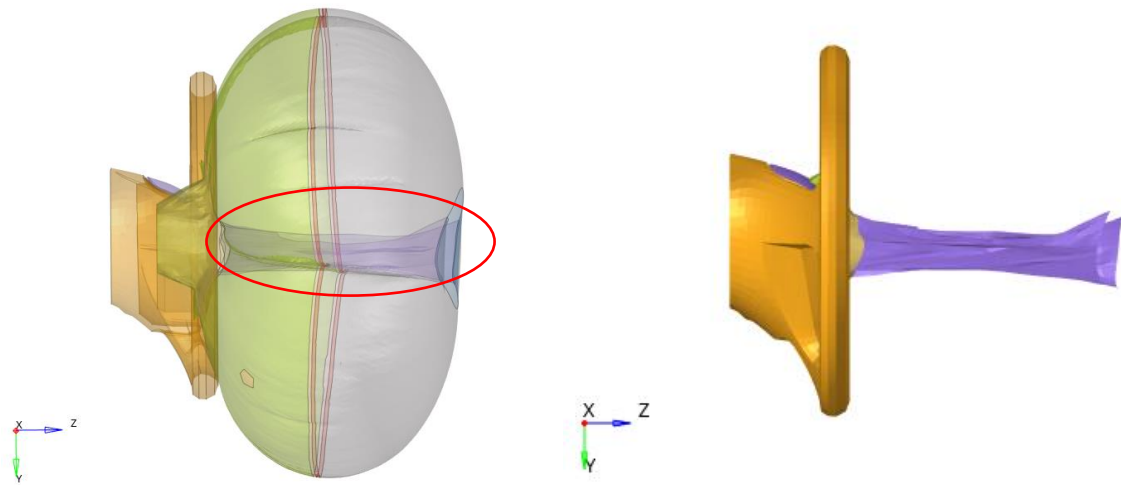


Figure 40: airbag straps

The *figure 40* shows another important element of the bag, the straps, that are the two purple bend in the red ellipse. Their role is very important in the inflating phase because they give to the cushion its particular form and stiffness, without them the bag would have a more spherical shape.

The last component is the vent hole, that can be seen in *figure 38* on the bottom right of the lower face of the bag and in transparency in *figure 40*, and that is reported also in *figure 41*. Even for the vent hole holds the same rule as for the porous surfaces, it must be divided from the other surfaces from a line of element to avoid problems in the nodes assignment.

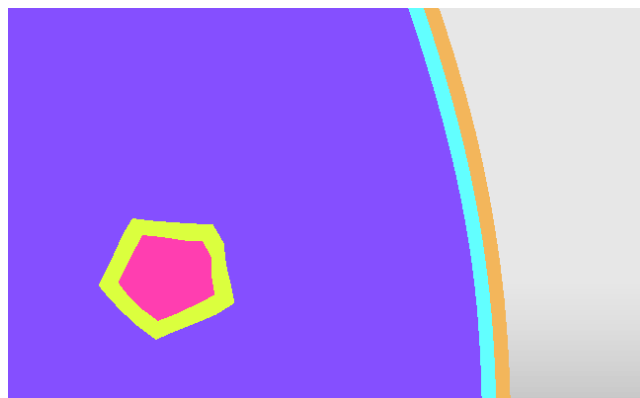


Figure 41: vent hole detail

The vent hole has a very important role in the correct functioning of the airbag because it is basically a hole in the fabric of the cushion but it lets the air out during the impact so that the stiffness of the bag is modified based on the force of the contact between the bag and the body hitting it during an accident. Without the vent hole the bag would work almost like a rigid wall and there would be more

dangerous consequences for the vehicle occupants, in this specific case for the driver being the study on the driver airbag.

### 5.1.3. Impactor

The impactor is a rigid plate made of steel of 250 x 700 mm with a thickness of 10 mm and two wings of 68 mm for a total weight of 36 kg. During the analysis it has two different configurations, one for the comparison with the Madymo model (*figure 42*) and the other for the one with the experimental test. The impactor for the experimental test is the same without the wings (*figure 43*).

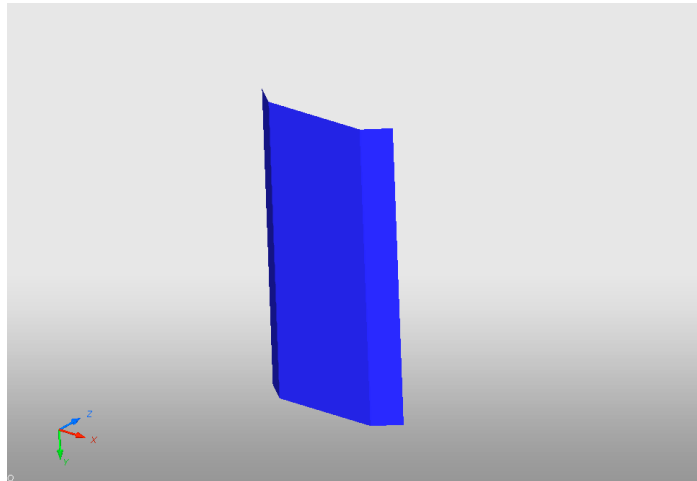


*Figure 42: impactor for Madymo comparison*

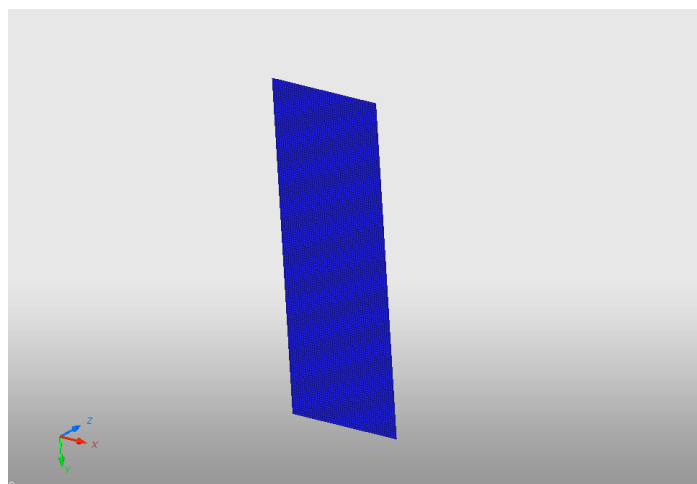


*Figure 43: impactor for experimental test comparison*

## 5.2. Airbag model parameters

Starting from the model provided by Iveco the first step is the characterization of the airbag comparing the results of the finite element model with the Madymo ones. This is done in three phases, so it is possible to divide the effects of the porosity by the one of the venthole on the global behaviour of the bag. Let's see then how all the characteristics of the airbag have been modelled.

### 5.2.1. Airbag volume and inflation definition

The airbag is defined through the /MONVOL card in Radioss, this is a card that permits to define the behaviour of a closed volume identified by one or more surfaces. In this work it has been used HyperMesh to create the FEM of the bag, specifically it is necessary that the surfaces defining the controlled volume are made by shell elements with three or four nodes (as can be seen in *figures 44 and 45*). So, once the FEM has been created, in HyperCrash it is possible to define the monitored volume card choosing from various types of them depending on which criteria it must be used to calculate the properties of that volume. In this case it is an /AIRBAG1 card, meaning that the volume defined by the upper and lower face and the seams seen in the previous section is a uniform pressure volume. This means that follows the ideal gas law

$$pV = mRT$$

where:

- $p$  is the uniform pressure inside the bag;
- $V$  is the airbag volume;
- $m$  is the mass of the gas inside the bag;
- $R$  is the gas constant;
- $T$  is the uniform temperature inside the bag.

In the /MONVOL card the external pressure has been putted equals to zero, so it is working with relative pressures only.

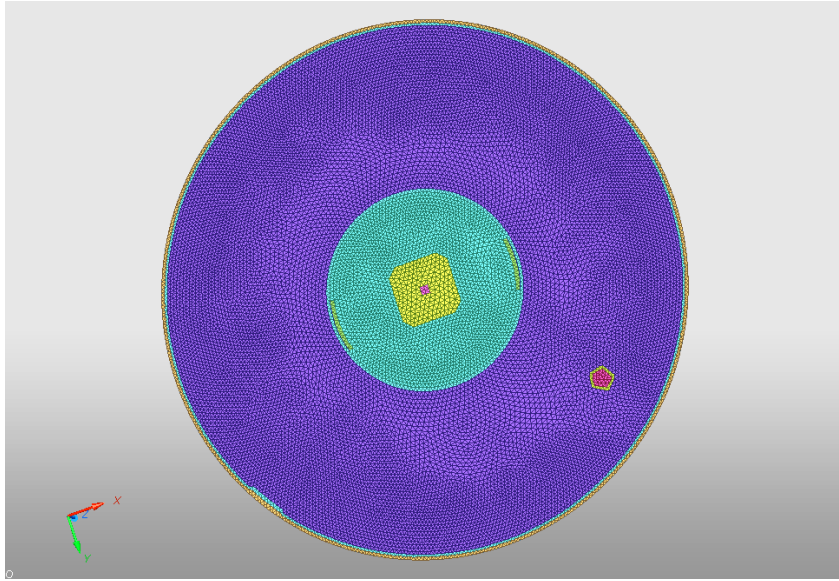


Figure 44: surfaces of the airbag monitored volume

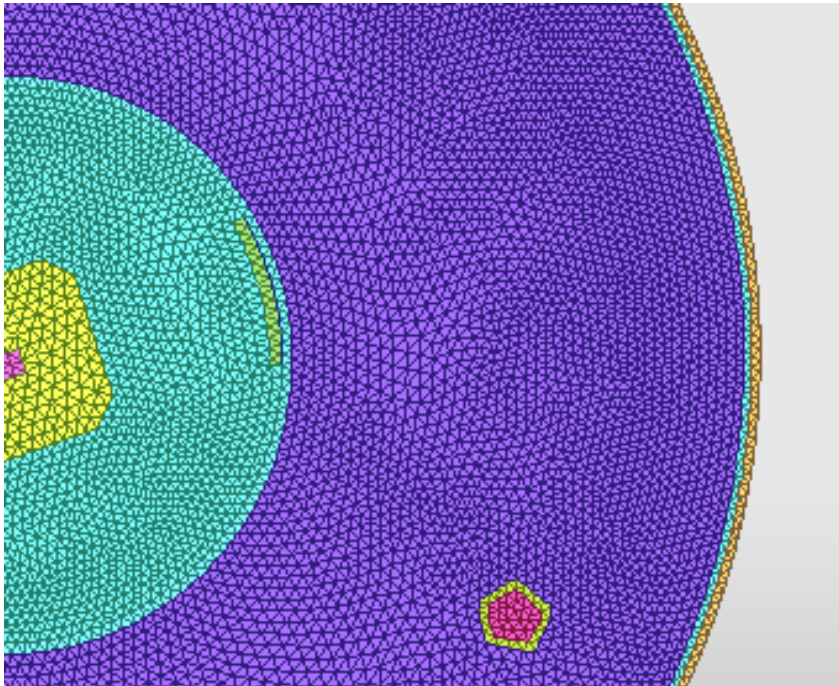


Figure 45: detail of the surfaces shell elements with 3 or 4 nodes.

Once the volume has been defined, it must be selected the material of the gas inside it. In this case it is air which properties were previously defined in a proper material card of type /GAS/MOLE. This card permits to define a gas by its molecular weight and the coefficients of the  $c_p(T)$  function.

The injector requires a property specifying the function of the mass flowing inside the volume and its temperature in time. These functions are derived from the Madymo model and they are presented in the *figure 46* and *figure 47*.

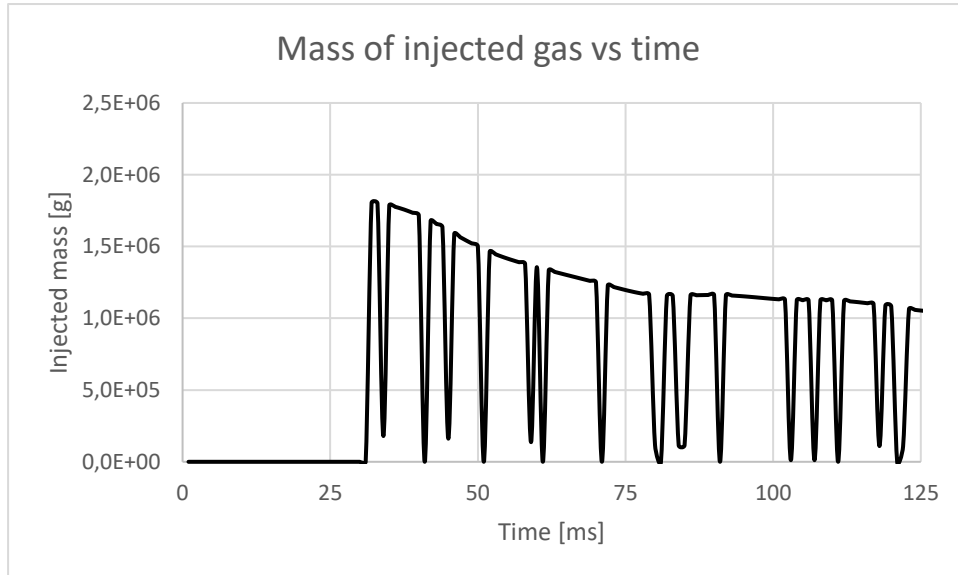


Figure 46: mass of injected gas function in time

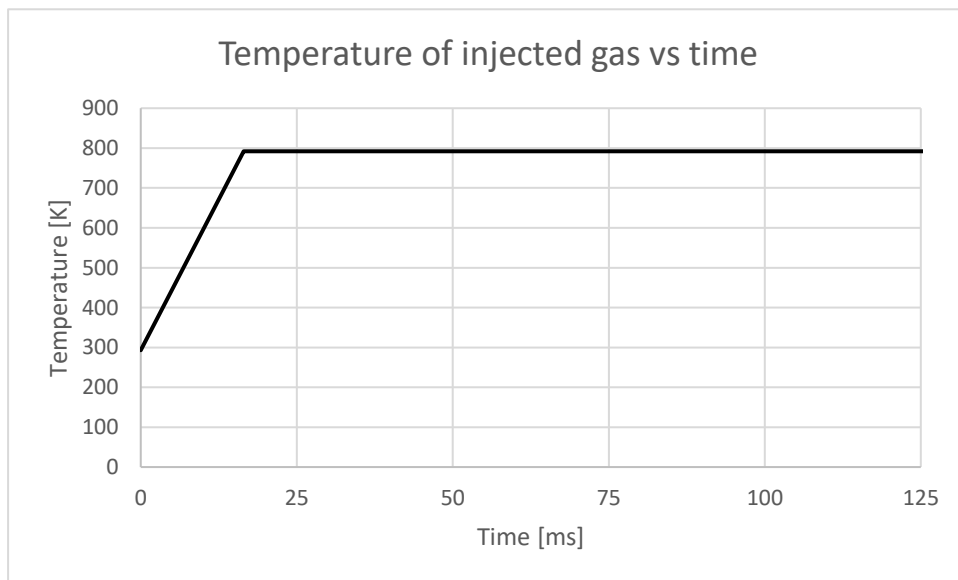
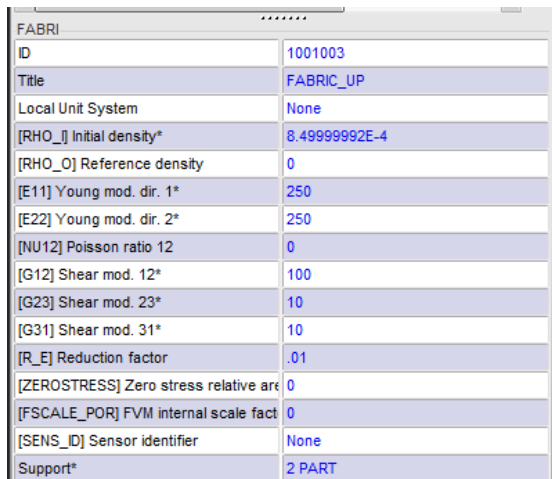


Figure 47: temperature of injected gas function vs time



### 5.2.2. Material properties

In the beginning the aim of the analysis is to identify the material properties to assign to the bag material of the parts described in the previous paragraph. All the airbag cushion parts are made by fabric so in Radioss their materials are all fabric cards in which it has to been defined the Young modulus (E), the shear modulus (G) and the Poisson ratio (Nu), as well as the material density.



FABRI	
ID	1001003
Title	FABRIC_UP
Local Unit System	None
[RHO_I] Initial density*	8.49999992E-4
[RHO_O] Reference density	0
[E11] Young mod. dir. 1*	250
[E22] Young mod. dir. 2*	250
[NU12] Poisson ratio 12	0
[G12] Shear mod. 12*	100
[G23] Shear mod. 23*	10
[G31] Shear mod. 31*	10
[R_E] Reduction factor	.01
[ZEROSTRESS] Zero stress relative area	0
[FSCALE_POR] FVM internal scale factor	0
[SENS_ID] Sensor identifier	None
Support*	2 PART

In *figure 48* there is an example of a material card, in this case it is the one of the upper part of the bag.

Except that for the density, that is the same for all the parts of the bag and it's equal to  $8.49 \cdot 10^{-4} \text{ g/mm}^3$ , the Young modulus and the shear modulus are different for the straps with respect to those of the other parts.

*Figure 48: Radioss material card*

To identify their correct values it has been analysed the inflating phase of the bag only, without the impactor hitting on it, modifying E and G to obtain the same shape of the bag between the finite element model and the Madymo one. In this case the material has been considered isotropic so that E11 and E22, representing the Young modulus in two normal directions are the same. E and G were modified in order to have about the same shape of the finite element and Madymo airbags at the end of the inflation.

In the *figure 49* and *50* is shown the comparison between the two airbags fully inflated with the finite element airbag in transparency. They do not have exactly the same shape, the finite element one is more circular from a bottom view and this is probably due to the fact that the cushion material is not really isotropic. Despite this little difference, as can be seen from a lateral view, the width of the bag is the same in both cases and this means that the straps in the finite element model well fit the Madymo behaviour of the same part.

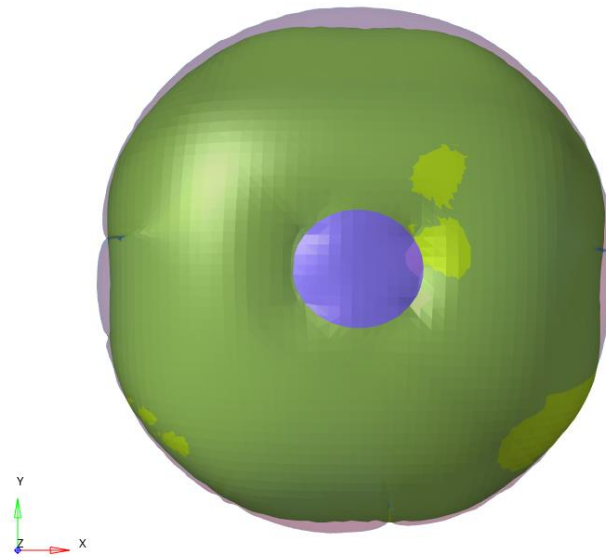


Figure 49: upper view of the comparison between Madymo and finite element airbag

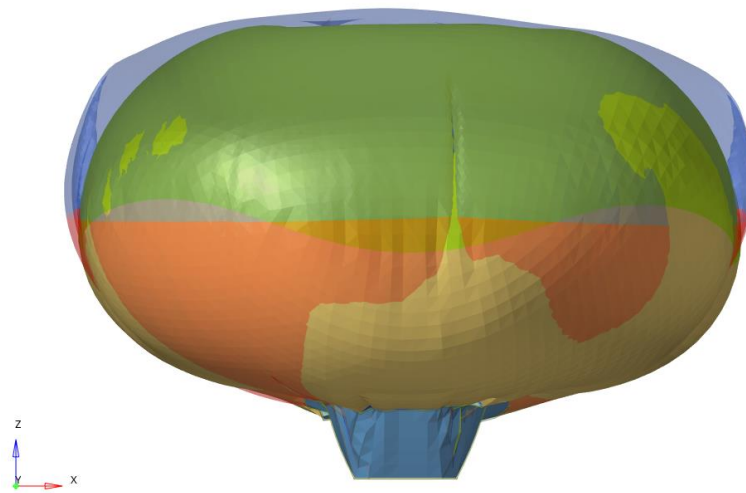


Figure 50: side view of the comparison between Madymo and finite element airbag

Following this method, the properties of the bag components have been identified.

	Fabric up	Fabric down	Straps
<b>E11</b>	250 MPa	250 MPa	15 MPa
<b>E22</b>	250 MPa	250 MPa	15 MPa
<b>G11</b>	100 MPa	100 MPa	100MPa

Table 1: material properties of the bag

With “Fabric up” are identified all the components of the upper part of the cushion and with “Fabric down” all the components of the lower part.

### 5.2.3. Porosity definition

Being of fabric material, the airbag is affected by loss of gas through the material. This effect must be taken into account and it must be formulated in the model identifying what is the mass loss due to material porosity. The porosity can be modelled in the monitored volume card, selecting the surfaces affected by this phenomenon and defining a function of the outflow velocity versus the pressure difference between the interior and the exterior of the bag. In *figure 51* are shown the two porous surfaces (in green), the upper and lower part of the cushion.

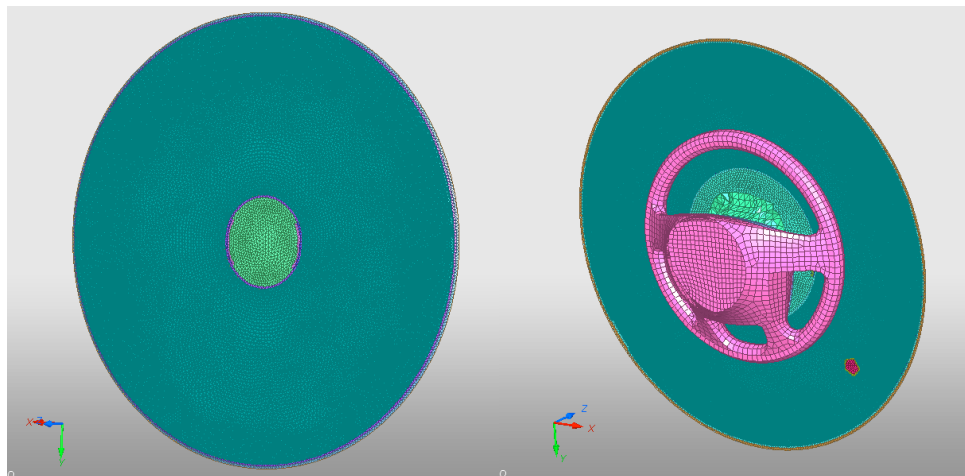


Figure 51: porous surfaces of the cushion

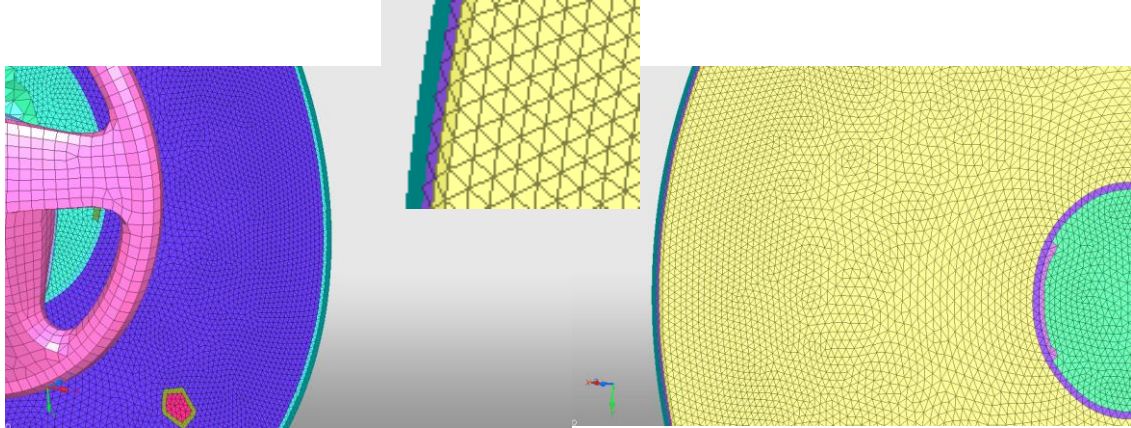


Figure 52: surfaces for seams porosity

There is a loss of gas mass through the seams also, showed in *figure 52*, and these two effects are different but both from the data of the Madymo model and of the experimental tests it is not possible to discern one effect from the other. So, in the model characterization it has been assigned a linear function of the outflow velocity to the seams and then only the surfaces porosity outflow function has been modified to tune the behaviour of the finite element model. The two functions are shown in *figure 53* and *figure 54*.

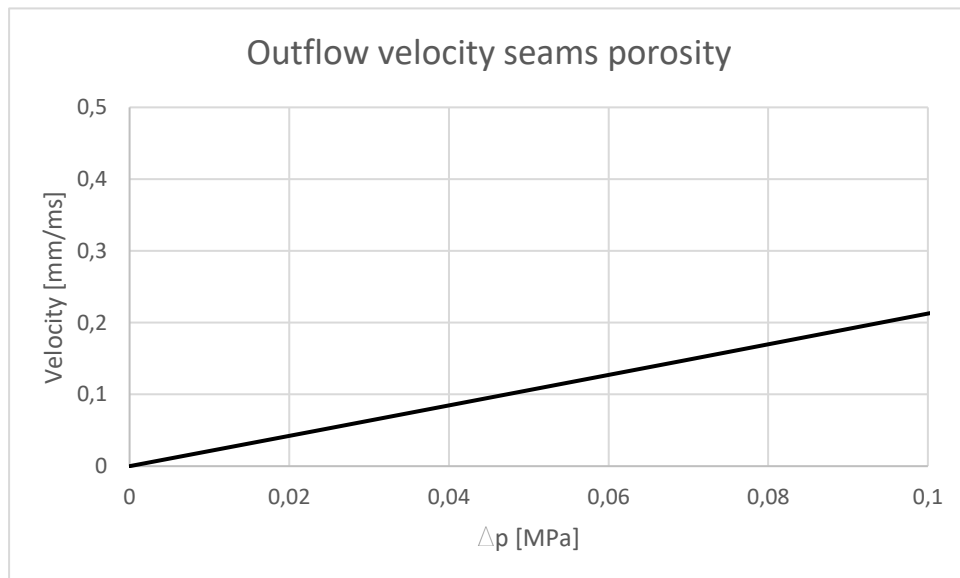


Figure 53: outflow velocity function of seams porosity

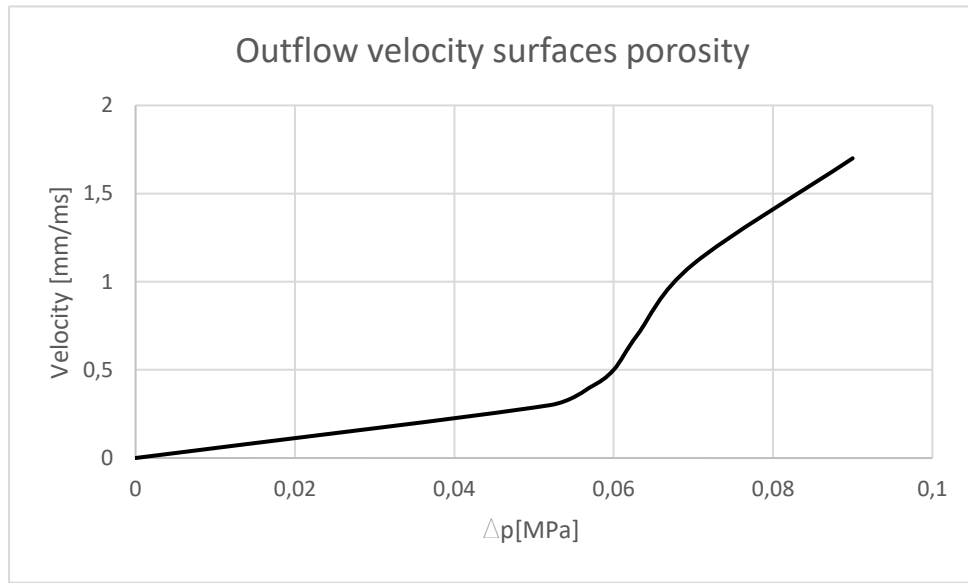


Figure 54: outflow velocity function of surfaces porosity

In this way the material porosity is formulated like a vent hole, defining the flux through a certain surface. It is possible to model it using the porous surfaces tool in the monitored volume card. From a mathematical point of view the formulation is the same as in the vent hole like definition. It is still possible to select from various type of flux formulation, define an outflow velocity depending on the pressure difference or define a time or a pressure difference for the activation of the porosity. In this case there are four parameters to define:  $T_{start}$ ,  $T_{stop}$ ,  $dP_{def}$ ,  $dtP_{def}$ .  $T_{start}$  and  $T_{stop}$  are the time instant at which the porosity effect starts and ends,  $dP_{def}$  is the pressure difference between the interior and the outside of the bag at which the porosity is activated and the  $dtP_{def}$  is the time for which the  $dP_{def}$  pressure difference must hold to activate the porosity. When using these parameters for the porosity formulation it is important to consider that they are all linked from a logic scheme. The porosity is activated if the time reaches  $T_{start}$  or the pressure difference is equal to  $dP_{def}$  for a  $dtP_{def}$  interval. So, if the porosity has to be controlled by the time, it must be defined a  $dP_{def}$  very high, never reached during the simulation, so that the porosity starts only depending on the time. Viceversa, if it has to be controlled from the pressure difference, the time instants  $T_{start}$  and  $T_{stop}$  must be higher than the simulation time to be sure that the porosity is activated only when  $dP_{def}$  is reached. These parameters are present in the vent hole definition also and they work exactly at the same way as for the porosity formulation.

#### 5.2.4. Vent Hole definition

A vent hole is literally a hole in the bag rear side that lets a certain amount of the gas, that inflates the bag, out so that the stiffness of the bag changes during an impact to decelerate properly the body hitting it and without serious damage for it, like said in paragraph 5.12. In the *figure 55* it is showed a deployed bag with the detail of the vent hole on the right. In the finite element model it is a surface divided from the bag surfaces through which it must be defines a flux. In *figure 56* it is reported the vent hole in the airbag model.



Figure 55: left, a deployed bag; right, zoom on the vent hole

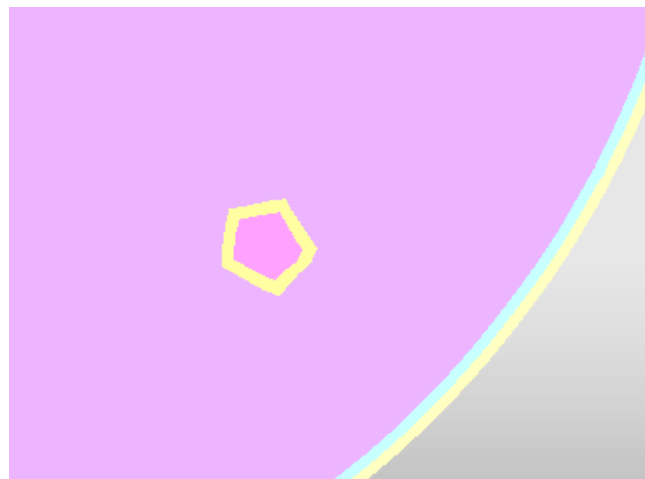


Figure 56: vent hole in finite element model

The vent hole behaviour is characterized defining the type of flow through the hole and the function “venting vs pressure” (fct\_IDP), a function defining a coefficient that multiply the mass of the air flowing out previously computed in the way defined with the *Iform* parameter. In this case the flow is isenthalpic, so it isn’t necessary to define the velocity outflow of the air, but this fct\_IDP is useful

because the model mustn't be changed to modify the air outflow. This function depends on the pressure difference between inner and outer side of the bag and has been modified to let the finite element model to behave like the Madymo one. From various simulations it showed out that the function characterizing the vent hole is the one reported in the *figure 57*.

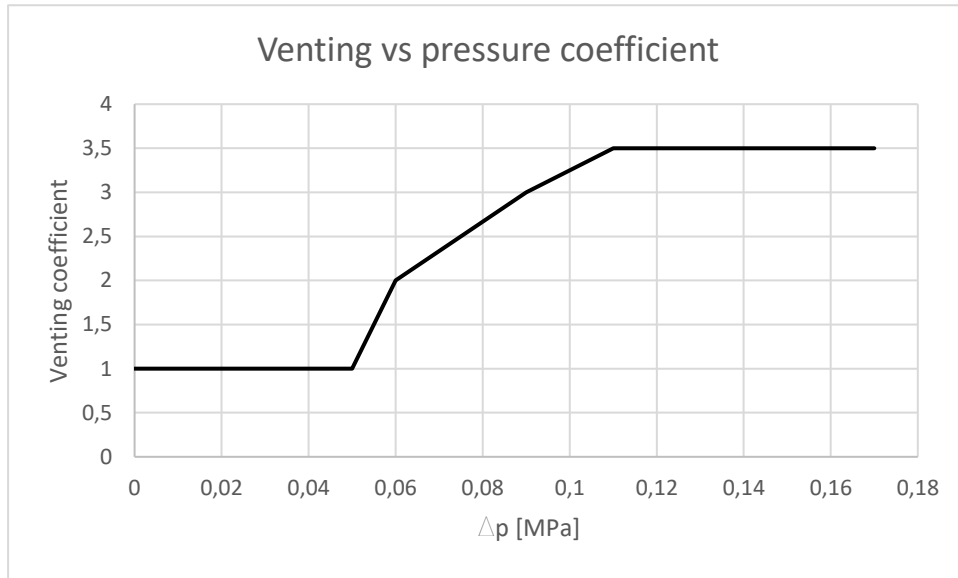


Figure 57: venting coefficient function

Another parameter used for the definition of the vent hole is the *Avent* coefficient, a coefficient that multiplies the area of the vent hole selected from the model. Like the *fct\_IDP* that multiplies the mass flowing out, the *Avent* changes the outflow without the necessity to modify the FEM. It turns out that the optimum value of *Avent* is 1,3.

As it will be seen in the next paragraph, the venting coefficient defined in this way doesn't represent the real behaviour of the bag in different conditions, even if it is good to correlate the finite element model with the Madymo's. When comparing the FE model with the ZF experimental tests (done in two configurations, high and low energy) results, it turns out that there is a divergence in the results of the two outputs in the case of low energy test. This led to the necessity of modifying the venthole definition. This fix has been done exactly in the *fct\_IDP*, that has undergone a better tuning to model properly the airbag behaviour in different conditions. From this further changing it came out a better correlated model, with a venting coefficient function as in *figure 58* and with the *Avent* coefficient equals to zero because it was no more necessary.

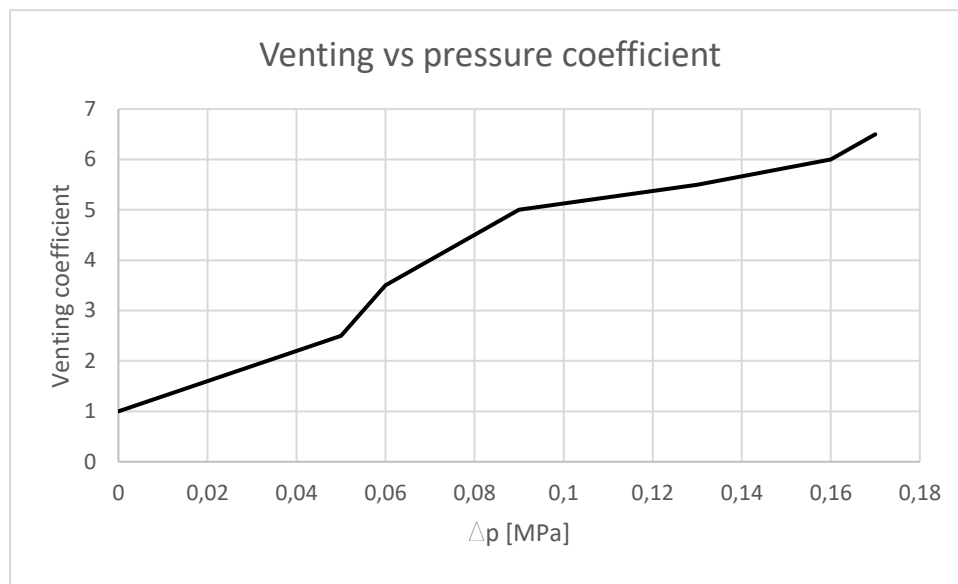


Figure 58: venting coefficient function of definitive model



### 5.3. Results discussion

In this section it will be presented the results of the optimized models discussed previously. The comparison with the Madymo ones has been done principally on the impactor deceleration versus time. In the following will be reported also the results of the contact force versus time, that has the same shape of the acceleration plot because it is just the acceleration multiplied the impactor mass. The comparison with the experimental tests is done instead on the contact force versus impactor displacement. Considering this output, it is taken a range around the experimental output of plus or minus the 5%, and the simulation result must fall into this range for the characterization of the model to be good.

The STELLANTIS Safety Center tests were afflicted by various energy losses due to the oscillation of the support and the deformability of the steering wheel, so the comparison with the experimental results has been done with the output of the ZF tests done for the airbag validation.

#### 5.3.1. Model with no porosity and no vent hole

As can be seen from the *figure 59* the finite element model behaves like the Madymo one, the two curves have the same slope and the minimum is the same also. The first part of the curve, from about 35 to 60 ms, represent the phase in which the impactor hits the bag and sink into it until it's stopped and goes back with the bag deflating (second phase of the curve from 60 to 100 ms).

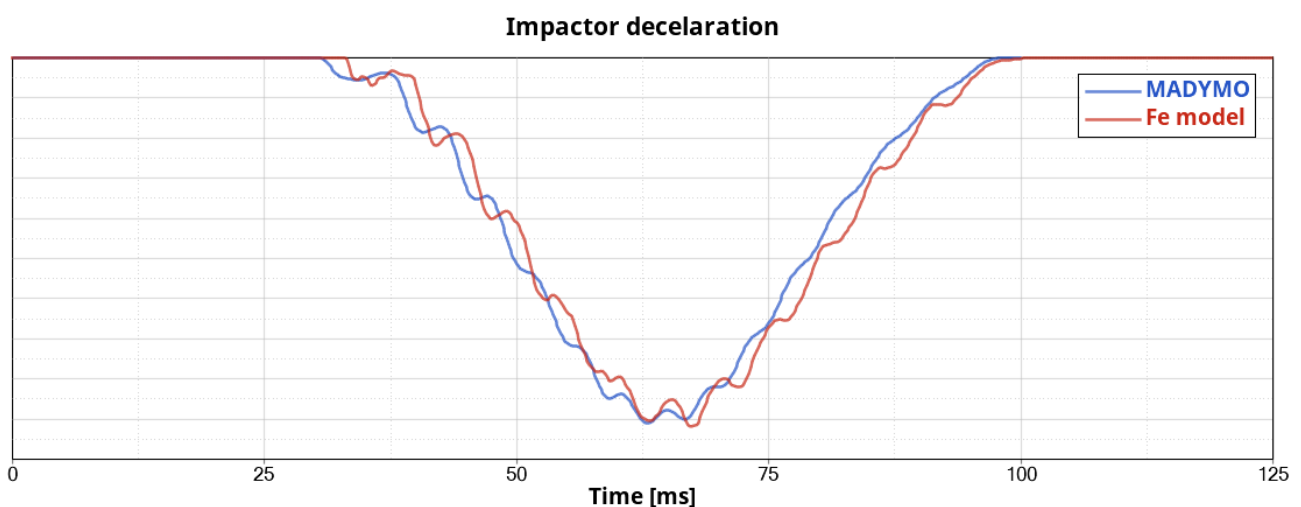
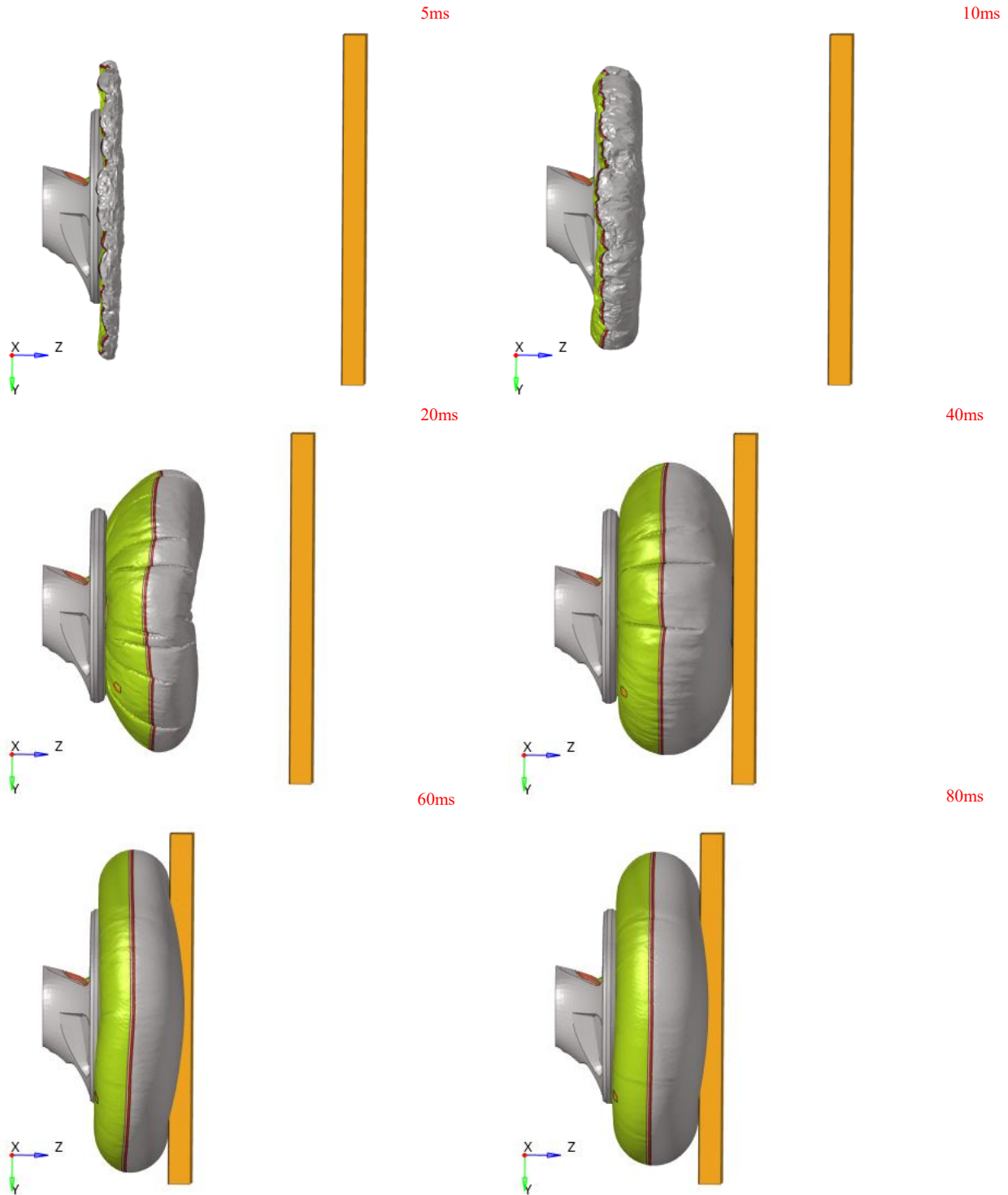


Figure 59: comparison between impactor deceleration of fe and Madymo models with no porosity and no vent hole.

In *figure 60* it is possible to see the frames of the linear impactor test simulation key instant. After about 35 ms the impactor hits the bag and starts decelerating (first phase of the curve), reaches the maximum deceleration after 60 ms and then is repulsed by the bag (second phase of the curve).



*Figure 60: simulation frames of linear impactor test*

The *figure 61* shows the contact force between the impactor and the bag and as expected it has the same shape of the deceleration. Instead, the *figure 62* shows the contact force versus impactor displacement. In grey there are the Madymo curves representing the offset of plus or minus 5% identifying the area in which the finite element curve should stay to consider the characterization of the model to be good. This is verified because the red curve (the finite element model one) falls exactly between them.

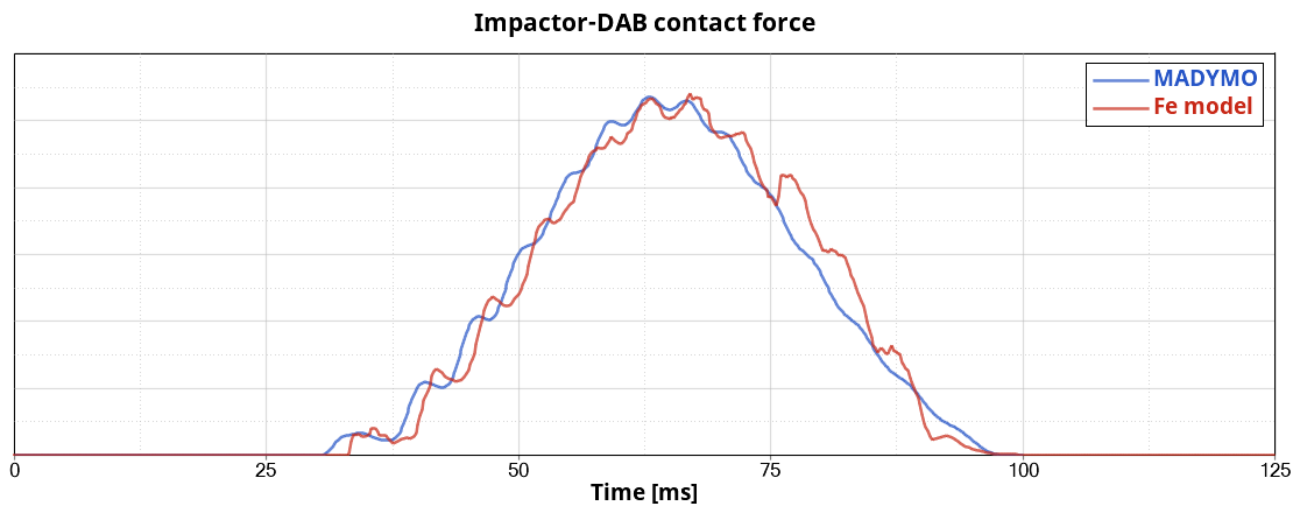


Figure 61: comparison between contact force of fe and Madymo models with no porosity and no vent hole

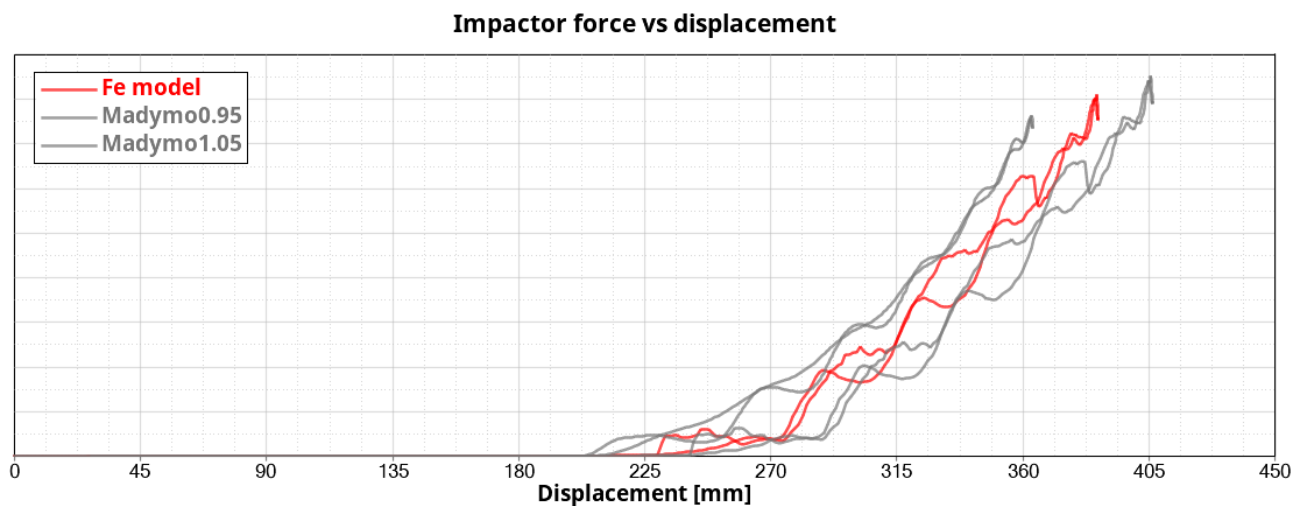


Figure 62: comparison between contact force vs displacement of fe and Madymo models with no porosity and no vent hole

### 5.3.2. Model with porosity definition but no vent hole

In the figure above is shown the comparison between the impactor deceleration of finite element and Madymo models. It has a good correlation in the slope on the curve in the first phase, the one where the impactor hits the bag, and in the minimum value also. In this case it is possible to see how the general values are lower than the latter case. This because, with the introduction of the porosity, there is a loss of air mass flowing through the fabric and reducing the stiffness of the cushion, with a less deceleration of the impactor consequently.

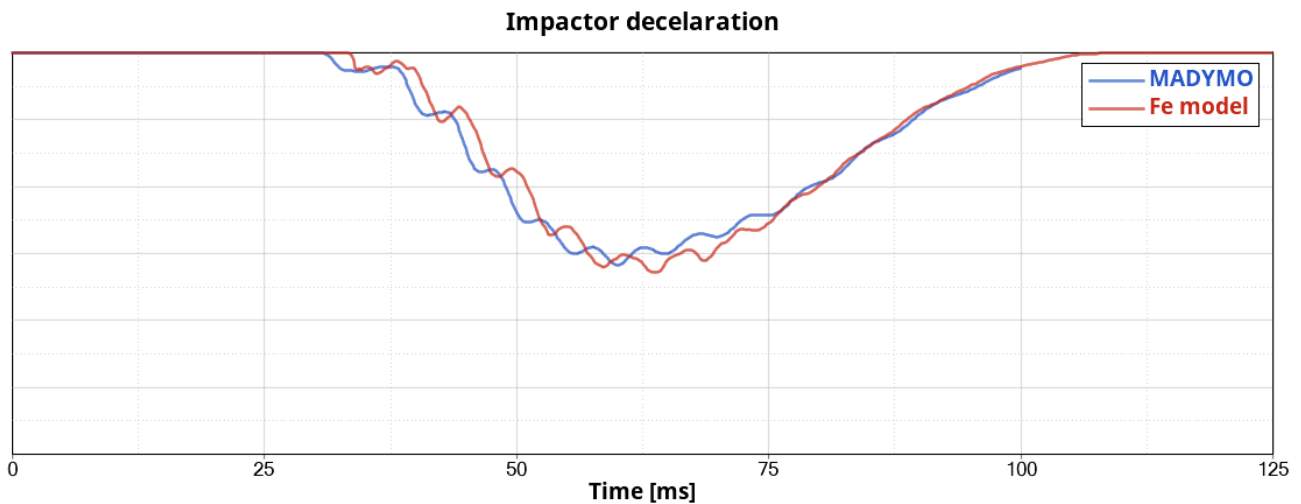


Figure 63: comparison between impactor deceleration of fe and Madymo models with porosity and no vent hole.

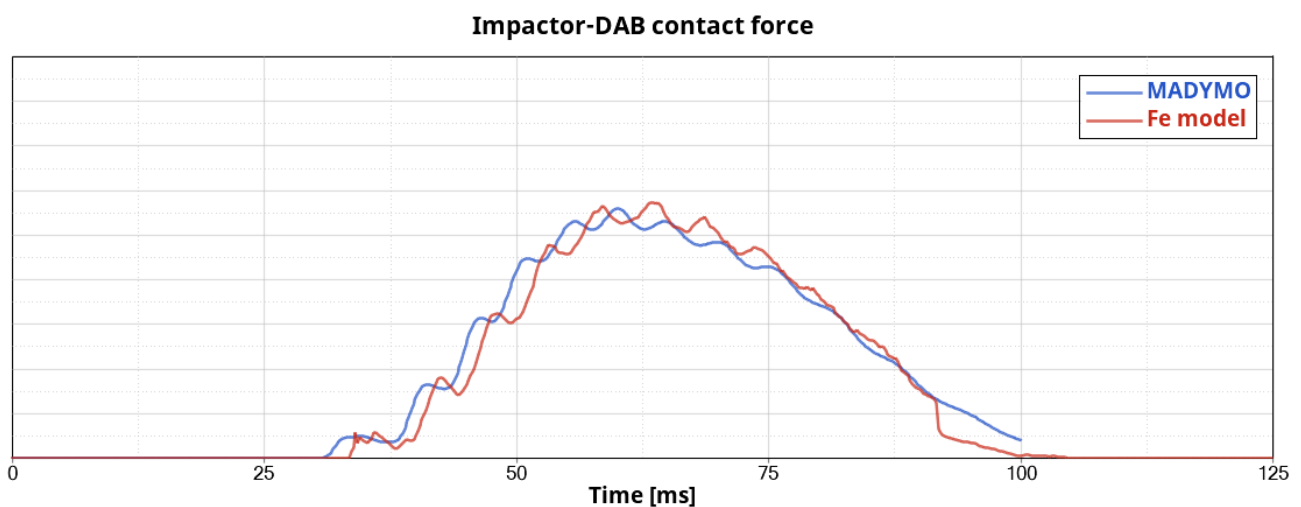


Figure 64: comparison between contact force of fe and Madymo models with porosity and no vent hole

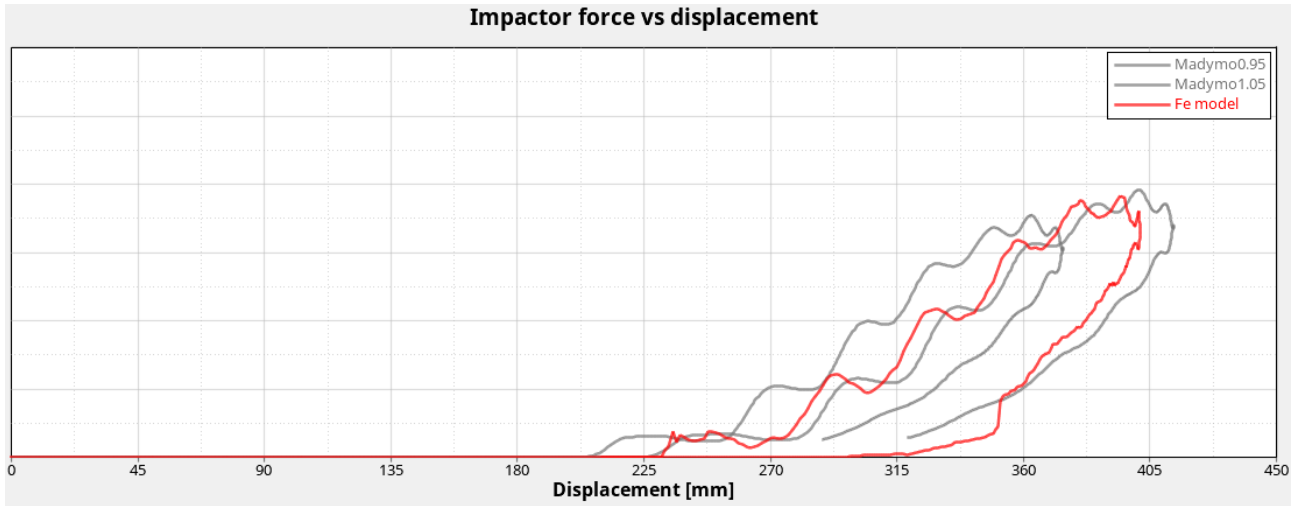


Figure 65: comparison between contact force vs displacement of fe and Madymo models with porosity and no vent hole

The same holds for what concern the contact force that is lower than the case with no porosity and no vent hole (figure 64). The comparison done with the contact force versus the impactor displacement shows that the contact force curve of the finite element model falls into the range identified by the Madymo curve, so the model is well characterized.

### 5.3.3. Model with porosity and vent hole definition

The figure 66 shows the results of the model with both the porosity and the vent hole definition, the finite element model is well behaving in this case also, with an impactor deceleration that fits the Madymo result almost perfectly. From the comparison between this curve and the one of the previous case it can be seen how the effect of the vent hole on the global working of the airbag is smaller than the one of the porosity, but nevertheless it is important, being the difference between the two curves (the one with porosity only and the one with also the vent hole) small but not negligible.

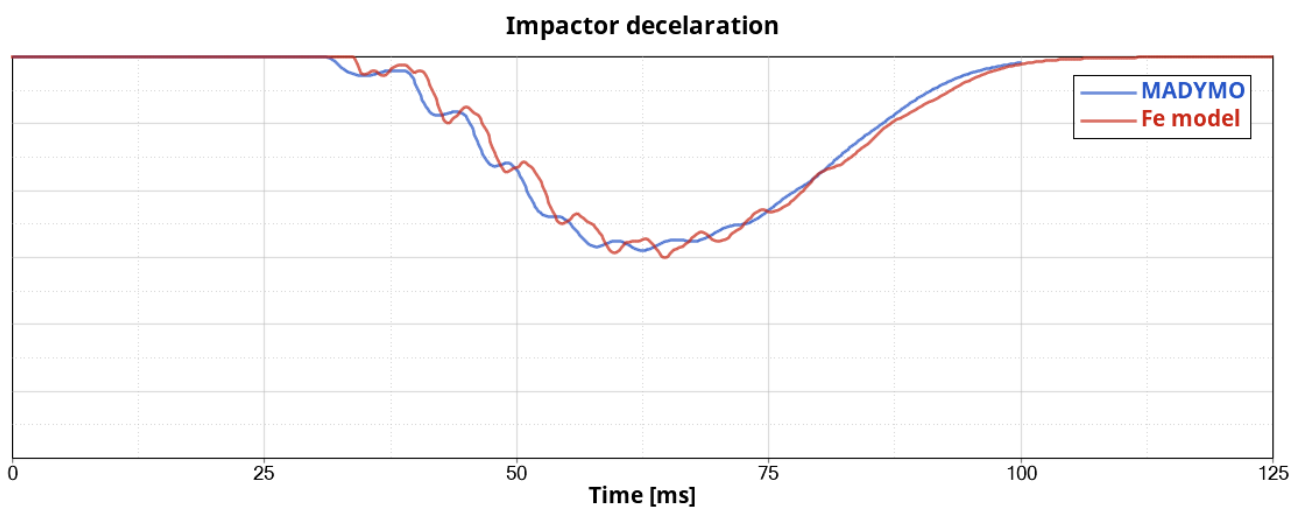


Figure 66: comparison between impactor deceleration of fe and Madymo models with porosity and vent hole.

The importance of the vent hole will be more appreciated in the comparison with the experimental curves, where the fine tuning of the model was done only modifying the definition of the vent hole.

In the following will be presented also the curves of the contact force versus time and versus displacement, to be coherent with the other cases above discussed but they do not give further information about the goodness of the model.

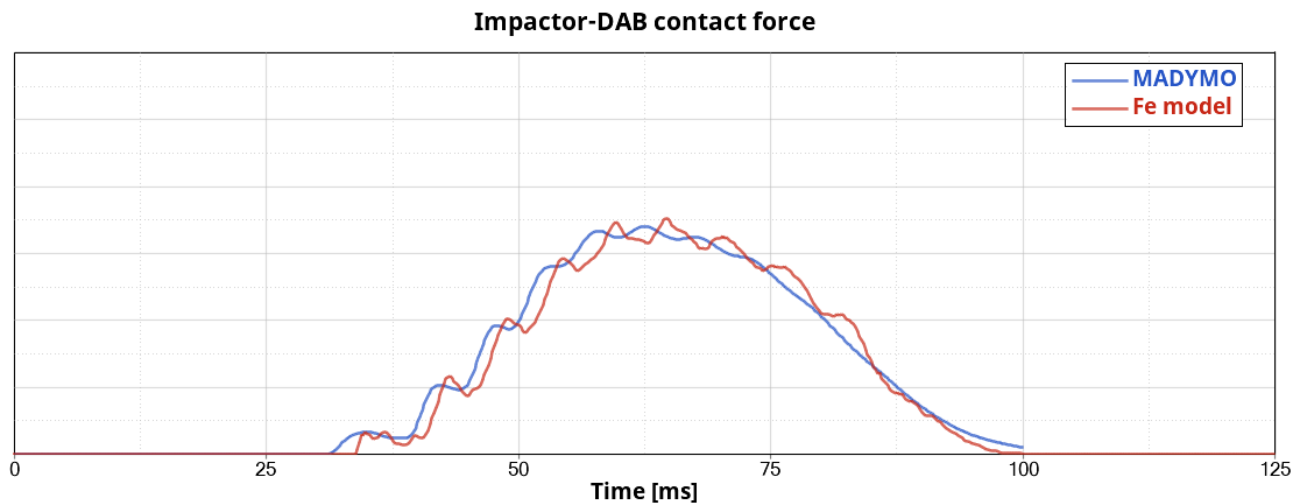


Figure 67: comparison between contact force of fe and Madymo models with porosity and vent hole

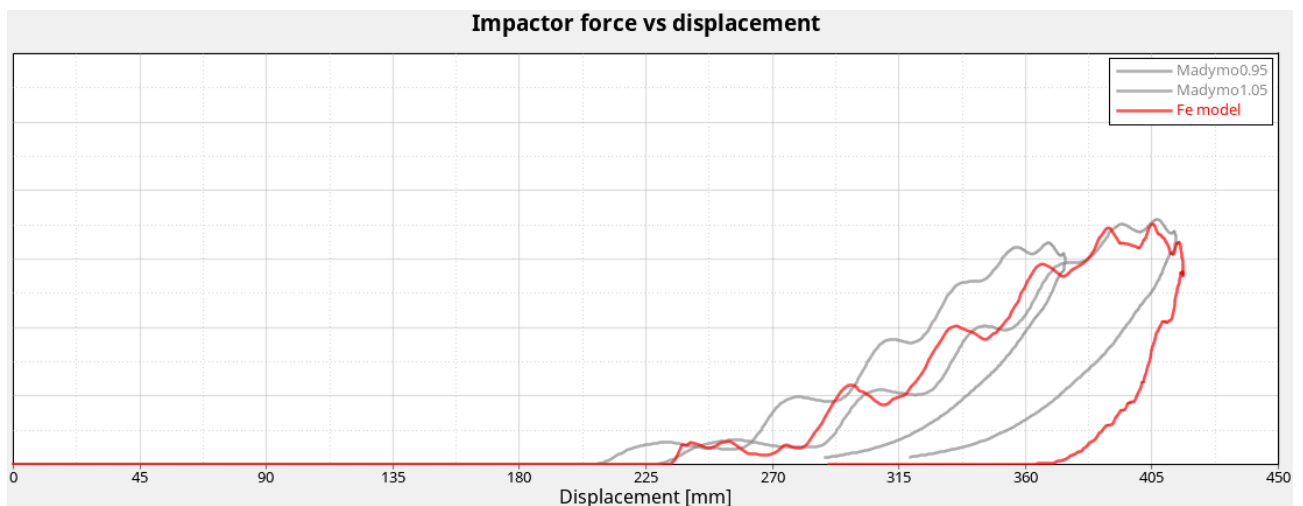


Figure 68: comparison between contact force vs displacement of fe and Madymo models with porosity and vent hole

#### 5.3.4. Comparison with experimental results

As said previously, the comparison has been done with the ZF validation test results, being the results of the tests done at the STELLANTIS Safety Centre afflicted by many energy losses due to how the tests were conducted. ZF, during the airbag validation process has done two different tests, one at high energy and one at low energy. The first with an energy of 882 J and the latter with an energy of 648 J, both with the same impactor but with a different initial velocity.

This tests by ZF gives the chance to improve the model because working with two different cases it is possible to define all the parameters so that the model represents the reality in various cases giving more confidence on the results. Indeed, the Madymo model used in the first step of the work to tune the model, was already correlated with the experimental results at high energy, so there was no doubt that in that case also the finite element one would be correlated. The problem figured out when the comparison has been done for low energy impact.

Like explained in the last paragraph, the initial formulation of the vent hole wasn't giving the desired results, so it has been modified until the model matches the real behaviour of the bag for the low energy case also. With this work it has been possible to find the best characterization of the vent hole with the parameters defined earlier.

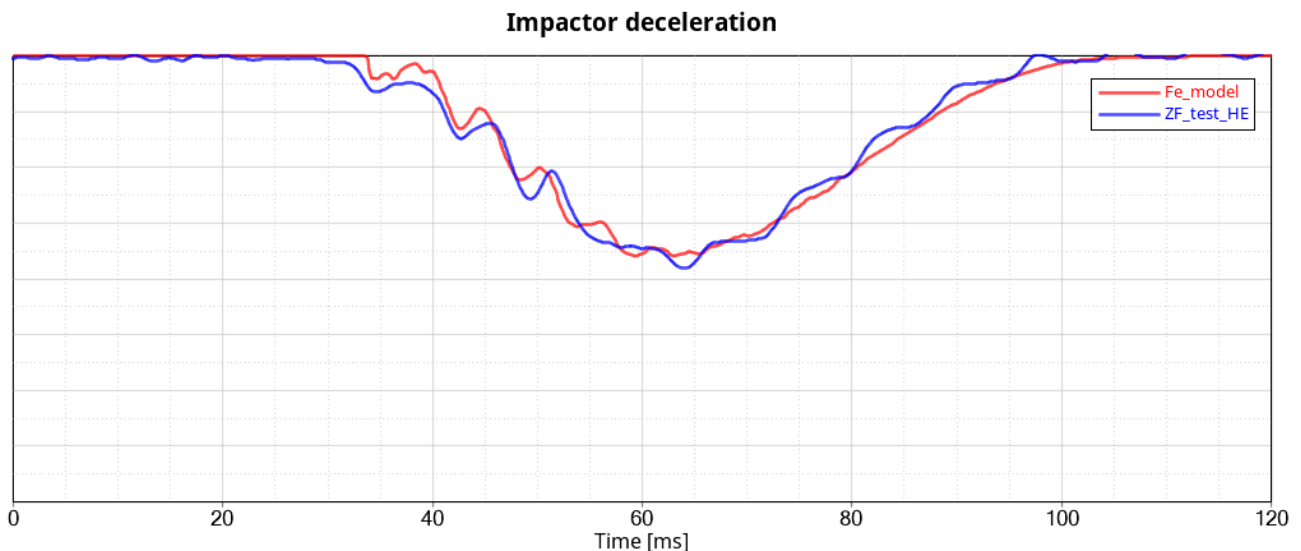


Figure 69: comparison between deceleration of finite element model and ZF experimental test at high energy

With the vent hole parameters discussed in paragraph 5.2.3 (figure 58), the correlation between the computer simulation results and the experimental ones is very good as can be seen in figure 69

reporting the deceleration plot for the high energy case. This result is also confirmed from the impactor force versus displacement curve in *figure 70* that shows how the finite element result fall exactly in the gap considered around the experimental results.

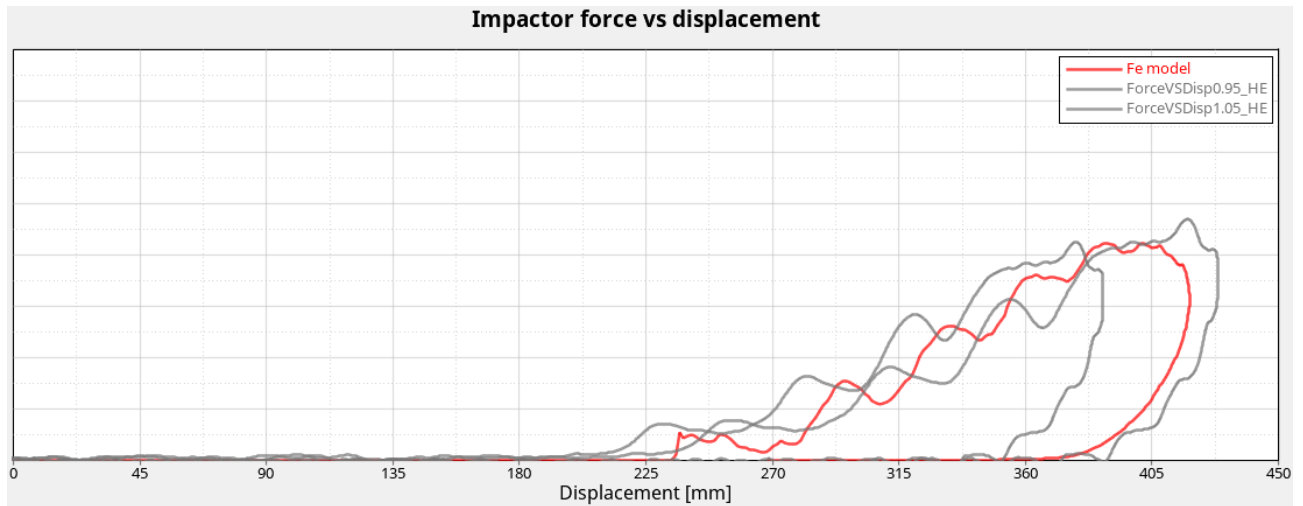


Figure 70: comparison between contact force of finite element model and ZF experimental test at high energy

In *figure 71* is showed the deceleration plot of the low energy case while in *figure 72* the contact force versus displacement of the same case. While the deceleration comparison could let think that the correlation is not at its finest, the contact force comparison shows that the computer simulation result fall perfectly in the range discussed above and so the result is acceptable.

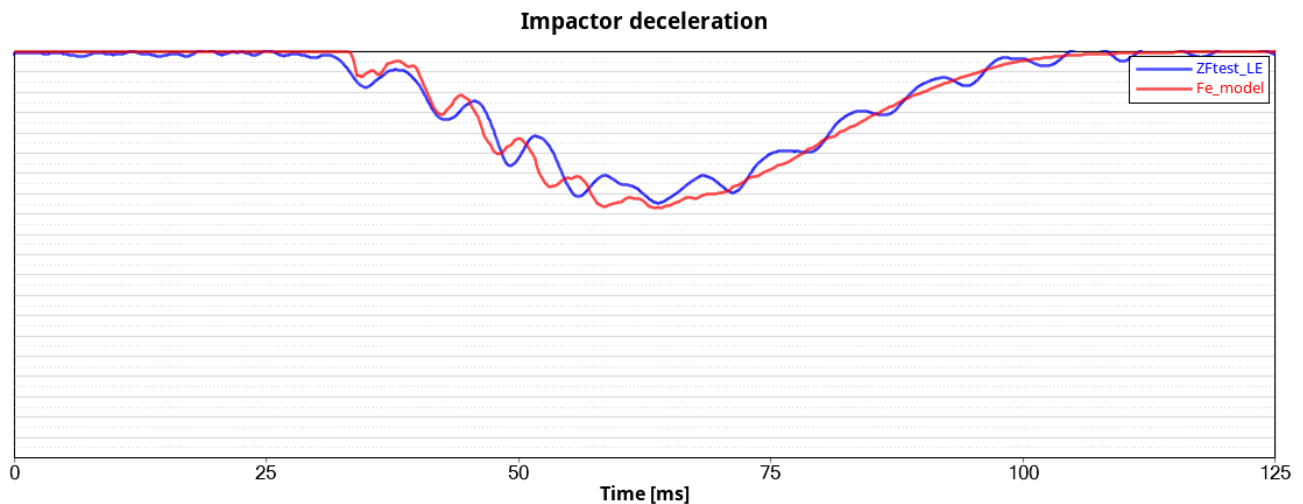


Figure 71: comparison between deceleration of finite element model and ZF experimental test at low energy



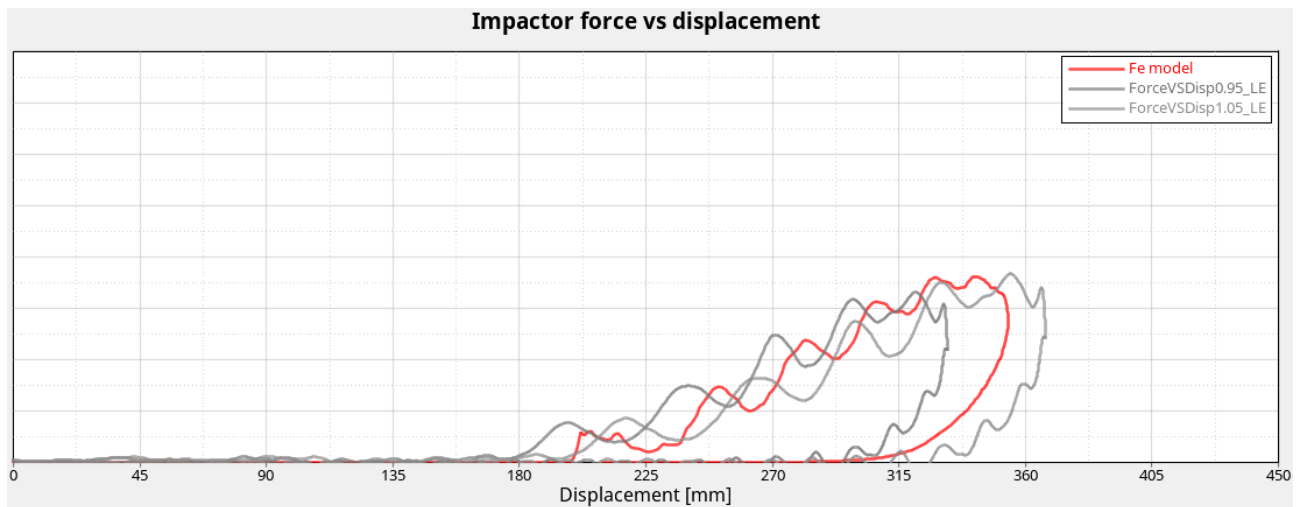


Figure 72: comparison between contact force of finite element model and ZF experimental test at low energy

### 5.3.5. Final results of Madymo comparison

After the vent hole definition was modified to tune the finite element model with the experimental results, a new comparison with the Madymo model has been done for the case of porosity and vent hole definition. So, in this case we have the Madymo model and the finite element model correlated with the tests results.

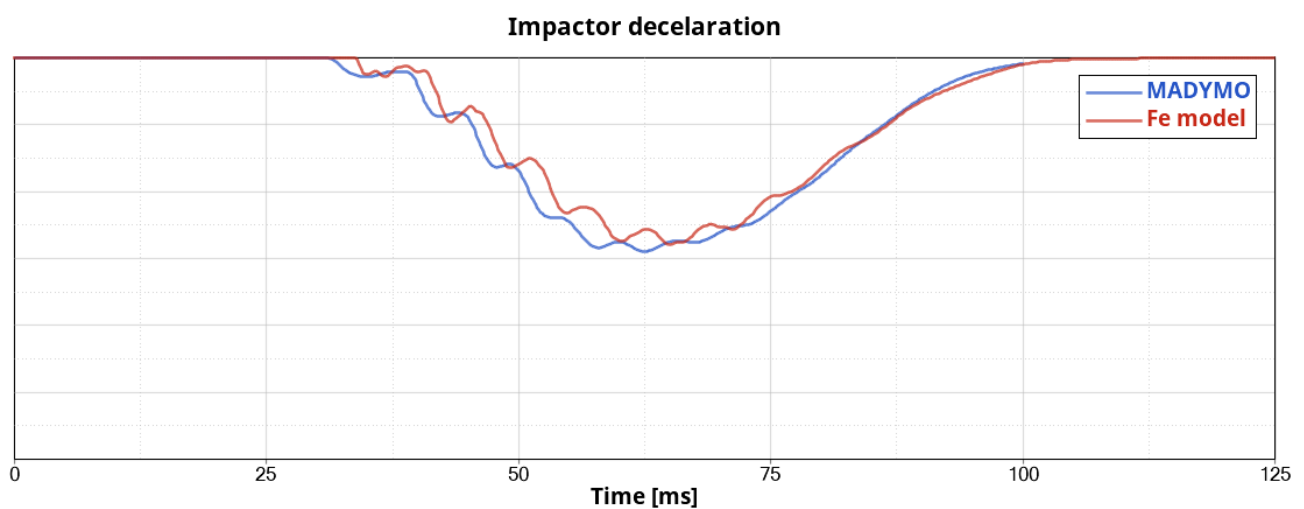


Figure 73: comparison between deceleration of finite element model and Madymo

As shown in the *figures 73* and *figure 74*, the deceleration, diverge a bit from the Madymo results. This happens also in the comparison of the contact force versus displacement (*figure 75*) in the second phase of the impact, when the impactor is repulsed by the bag, where the finite element curve falls outside the range identified by the Madymo results. Being the contact force of the finite element model higher this shows that the model is stiffer than the Madymo one.

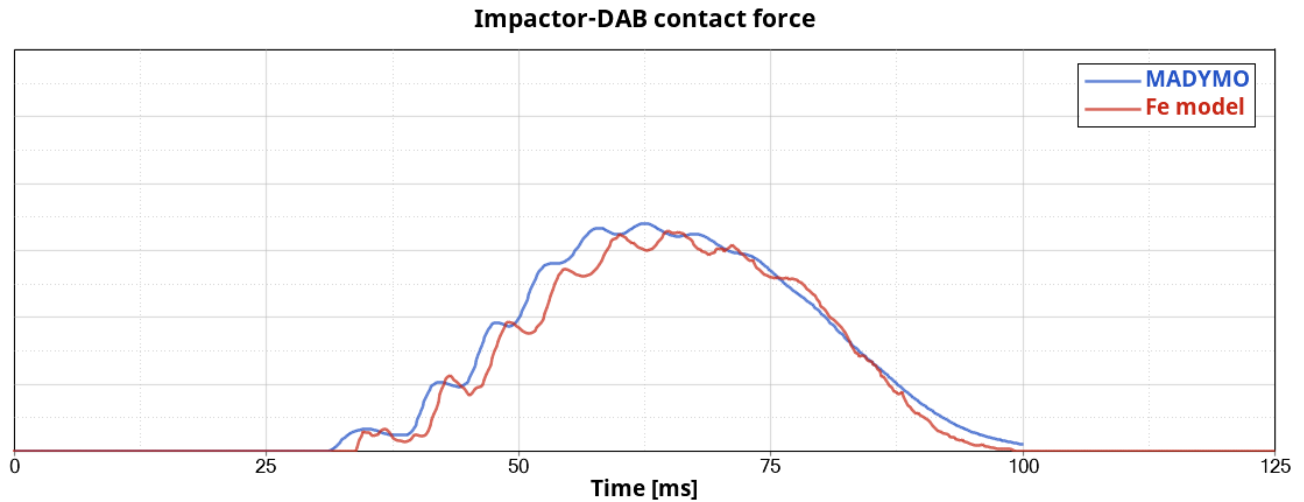


Figure 74: comparison between contact force of finite element model and Madymo

These differences showed in the acceleration and force plot are not so big and they are negligible because the aim was to correlate the finite element model with the experimental tests, the Madymo results were an intermediate step only, so the model can be considered to have a high level of correlation

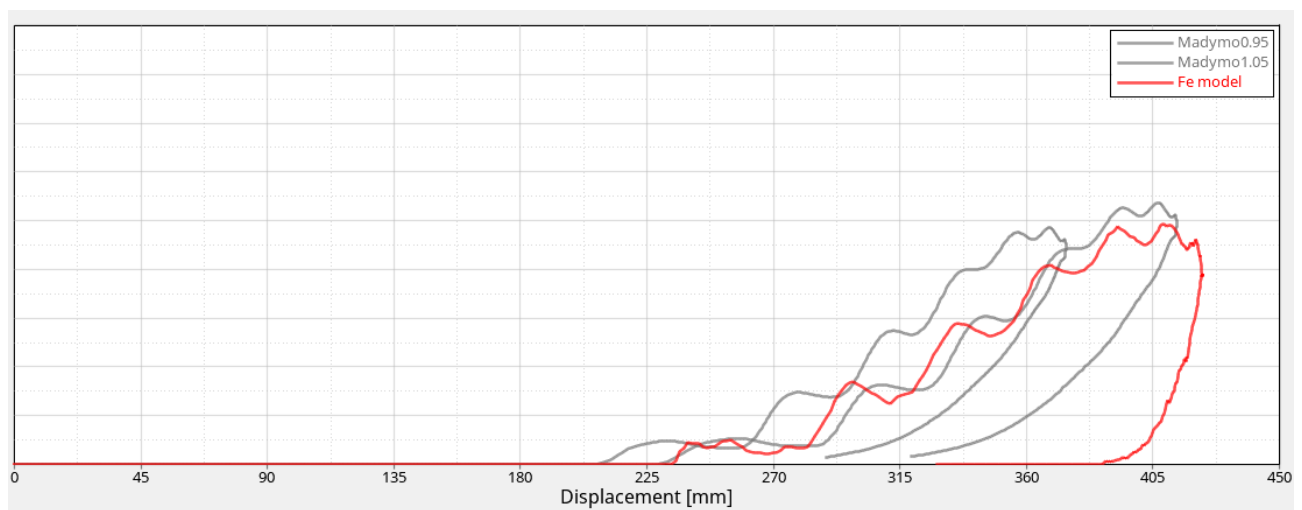


Figure 75: comparison between contact force versus displacement of finite element model and Madymo

## 6. Body Block

### 6.1. Model description

The body block test is about a mannequin (i.e. the body block) crashing into the steering wheel with the bag inflation. So, in the finite element model also, it is necessary to model these various parts. The airbag is characterized as described up to now in this thesis, being this simulation used primarily to verify the goodness of the bag model when it has to be putted in a more complex subsystem in order to study a real-world situation. The body block, the steering wheel and the steering column were already characterized from Iveco in a previous work. In the *figure 76* and *77* it is reported the model characterized from Iveco, where can be identified the steering column with the plate to fix it, the steering wheel that, differently from the previous case, now is deformable, and the body block.

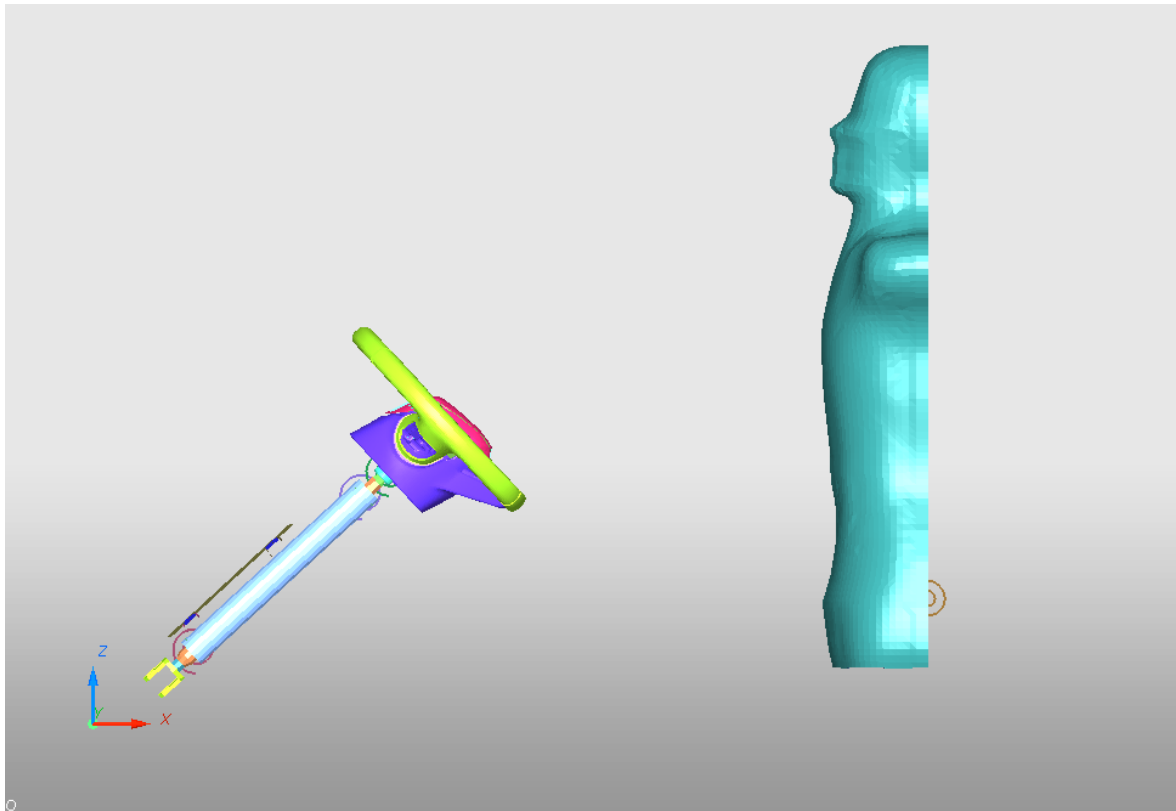


Figure 76: body block finite element model

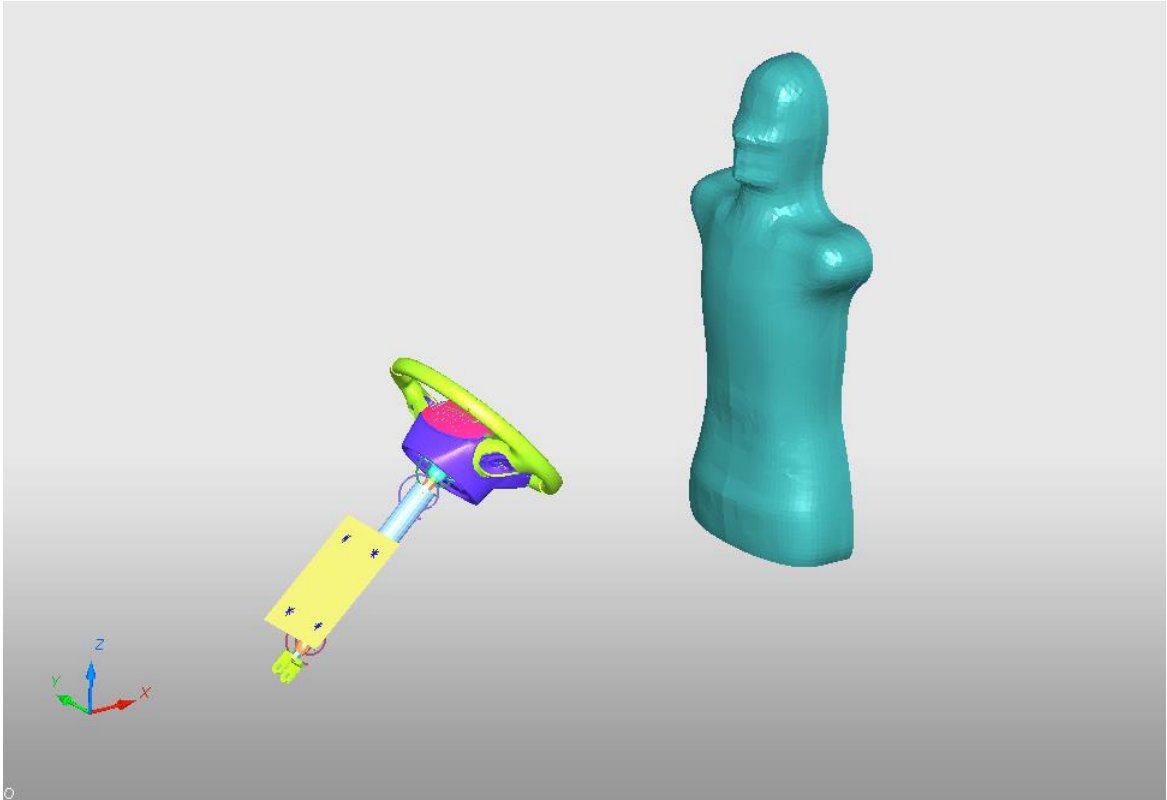


Figure 77: body block finite element model, 2nd view

### 6.1.1. Body Block

The body block test is normed by the UNECE R12 that defines the safety standard for the “protection of the driver against the steering mechanism in the event of impact” and how the test must be done, defining also how the body block must be made. On the Regulation there are defined the materials, the dimension and how the body block must be characterized for a 50<sup>th</sup> percentile mannequin. The mass of the body block must be 34-36 kg.

In *figure 78* it is reported the drawing of the body block with his components and in *figure 79* are reported the components modelled in the finite element model.

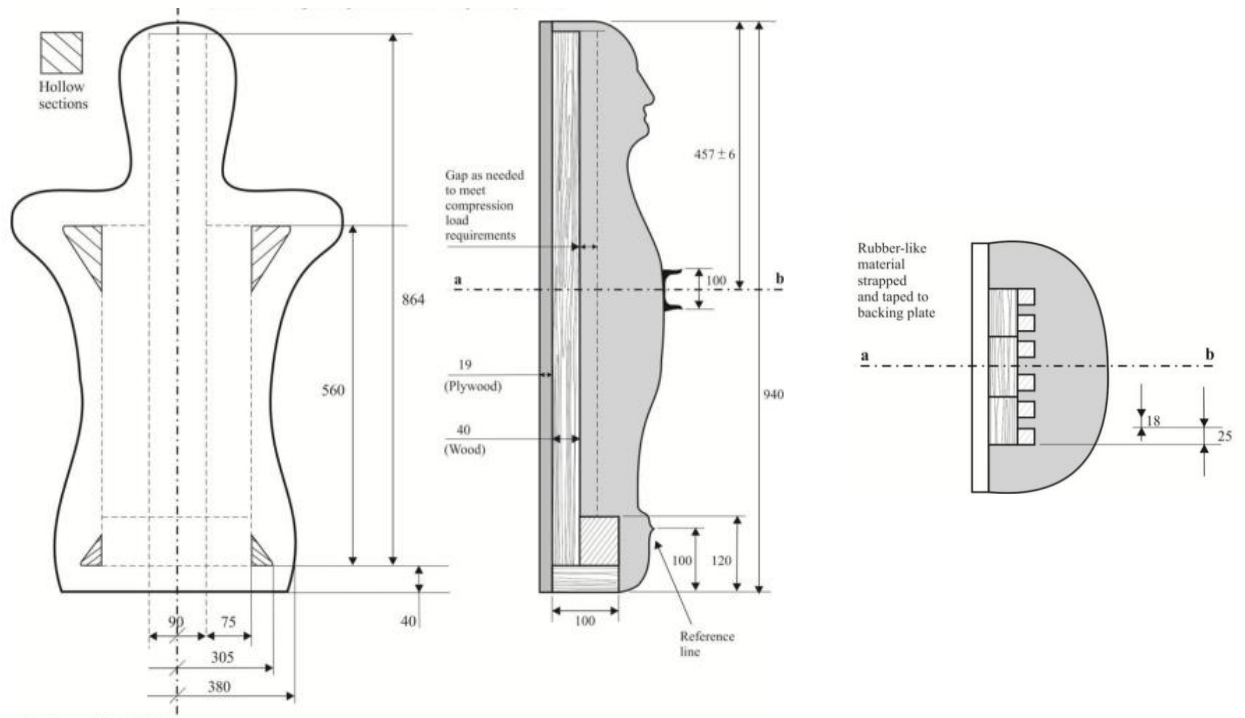


Figure 78: drawing of body block as described in the UNCE R12 normative.

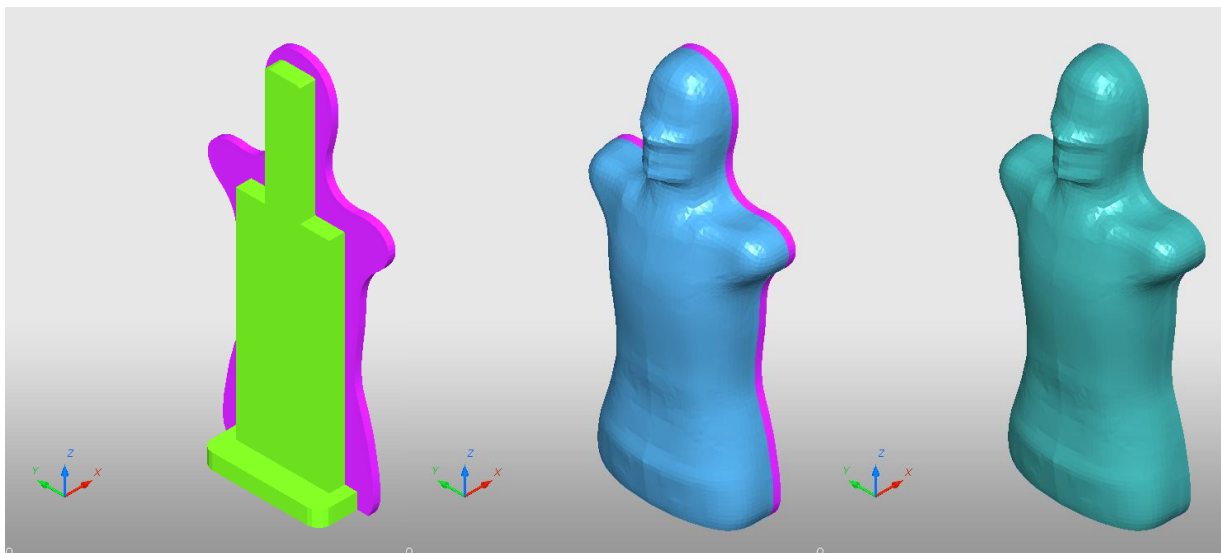


Figure 79: body block finite element model. Left: plywood (rear of the body block) and wood. Centre: wood covered by elastomeric material. Right: all the components are covered with scotch tape.

The back of the body block has a plate of plywood that in the model has been formulated as a rigid body while all other components are deformable. It has a wood hollow, in green in *figure 79*, and a

major part defining the shape of the mannequin made by elastomeric material with a proper Young Modulus and a proper deformations-stress curve defined in the model. These three components are completely covered by scotch tape to bring all together. The normative defines also how the mannequin H point should be positioned to define the relative distance between the body block and the steering wheel.

### 6.1.2. Steering wheel and steering column

In this case the steering wheel is the one characterized following the UNECE R12 Regulation: it is a deformable one, instead of the one used in the linear impactor tests that was rigid.

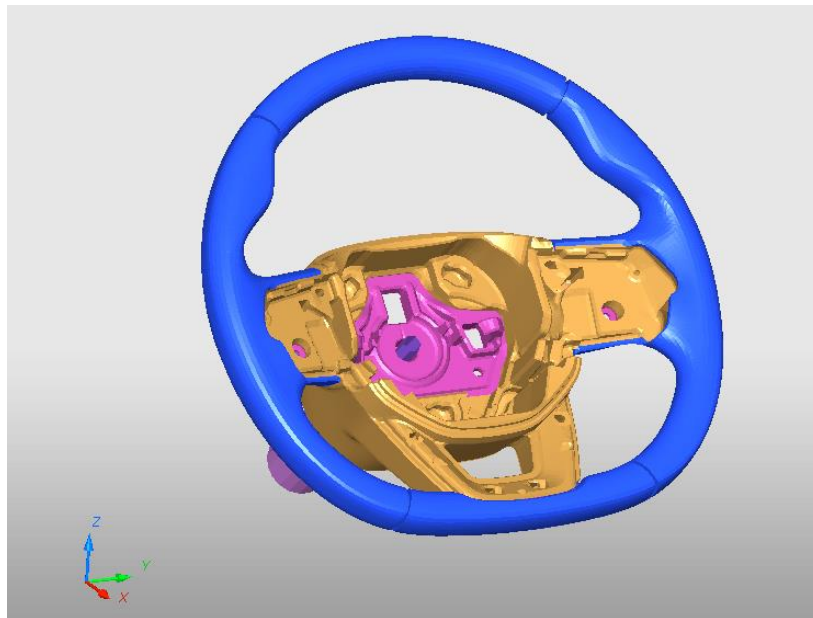
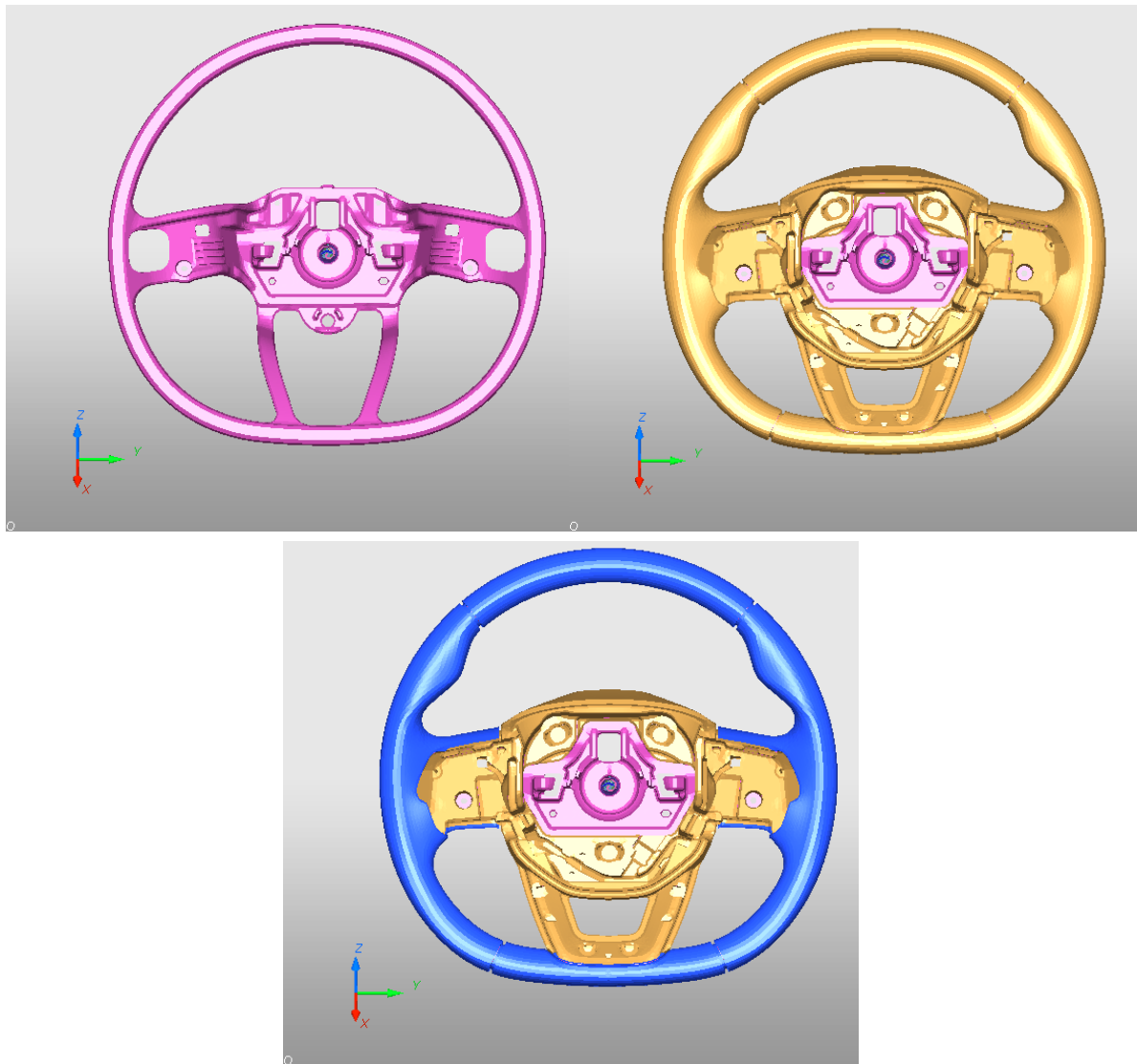


Figure 80: deformable steering wheel

As can be seen from the *figure 80*, the steering wheel is different from the linear impactor one. This is a new one, introduced in the last versions of the Daily. The main differences are that it is not perfectly circular but has a cut lower part; it also has the steering wheel controls that are located into the two side-housing. Furthermore, this steering wheel has an armor of magnesium alloy covered by a rubber material and by the leather, these “layers” of which it is made are showed in *figure 81*.



*Figure 81: steering wheel model definition*

For what concern the steering column, it has been needful to adjust it to the test conditions so, being the steering wheel fixed on a rigid support, also the steering column has been cut and fixed in its free end blocking all the degrees of freedom of the end nodes. The section of the beam also has been modified to make the support of the finite element model more like the experimental one.

In *figure 82* is reported a comparison between the experimental set and the simulation model.



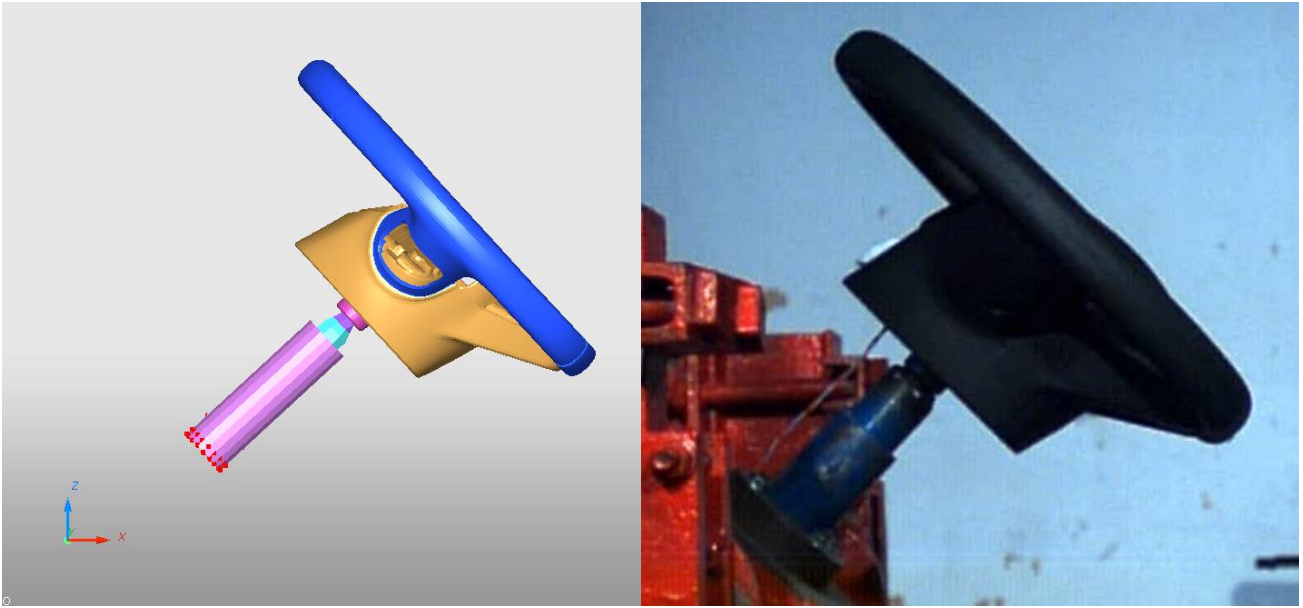


Figure 82: comparison between steering wheel set in finite element model and experimental test.

Originally the beam section of the column was modelled on the real column, being the test done with the steering wheel mounted on the steering column. In this case the steering wheel is mounted on a fixed support that has also a higher inertia with respect to the column, so the section of the beam has to be increased (on the right in *figure 83*). This turned out from a video comparison also between the experimental test and the video of the simulation done with a beam section like the column one (on the left in *figure 83*). In this case the deflection of the support was too high with respect to the real one that is barely visible on the video.

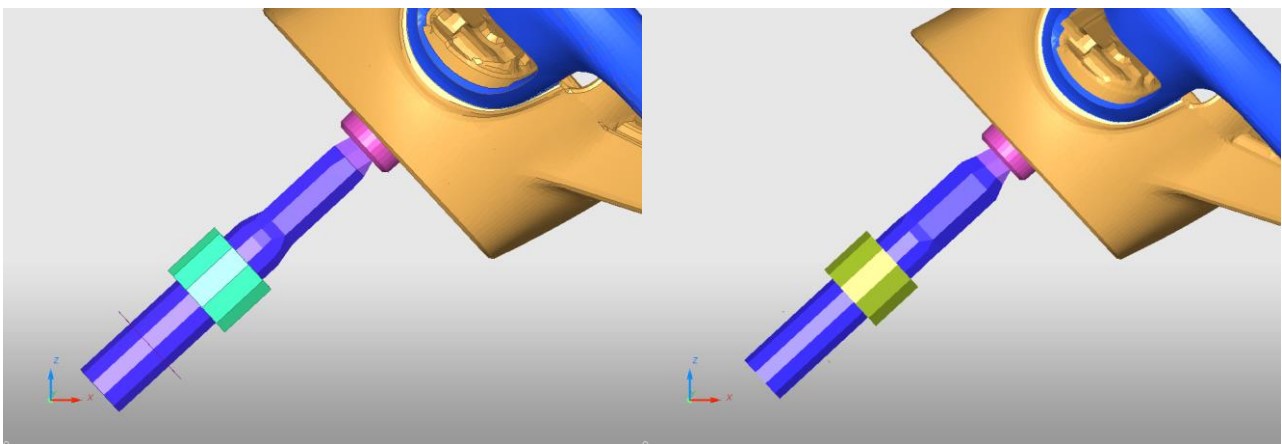


Figure 83: Left, original section of the support derived from the column one. Right, section of the support that more fit its real behaviour

### 6.1.3. Final configuration of body block model

With the changes done principally on the steering wheel and column, it has been introduced the airbag with the punch. These two components are the same defined and whose characteristics have been already explained in the last chapter so it not necessary define them again. The positioning of the body block has been done computing the trigger distance considering the space occupied by the bag once it is fully inflated plus the distance covered by the body block, with a speed of at least 24,1 km/h, in the time that take the bag to inflate.

As the experimental tests, the simulations also have been done with the three different configurations:

- The first one, with the steering wheel at 0 degrees (*figure 85*);
- The second one, with the steering wheel at 90 degrees (*figure 86*);
- The third one, with the steering wheel at 180 degrees (*figure 87*).

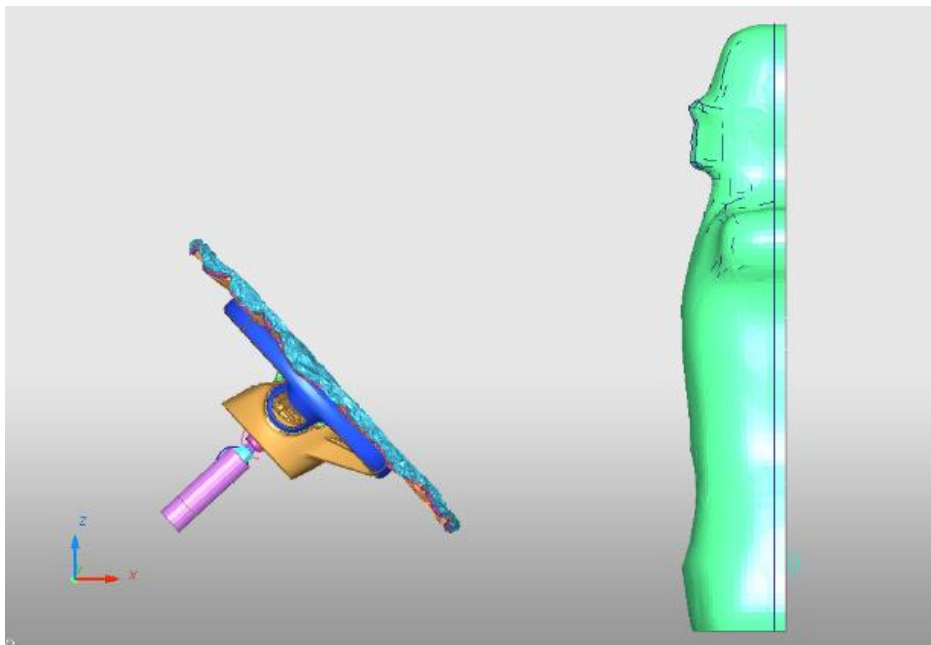


Figure 84: final body block model, side view

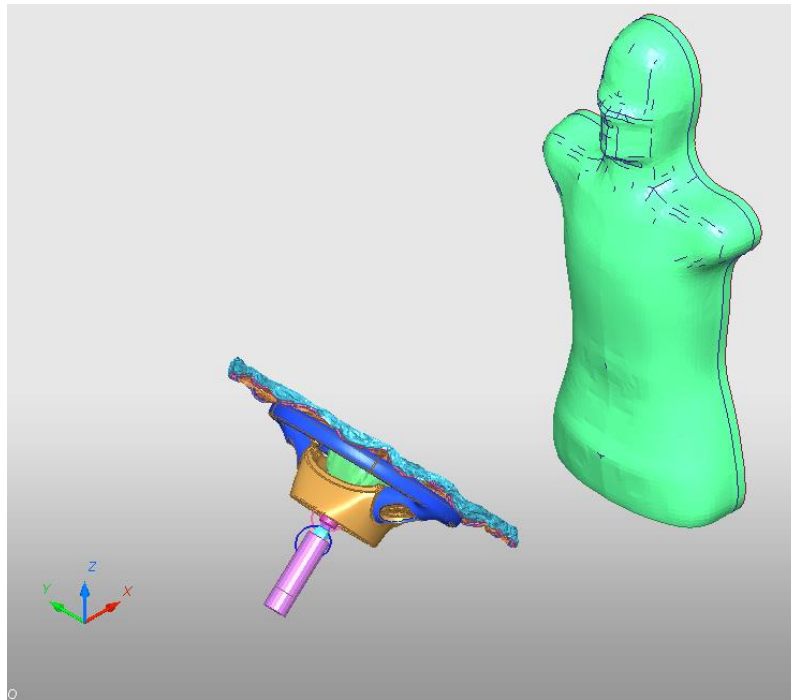


Figure 85: body block model with 0 degrees steering wheel.

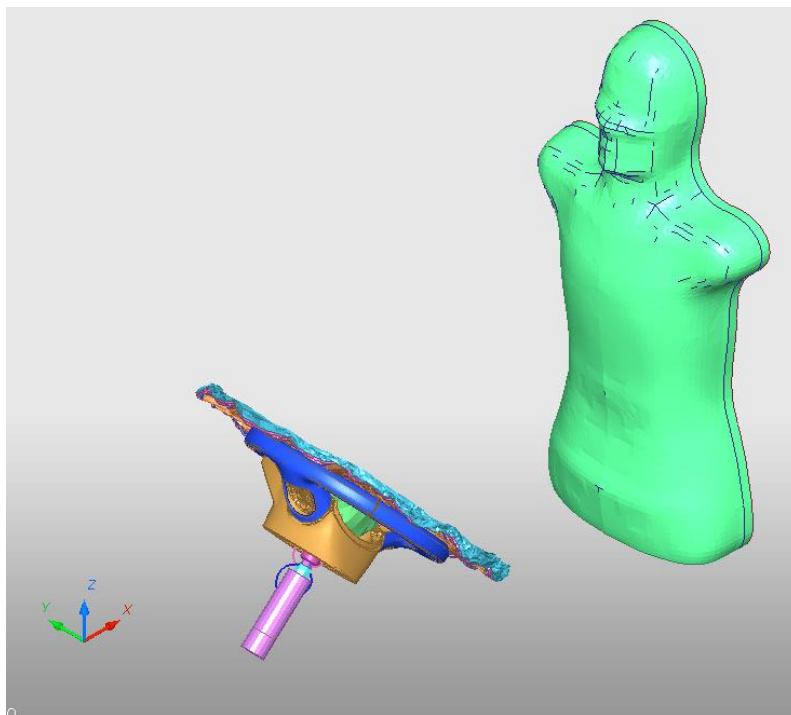


Figure 86: body block model with 90 degrees steering wheel.

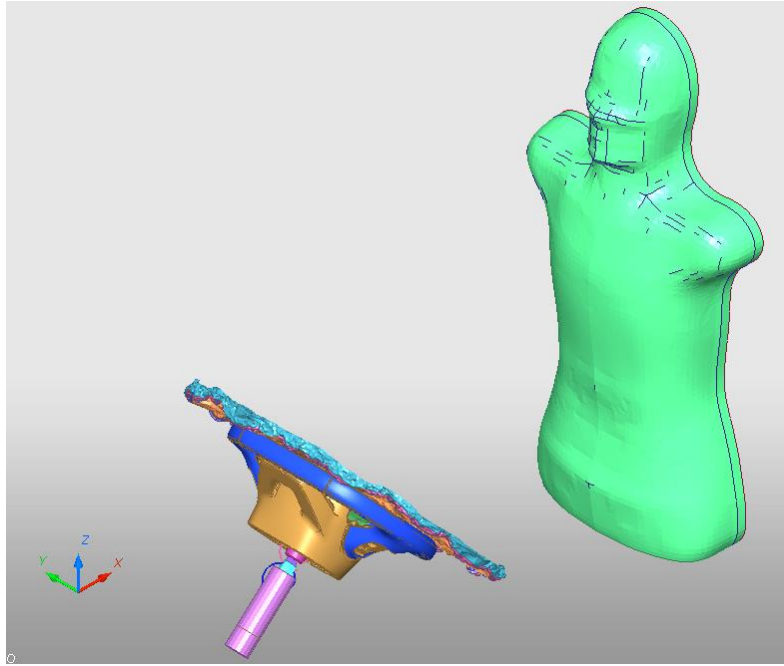


Figure 87: body block model with 180 degrees steering wheel.

## 6.2. Results discussion

This time the comparison between the experimental results and the simulation ones was done on the acceleration, or better, the deceleration of the body block during the impact with the bag.

### 6.2.1. 0 degrees steering wheel

From the deceleration curve (*figure 88*) can be recognized the different phases of the impact:

- The first phase, from about 40 ms to 75 ms, is about the body block hitting the airbag;
- The second one, from 75 ms to 85-90 ms, is when the stiffness of the steering wheel also intervenes. This can be seen from the slope of the curve that changes suddenly, and the deceleration values become higher.
- The last one is the discharge phase, from the peak, and this is when the body block is repulsed from the system composed by the airbag plus the steering wheel.

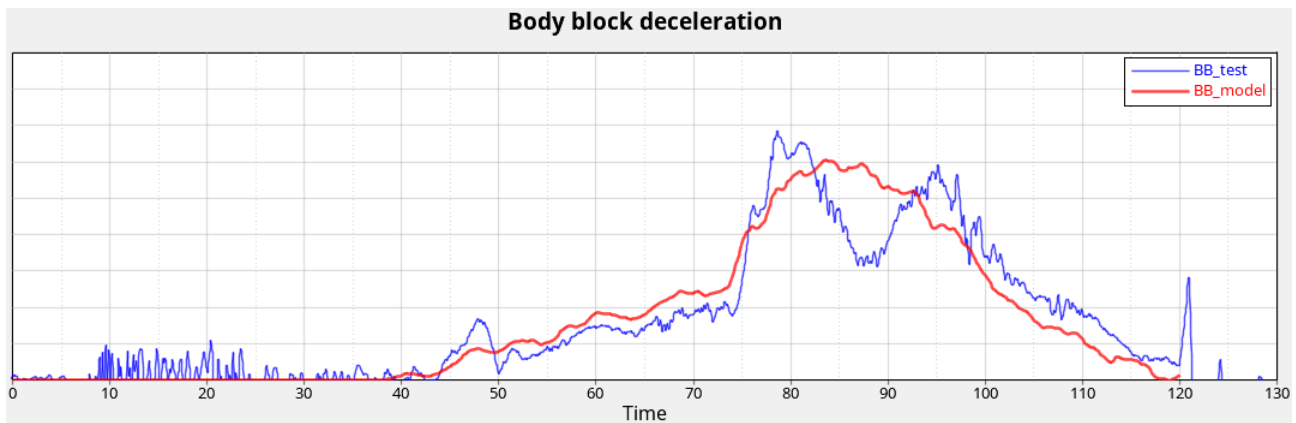


Figure 88: body block deceleration with 0 degrees steering wheel

As can be seen from the comparison in the deceleration plot from *figure 89*, the behaviour of the two systems is a bit different. In the simulation plot there is only a pic, more or less of the same height of the experimental first one, while in the test plot there are two pics, this is probably due to a fracture in the steering wheel occurring at a certain instant during the impact, that is not happening in the computer simulation because of how the material of the steering wheel is characterized.

From the first phase of the impact it is possible to see how, in any case, the bag works like the real one, in fact this phase is the one where only the airbag functioning is decelerating the body block.





Figure 89: body block test with 0 degrees steering wheel

In figure 89 and 90 there are reported the frames of the experimental test and of the simulation, respectively, and from the images analysis also it can be seen how the behaviour of the body block is a bit different, specially in the final phase with the body block rotating clockwise after the impact before falling down under the gravity effect, while in the simulation the body block has an anti-clockwise rotation. This happens also in the other tests, with the steering wheel at 90 and 180 degrees, and is probably due to the characterization of the body block, particularly to its inertia distribution.

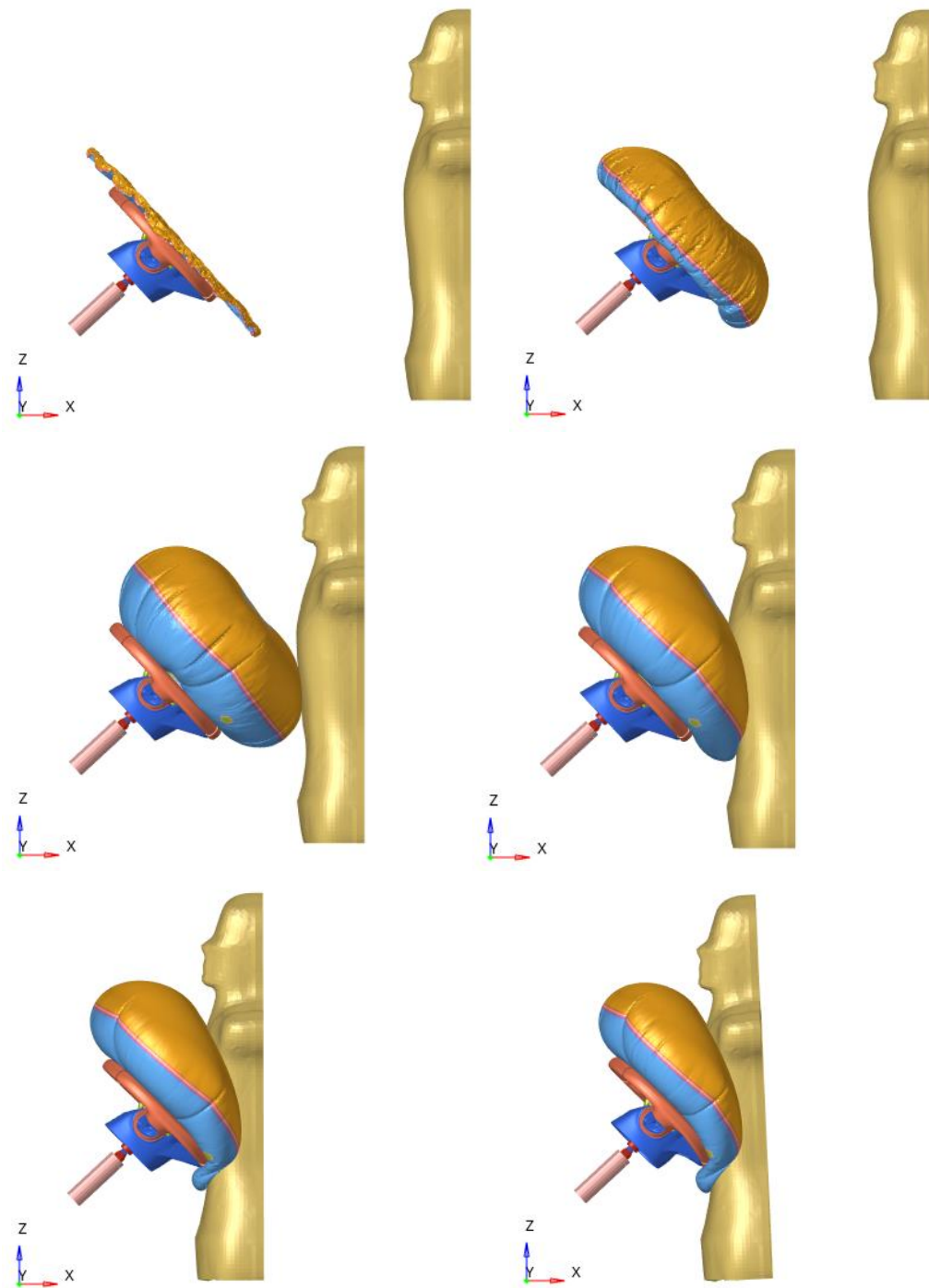


Figure 90: body block simulation with 0 degrees steering wheel



### 6.2.2. 90 degrees steering wheel

In this case also can be identified the three phases described before, and how can be seen in the *figure 91*, in the second phase there is a different slope between the test output and the computer simulation one. This means a different stiffness in the steering wheel and this is caused by the absence of the steering controls in the finite element model. Normally they are embedded into their housing on the sides of the steering wheel and are also fixed with two screws from the back of it (*figure 92*). So, in the global behaviour of the system, the absence of the steering controls has a relevant effect being the steering wheel at 90 degrees with the body block hitting exactly the zone where they are fixed.

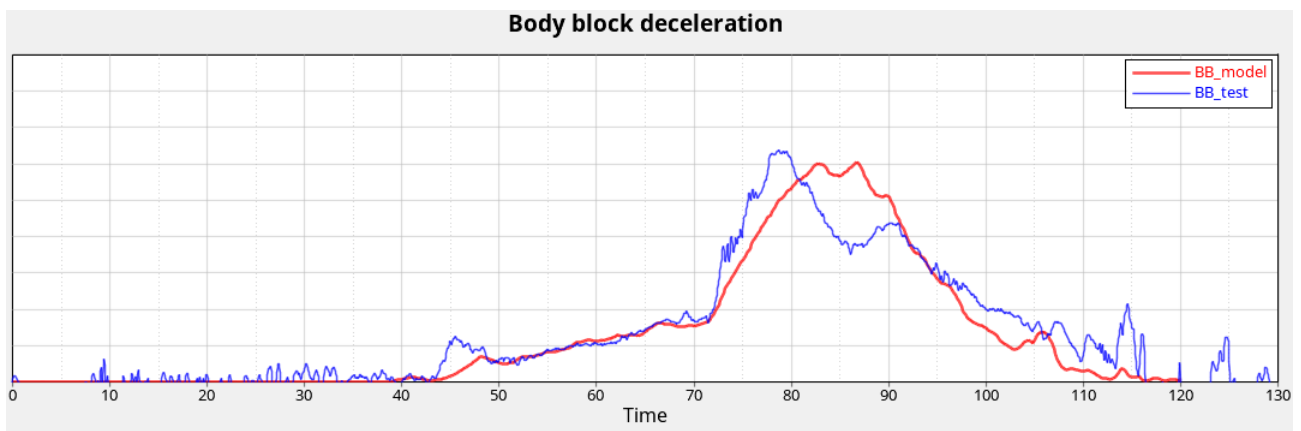


Figure 91: body block deceleration with 90 degrees steering wheel

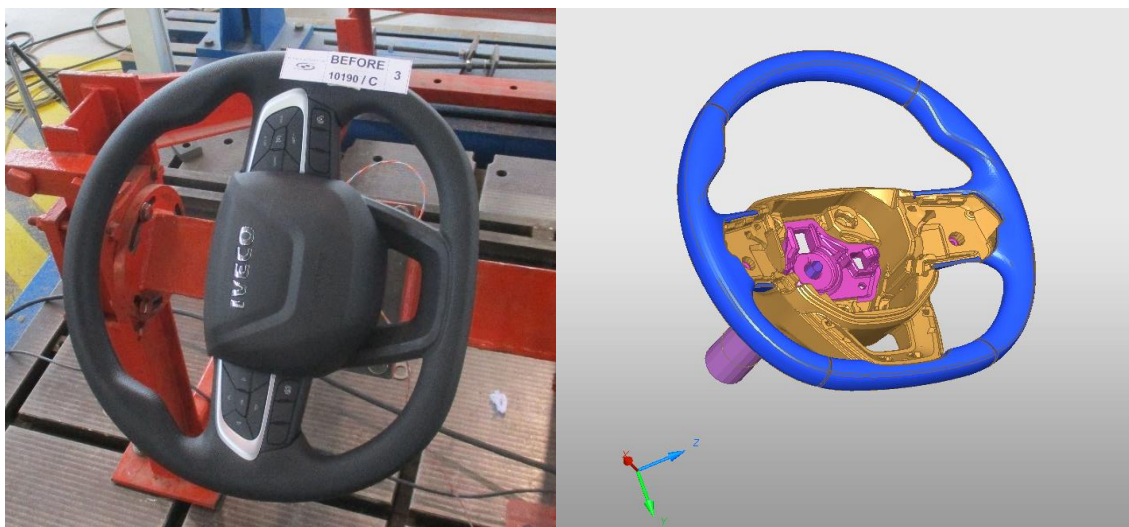


Figure 92: comparison between the real steering wheel and the model, where the are the controls missing

In the *figures 93* and *94* there are reported the frames of the test and of the simulation. As can be seen there is a correct correspondence between the two, with also the bag that in the simulation remains caught between the body block and the steering wheel.



*Figure 93: body block test with 90 degrees steering wheel*

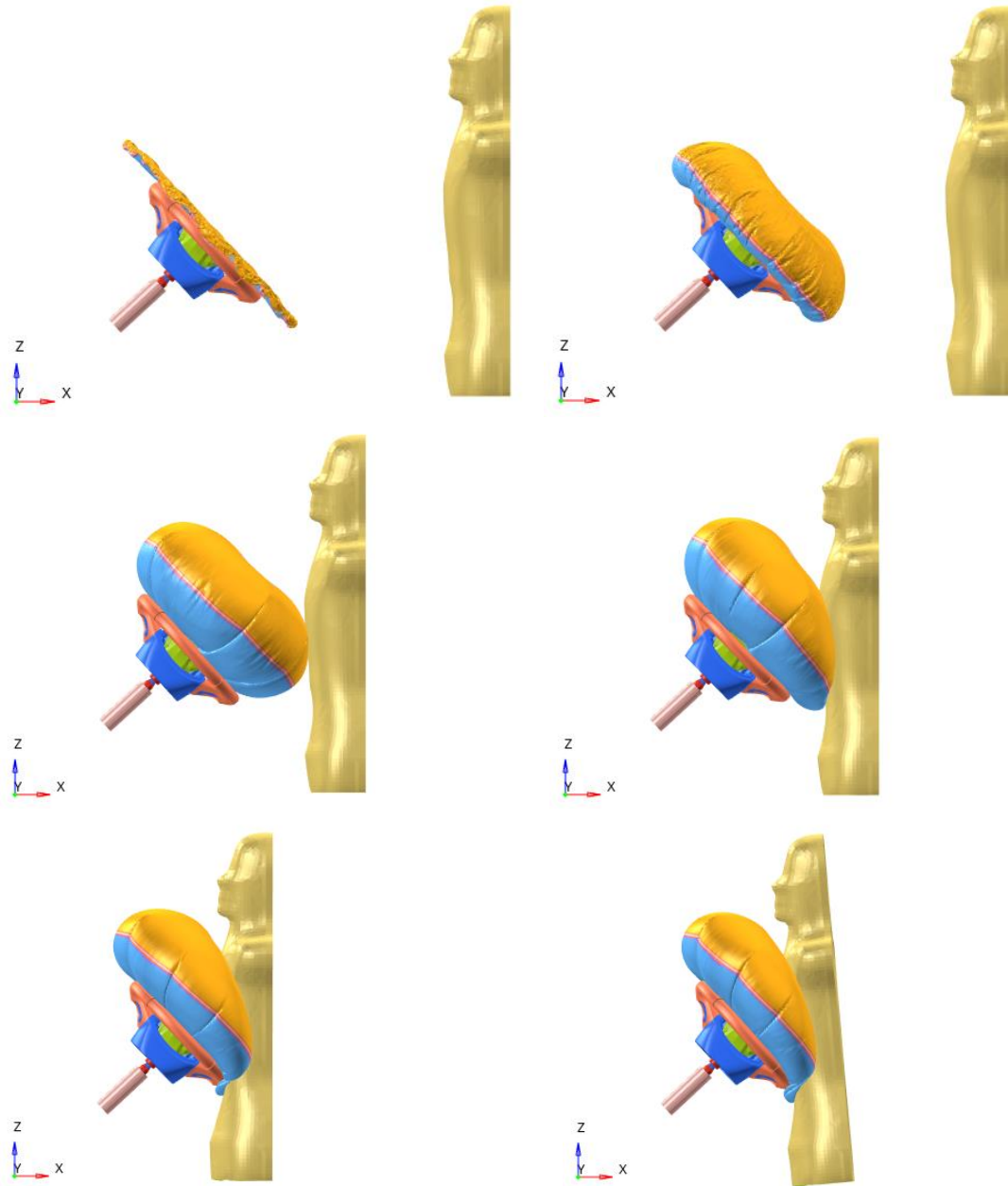


Figure 94: body block simulation with 90 degrees steering wheel

### 6.2.3. 180 degrees steering wheel

In this case the difference between the first and the second phase of the impact is less marked but can still be identified the moment when the steering wheel stiffness become relevant in the system behaviour, at about 75 ms. As showed by the plots in the *figure 95* there is a different behaviour between the test and the computer simulation during the phase in which the steering wheel stiffness become important, this because the steering wheel of the finite element model is stiffer than the real one and this results in a higher deceleration of the body block.

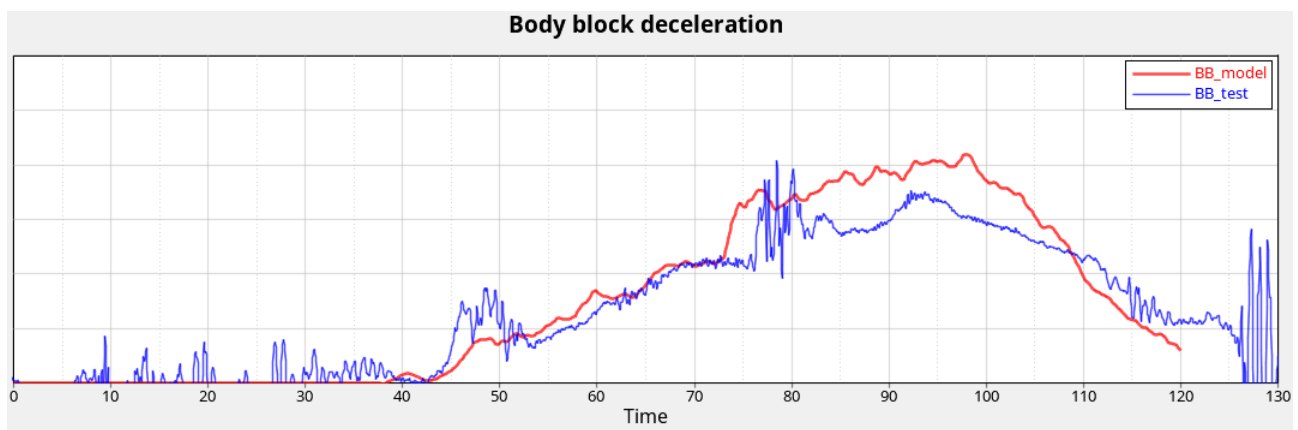


Figure 95: body block deceleration with 180 degrees steering wheel

The *figure 96* shows the different deformation between the two cases, with the long arc of the steering wheel deforming more in the test (*figure 97*) than in the simulation (*figure 98*). As can be seen from the first phase of the impact, the behaviour of the bag is fully correlated being the finite element and the test outputs coincident.

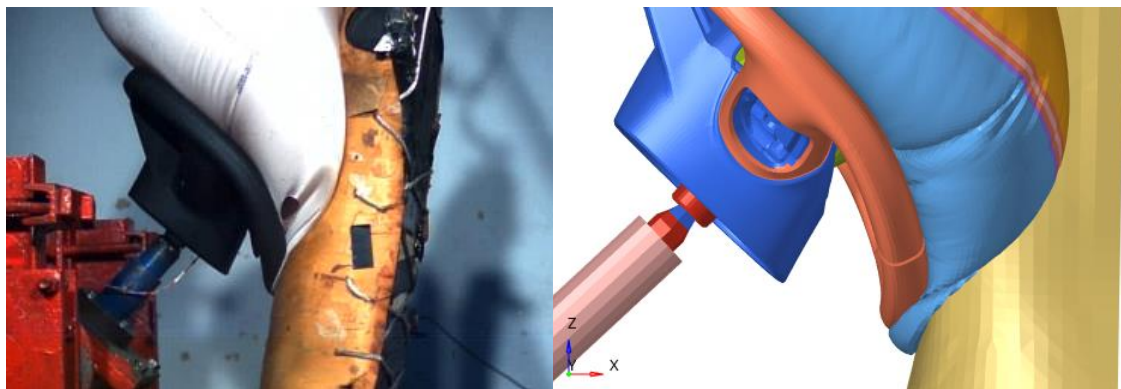


Figure 96: comparison between the long arc deformation in experimental test and in finite element model





Figure 97: body block test with 180 degrees steering wheel

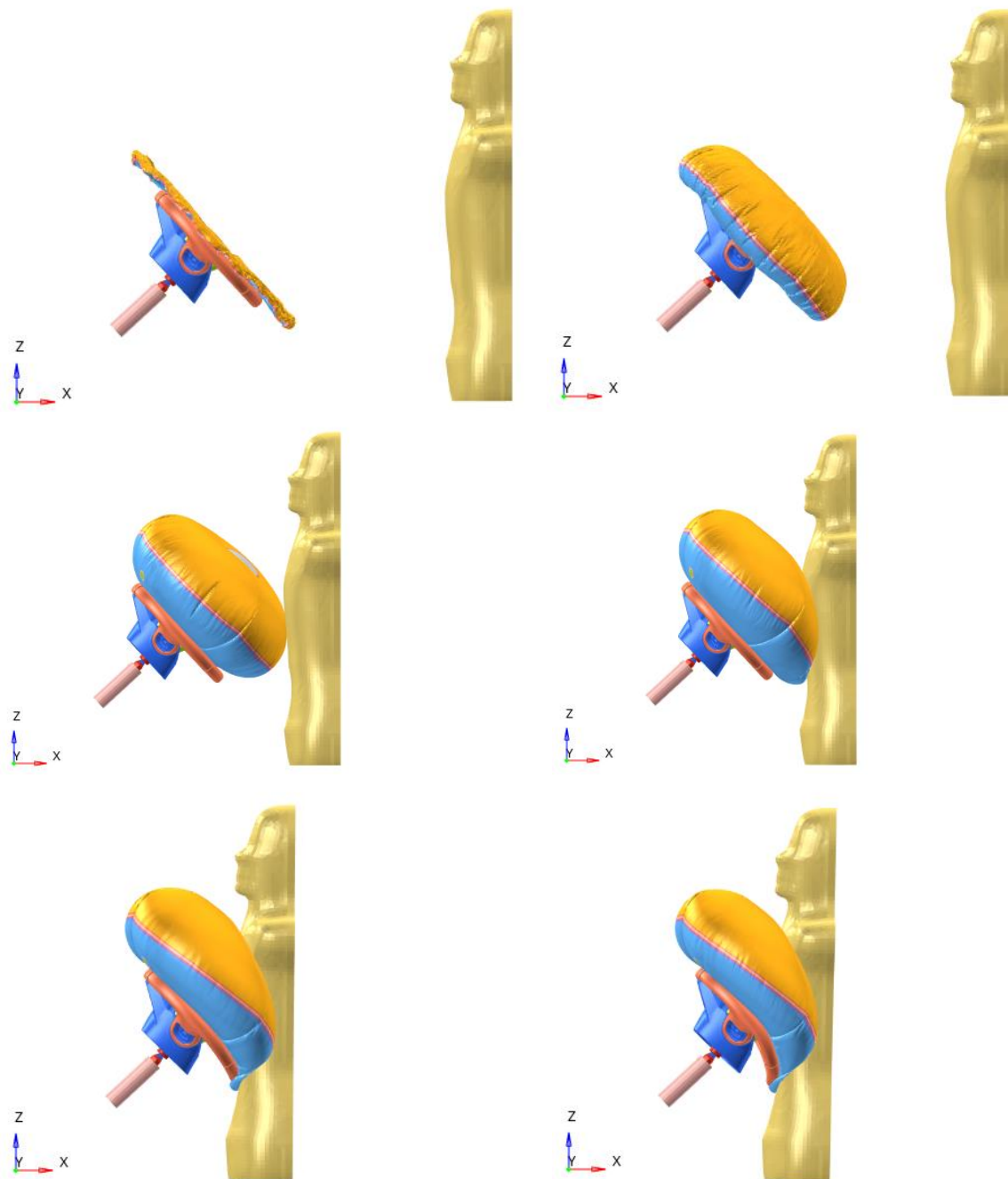
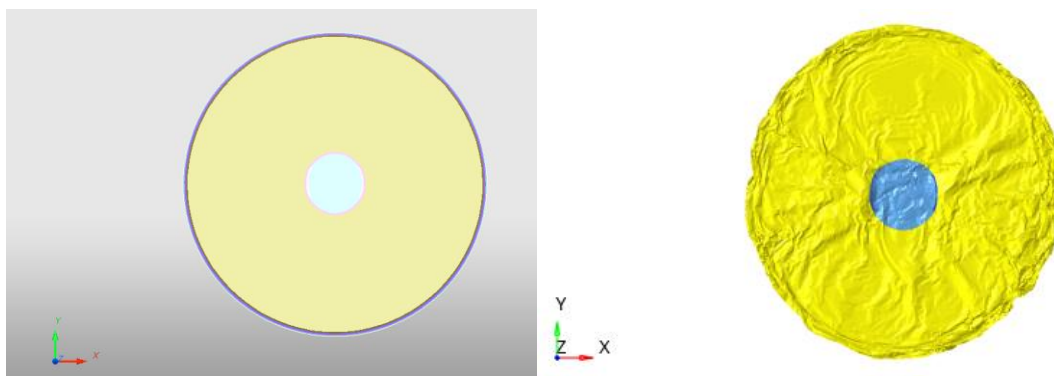


Figure 98: body block simulation with 180 degrees steering wheel

## 7. Airbag folding

Since the beginning of this thesis work it has been used an airbag in its unfolded configuration, as we have already discussed, because the important thing is not the deployment of the airbag but its behaviour during the impact test. So we have the initial airbag configuration where it is outside its housing and unfolded and the second configuration used where the airbag is pre-formed inside the punch to give him the correct shape before the inflation starts, like it was folded into to housing (*figure 99*). Now what it has been done is the folding of the airbag to fit it inside its housing and have a more realistic model.



*Figure 99: left, unfolded airbag initial configuration; right, pre-formed airbag second configuration*

The folding process is important because it could determine the functioning of the airbag or not, and also it is different from an airbag to another (for example, the driver airbag is folded in different way from the passenger or the side airbag), depending on the airbag shape and on the dimensions of the housing. So there are various folding techniques like zig zag folding, roll folding and tuck folding.

It happens that, once the airbag is folded into its housing its geometry is too complex to be easily defined in a finite element model, so Altair has developed a new and innovative tool that permits to the user to fold the airbag in a simple way, starting from the unfolded airbag geometry. This tool is present from the 2021.2 HyperWorks version and beyond.



## 7.1. Airbag folding tool in HyperWorks 2021.1

Since the 2021.2 version of HyperWorks, Altair has introduced a new tool to help the user folding the airbag, starting from its unfolded configuration. To use this tool is sufficient to have a model of the airbag with only the geometry and the material properties of the parts, no more cards have to be defined in the model. The tool allow to make the simplest folding that can be made on the airbag, so, as can be seen in the *figure 100*, it is possible to choose the folding among four different types:

- simple fold: meaning that a flap of the airbag will be folded along a line over the other side of the bag;
- roll fold: to roll a flap of the airbag until a stopping point defined by the user;
- tuck fold;
- zig zag fold;

plus a flatten fold, that is a process where the airbag, once has undergone to one of the other folding types, is pressed against a plane to reduce its size.

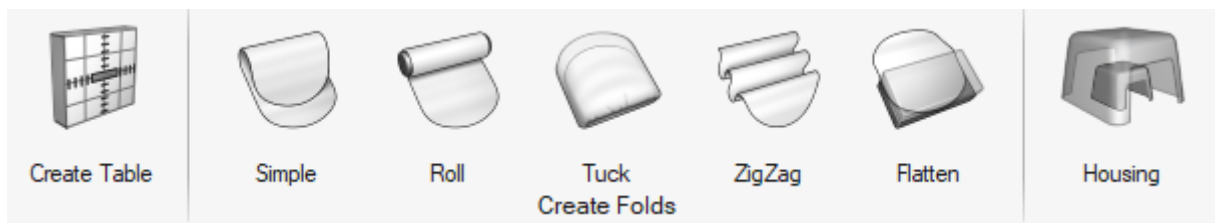


Figure 100: HyperWorks airbag solution options

Lastly there is the housing, i.e. the process of closing the airbag inside its housing, in this one an housing for the airbag must be created and imported into the model because the software needs the housing geometry to define a bigger one of it that will be scaled back to be sure that all the airbag is, in the end, enclosed into its housing.

From the 2022 HyperWorks version it is possible to do also a symmetric folding for the various folding types described in this paragraph. For the folding of the airbag studied in this work, it has been used this version of the software because being the driver airbag a circular one, with the symmetric folding it is possible to reduce the time needed for the folding process.

## 7.2. Airbag folding process

### 7.2.1. Folding plan

Before starting the folding, it is necessary to have a folding plan, i.e. how the airbag has to be folded in terms of type of folding that have to be done and their sequence. The folding plan is crucial in the folding process because it determines if the folding will be successful or not.

For example, in the folding plan presented below (*figure 101*), is it possible to see a driver airbag that in a first phase is folded on its lower face and then in the other sense, in its upper face. Then the two ends have been rolled and folded along the two black lines to have a final configuration where the airbag is packed around its inflator.

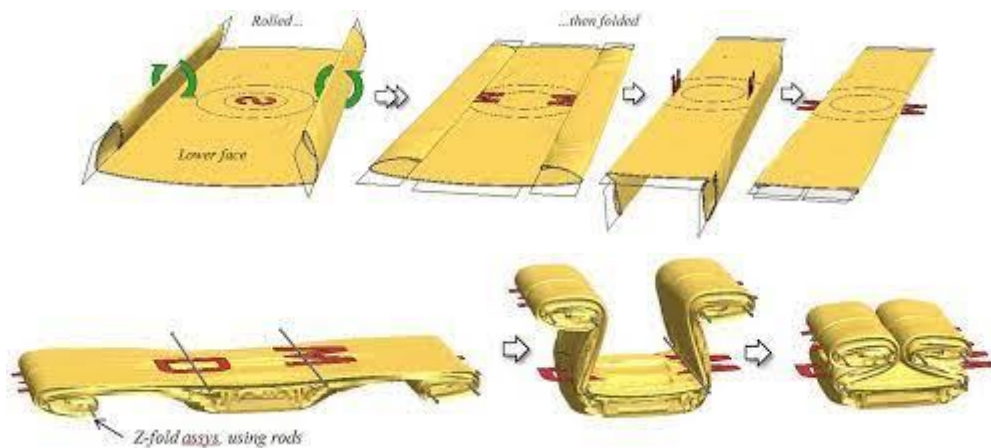


Figure 101: folding plan example for driver airbag

About the airbag subject of this thesis work, it has been defined a folding plan similar to the one up here, that will be showed in the following along with the folding process carried on with the HyperWorks tool.

### 7.2.2. Airbag folding process

The folding has been divided in four steps, consisting of two simple folds, one roll fold and one housing.

- First symmetric simple fold: the two airbag ends are folded on the lower side of the airbag with a symmetric folding process (*figure 102*).

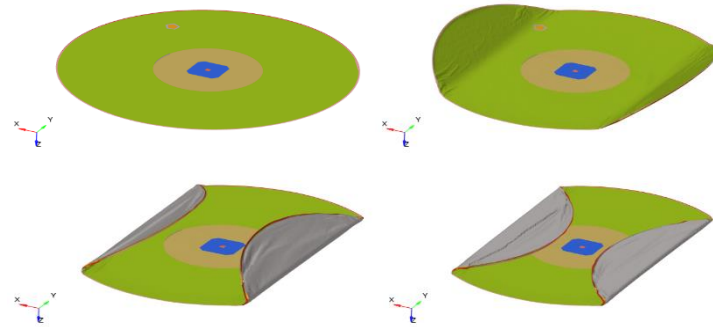


Figure 102: airbag first symmetric simple fold

- Second symmetric simple fold: after the first fold, the same symmetric fold has been done on the other sense, on the upper side of the bag (*figure 103*).

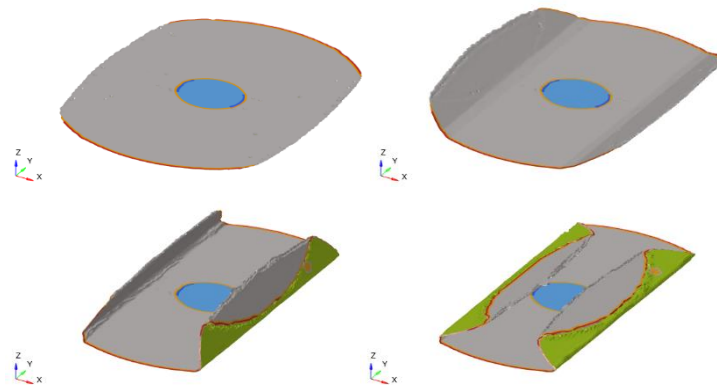


Figure 103: airbag second symmetric simple fold

- The third step is a symmetric roll fold so that the two flap of the airbag will be rolled upon the inflator (*figure 104*).

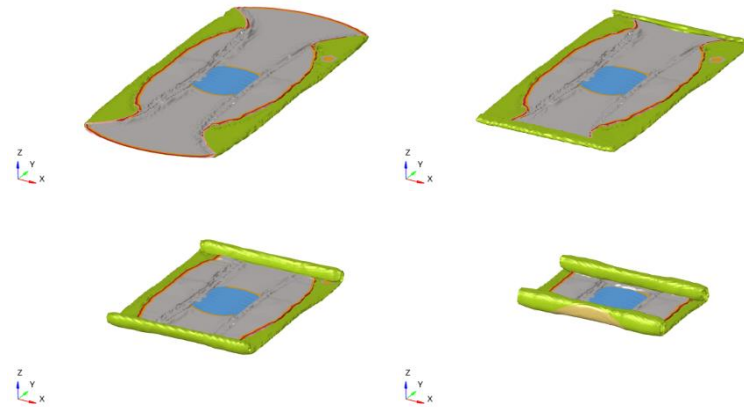


Figure 104: airbag symmetric roll fold

- Finally, the last step is to fit the airbag inside its housing (*figure 105*).

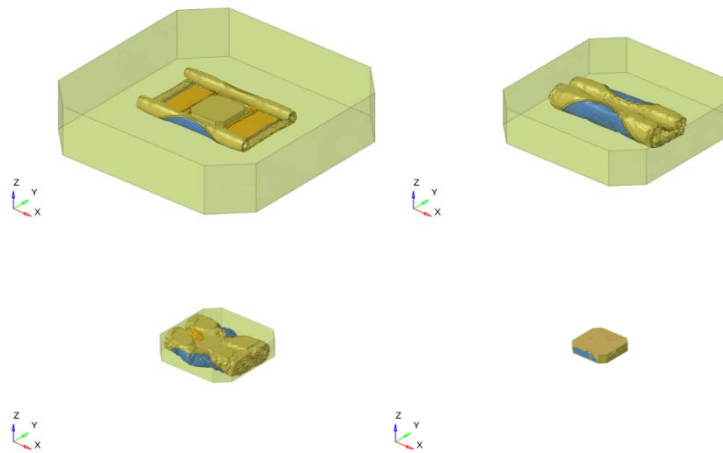


Figure 105: airbag housing

And what is obtained is the airbag fully enclosed in its housing as can be seen from the *figure 106*

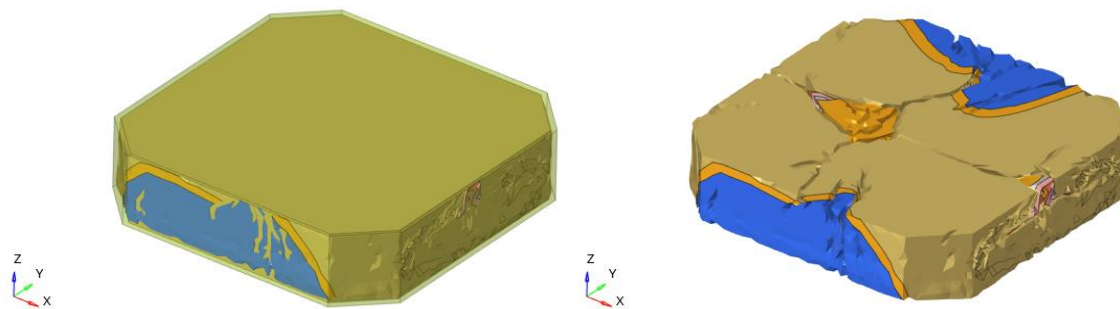
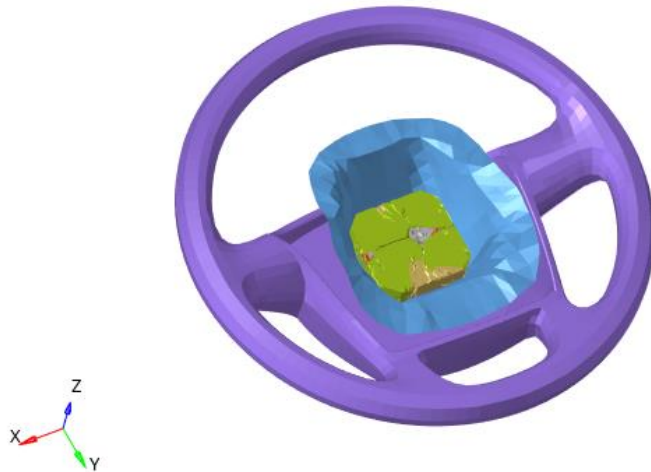


Figure 106: final folded airbag configuration

Despite the airbag has been folded it is still necessary to maintain the punch in the model because of the missing of all the detailed parts of the airbag housing in the steering wheel model. The punch is then still important for having a correct deployment of the airbag being the component that gives to the airbag the correct form during the deployment. The *figure 107* shows the final configuration of the steering wheel with the folded airbag.



*Figure 107: steering wheel and folded airbag*

### 7.2.3. Folded airbag deployment

As can be seen from the *figures 108* and *109*, starting from a folded configuration, the airbag inflates in a more natural way and its behaviour is comparable with the real one used for the experimental tests.

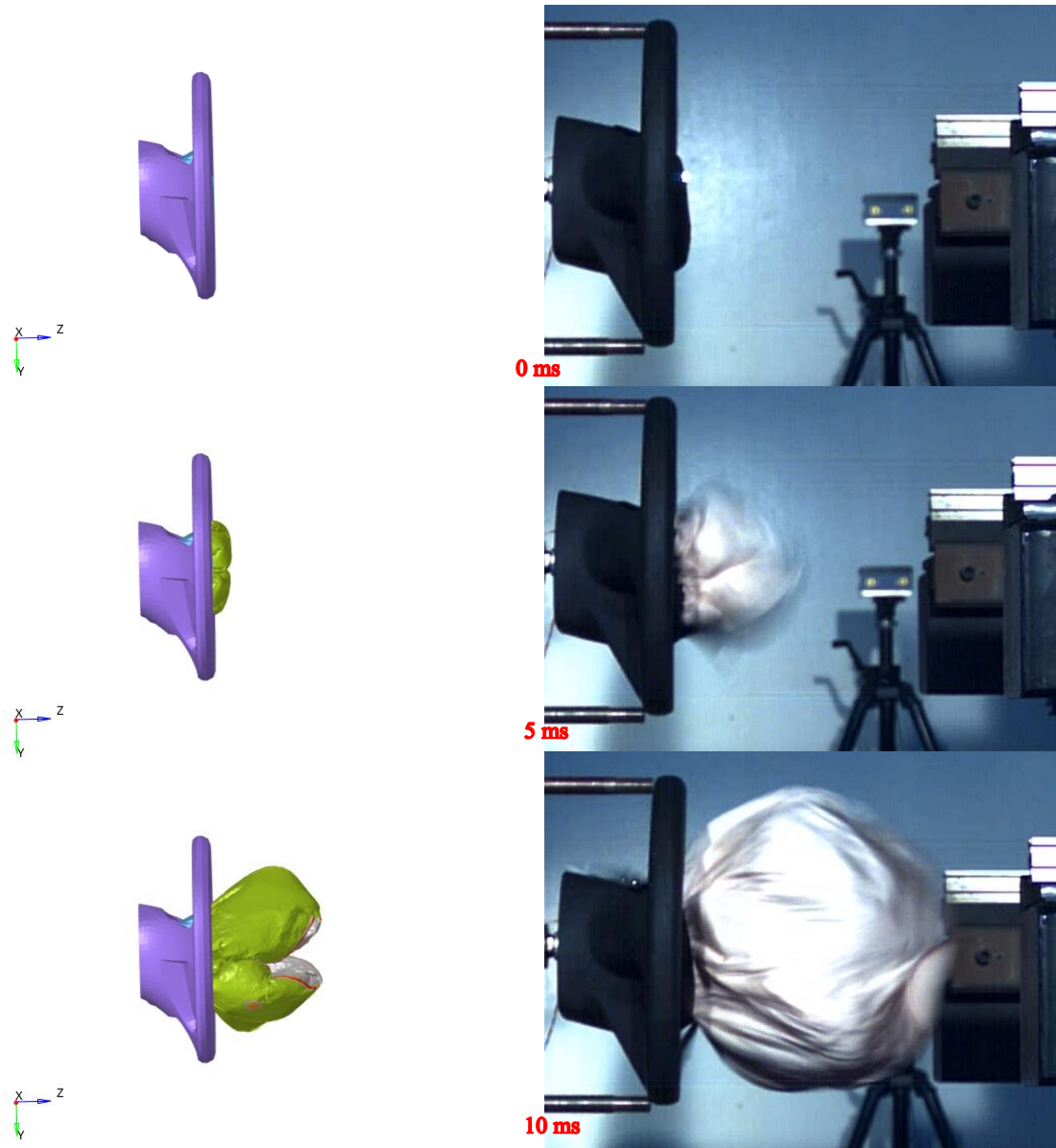


Figure 108: comparison between finite element folded airbag and real airbag deployment, part 1

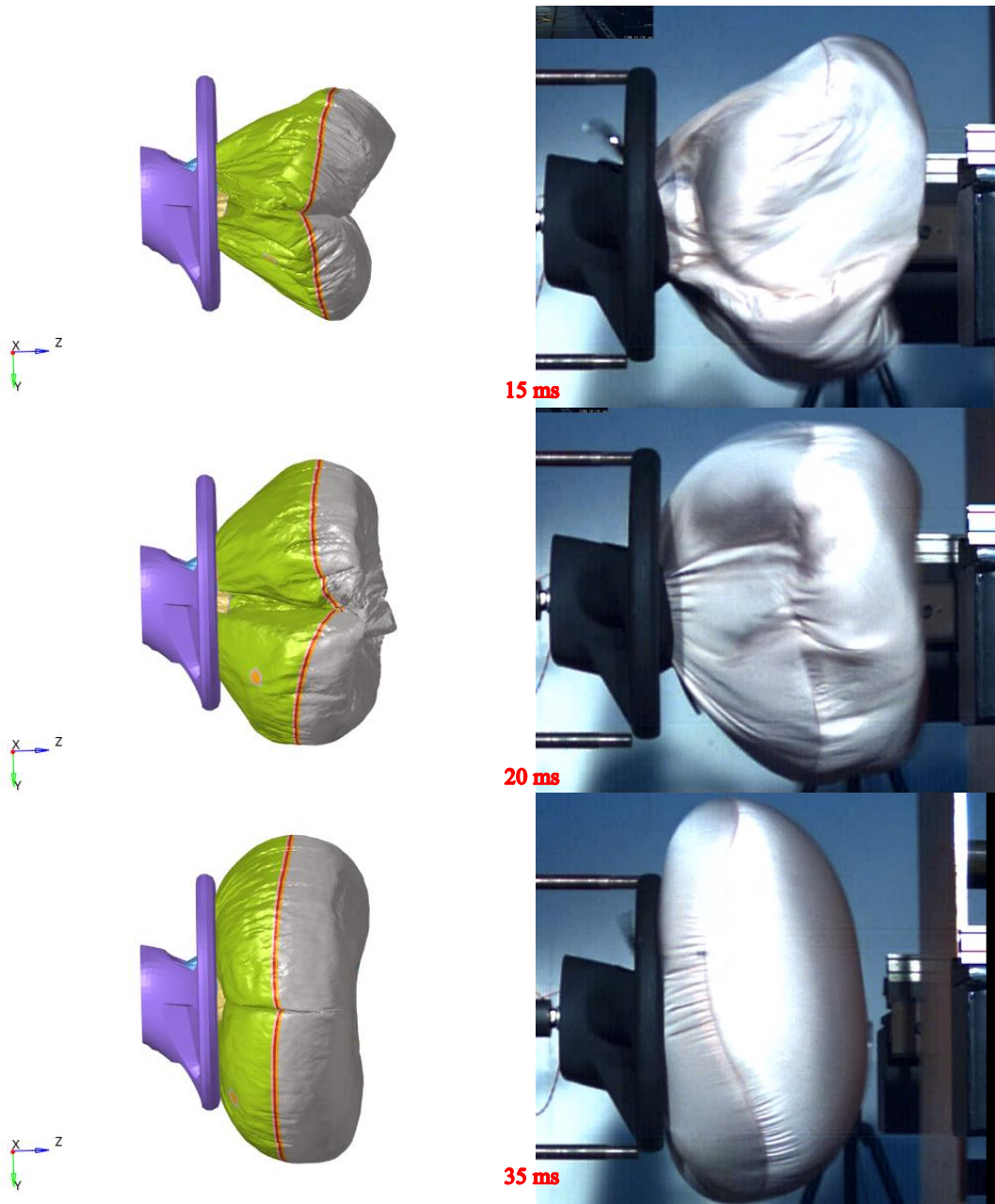


Figure 109: comparison between finite element folded airbag and real airbag deployment, part 2



## Conclusions

The aim of this work was in a first time the characterization of an Iveco Daily airbag finite element model. In a second time this airbag model has been used to simulate a real accident situation with the driver impacting on the steering wheel. The characterization has been done in different phases starting from the comparison between the behaviour of the finite element model with the Madymo model of the same airbag (a multi-body model). This allowed to define the material properties of the various parts, as well as the porosity and the characteristics of the vent hole. Then the finite element model results were compared with the one of the experimental tests done by the airbag manufacturer, ZF Friedrichshafen, and this allowed to make the model more robust. This characterization process showed very good results since the behaviour of the modelled airbag is correlated with the real one.

In a second phase the airbag model has been used to simulate a mannequin impacting on a steering wheel (like after an accident) with the airbag deployment, the so called body block test. The results of the computer simulation have been compared with the tests one conducted at the STELLANTIS Safety Center and the comparison has been done with three different configurations of the steering wheel. In this case the comparison between the simulation and the experimental results show very few differences. From an accurate analysis of the tests videos and of the simulation, it has been deducted that the differences between reality and simulation can be due to the steering wheel model, that behaves in a different way from the real steering wheel. Also in these tests the airbag model is well correlated with the real one.

In the end, a new tool available in the HyperWorks 2021.2 version has been used to fold the airbag and put it inside its housing.

## Bibliography

- [1] Vehicle Categories, EU [https://ec.europa.eu/growth/sectors/automotive/vehicle-categories\\_it](https://ec.europa.eu/growth/sectors/automotive/vehicle-categories_it);
- [2] 2021 Commercial Vehicle Safety, Euroncap <https://www.euroncap.com/en/vehicle-safety/safety-campaigns/2021-commercial-van-safety/>;
- [3] Altair Support, Altair Engineering,  
[https://support.altair.com/csm?id=altair\\_product\\_documentation](https://support.altair.com/csm?id=altair_product_documentation);
- [4] UNECE R12 Regulation,  
<https://unece.org/fileadmin/DAM/trans/main/wp29/wp29regs/R012r4e.pdf>



*I would like to thank a lot firstly the professor Alessandro Scattina, who gave me the opportunity to work on this project and from whom I have learned a lot during this period.*

*Thank you also to Marco and Giuseppe, that followed me and supported me constantly.*

*The biggest thanks goes to my family, because without them I wouldn't have been able to do anything of all I did in, unfortunately, more than five years. All that I've achieved from when I left home is in the biggest part for and thanks to them.*

*Thanks to Serena, she knows.*

*Thanks to all the others, the old and the new ones. Thanks to the ones I know since I was born, I can even imagine how all of this could have gone if you weren't here. Thanks to those who are still wondering of the ice creams prices in Lubiana, who is always late and who don't need words to speak. Who don't know if he is from Terni or Perugia and who shared the house with me for too much years. Who loves to sleep on the ground and who learned the Hungarian in a day. Everyone from Miranda, no words are needed.*

*And to everyone that doesn't recognize himself in the previous descriptions, I've only few lines and very poor imagination so thanks also to you.*